MODELING THE NATURAL FREEZEBACK OF PILES USING COMSOL MULTIPHYSICS®

By

Elliot D. Clausen, B.S.

A Thesis Submitted in Partial Fulfillment of the Requirements
for the Degree of

Masters of Science
in
Arctic Engineering

University of Alaska Fairbanks
May 2017

APPROVED:

Dr. Robert Perkins, Committee Member
Dr. Rorik Peterson, Committee Co-Chair
Dr. Yuri Shur, Committee Co-Chair
Dr. Leroy Hulsey, Chair
Department of Civil and Environmental Engineering
Dr. Douglas Goering, Dean
College of Engineering and Mines
Dr. Michael Castellini, *Dean of the Graduate School*

Abstract

Slurried pile foundations installed in predrilled holes are one of the most common foundations for building major structures on permafrost. This installation method relies on the cold permafrost to freeze the backfilled slurry around the piles to provide the strength required to support loads of a structure. Nearly all evaluations of freezeback time to date stems from the work of Frederick Crory presented to the First International Conference on Permafrost in 1963 and published in 1966. Crory never published field data but he provided an equation to determine freezeback time. This work was later expanded upon by G.H. Johnston in 1981 however Johnston gives no explanation for how or why he varied from what Crory had done. The purpose of this research is to check the results predicted by both Crory and Johnston with a contemporary computer modeling using COMSOL ® Multiphysics. Due to the advancement in technology and the power of COMSOL as a program more variables and situations will be able to be examined than what was available to Crory or Johnston at the times of their publications. This will be the first research in over 50 years to revise the work first published by Crory and show that his equation produces results that are significantly shorter than what the model calculates.

Table of Contents

List of Figures

Page

List of Tables

Page

Section 1: Introduction

1.1: *Background*

There are many challenges for people and projects directly impacted by the presence of permafrost. While frozen, permafrost is a strong foundation material capable to carry loads much larger than could be achieved if the soil were not saturated with water and ice. However, when non-thaw stable permafrost thaws the soil loses a significant amount of its strength and will typically differentially settle. This differential settlement will ruin a structure often condemning it or requiring massive, expensive overhauls. This thaw settlement is also an issue in the layer directly above the permafrost called the active layer which freezes and thaws each winter and summer.

Another issue is when the active layer refreezes in the winter. Water in the ground will freeze and expand causing frost heaving. If the pore size in the soil is small enough, water will even be drawn in towards the freezing front allowing the permafrost to heave greatly beyond the nominal 9% that water goes through. The cause of this phenomenon is not entirely understood however it leads to problems for structures placed directly on top of the permafrost. Problems also arise when objects, such as piles, are placed into or through the active layer. As the active layer freezes the ice will create a strong bond to the object and lift it out of the ground in an action called frost jacking. These problems, along with several others, contribute to many of the issues that people living in or designing for permafrost areas encounter.

1.2.1: *Common Structural Designs for Permafrost Areas*

There are three design approaches when it comes to building structures on permafrost being the passive and active methods as well as using standard practices. The most basic method is to determine whether or not the soil is thaw stable or if there is little or no chance of frost heave or jacking. This type of situation is typically found in what are called non-frost susceptible soils or NFS. These soils have pore sizes that are large enough to not be influence by the phenomenon that draws water towards the freezing front. If these soils are present then regular design practices can be implemented and there is no added concern from the presence of permafrost.

The other two methods are the most common in permafrost regions where frost susceptible soils are present and their thawing will cause what is known as thaw settlement. They are the passive and active methods. These methods are not a rigid set of procedures but rather design concepts that are implemented in different styles for different projects.

1.2.2: *Active Method*

The active method is a design protocol that begins with altering the in situ soils in some way. This can be done by pre-thawing the soil and allowing the settlement to occur prior to construction. Pre-thawing is a familiar technique used by miners in the early gold rush days to thaw the frozen ground before excavation. It was widely used in the Yukon and Alaska placer gold fields before activity in that area dwindled (Johnston, 1981). Another practice following the active method guideline is to remove the thaw susceptible soil prior to construction.

Both pre-thawing and removing the thaw susceptible soil are rare to see because of their limitations of only being practical in the discontinuous permafrost zone where permafrost depths are not typically thick and the presence of permafrost itself is a delicate balance of several factors. Pre-thawing works where the heat of the building will keep the soil thawed even during the winter as the surrounding soil begins to refreeze. It also assumes that the soil is stable once thawed, and typically drained, which is not common. Excavating the soil is also limited to shallow areas of permafrost because the soil must be completely thawed. If the soil is sufficiently thick the soil will have to be manually or artificially thawed. If this practice were done in the continuous zone, where temperatures are significantly colder and the permafrost layer is thicker than the discontinuous zone, the stability of the thawed soil not removed would likely not be able to support the loads placed on it or cause heaving when it refreezes. In general, the active method is typically not employed due to the lack of application and lack of control on the resulting thermal regime.

Creating a structure with a rigid base is often considered an alternative to the active method. The basic design philosophy is that if the base of a structure is stiff enough that it will not allow deflection when the ground moves. This is not a common practice due to there being no control over the thermal regime of the soil and its limited applicability to small structures such as

houses. It can be used as a complementary procedure for some of the other practices, however, as an added factor of safety. It is considered the cheapest option because the only extra cost is in the minor increase in materials cost.

1.2.3: *Passive Method*

The passive method is based on preservation of frozen state of soil. This option has been used much more frequently due to the fact that they can be applied to any situation, they give the designer more control over the resulting thermal regime of the soil, and there is a range of options varying in terms of cost, labor expertise, and materials required.

One of the most common designs for small structures is a post and pad foundation. This design is highly popular for several reasons including its simplicity, constructability, cost, and effectiveness. A post and pad foundation places several spread footings, often constructed of all weather wood over a pad of NFS material. The thermodynamic justification for this practice is that the bottom of the structure rests 2-3 feet above the ground creating a thermal break. This air gap prevents the heat from the structure from traveling into the ground and influencing the permafrost. There is an added benefit where the building provides shade for the ground during the summer while allowing the cooler winter air to circulate underneath. This air flow supercools the soil as the surrounding ground will have a layer of snow insulation. Also, gravel pads act as a permanent insulator shielding the permafrost from any temperature influence. This reduces the need for special construction techniques and what is required is relatively simple. It is also inexpensive in materials and labor required making it one of the most cost effective options available. After construction, this design often times allows for the quick and convenient leveling of the structure if there has been any shift in the. When combined with another technique, such as a rigid foundation, this becomes one of the best foundation options available. The biggest limitation of a post and pad foundation is that it is not well suited for large loads such as a multistory concrete building, hangar, or any other large building.

If the material for a NFS pad is unavailable, which is often the case for small remote communities, this practice also works without the gravel pad so long as extra attention is paid to the thermodynamic stability of the building and the permafrost. Similarly, if ample NFS material is available then a pad thick enough to protect the permafrost from the structure's heat influence can be used.

A unique practice that modifies the basic NFS pad design is a duct bank foundation. This technique uses buried duct pipes in the NFS pad that are left open in the winter to allow cold air to supercool the ground. This design is typically only used for structures that exert a large load and have a significant thermal impact. Specifically, this practice is almost exclusively used for large liquid, mostly water, storage tanks. The large load from the liquid makes other designs impractical and the thermal energy stored in the water poses a serious threat to the stability of the permafrost below. One important maintenance note for this design is that it requires that the ducts be capped at the end of each winter to prevent the warm summer air from thawing the permafrost.

One of the most well known designs used is a thermosyphon to continuously remove heat from the ground year round to keep the ground below the freezing point. They use either a single or two phase fluid to extract heat from the permafrost and active layer to the air via convection. In a single phase thermosyphon a single fluid fills the thermosyphon. At the bottom of the thermosyphon, placed in the permafrost, the fluid is colder and thus denser than the fluid at the top. As heat flows downward the fluid heats up, becomes lighter, and rises to the top using natural convection. At the top of the thermosyphon there are fins which help radiate the heat outwards. In a two phase thermosyphon the liquid is allowed to change phase from a liquid to a vapor at the bottom. When it rises to the top it condenses and runs down the sides of the thermosyphon back to the bottom. Two phase thermosyphons are much more efficient than single phase because they use latent energy of phase change to remove the heat which is much more effective than natural buoyancy. They are, however, much more costly and the working fluid has more stringent requirements. There are many variations on the thermosyphon that utilize the same concept. A thermopile is a thermosyphon that also has a structural component

that supports a structure. The Trans Alaska Pipeline uses these across much of its span from Prudhoe Bay to Valdez. Another variation is the aeropile which simply has an open top and allows cool air to travel freely into the pile and sink to the bottom. Lastly, a heat pipe uses a wick to accelerate the return of the condensed liquid to the bottom of the thermosyphon. While these systems are highly efficient and stable they are also the most expensive option and a single thermosyphon may cost upwards of ten thousand USD. Due to this limitation they are often only used in the oil and gas industry or for large government buildings.

The final design used in permafrost construction is a pile foundation. These have a varying degree of popularity and use. In the continuous permafrost area where the permafrost is cold, stable, thick, and abundant they provide substantial strength through the adfreeze bond strength. The adfreeze bond is caused by the lateral freezing of the permafrost to the pile supporting the structure through the shear strength of the permafrost. The piles themselves can be made of timber or steel. Concrete piles have been used however there is difficulty in ensuring that no tensile cracks form that would allow moisture into the reinforcing steel. Cast in place concrete piles should not be used due to the introduction of heat from the cement-water reaction to the permafrost.

Pile foundations are not uncommon in more temperate climates however there are some specific things that need to be considered for cold regions. A common practice in warmer areas is to drive the piles utilizing equipment such as a vibratory hammer. However, the strength of permafrost will almost never allow this and will likely cause the pile to be crushed. Driving can be accomplished more easily if a pilot hole is drilled first. Steam or water can also be used to thaw the ground however extreme care should be used not to thaw the permafrost any more than what is necessary. The best way is to thaw a small hole and place or drive the pile into that. Larger holes should only be used as a last resort as the thermal disturbance may cause long lasting thawing effects if the permafrost is especially warm. A common method of installation is to drill a hole larger than the pile and backfill with a sand-water slurry. The slurry, composed of NFS sand, will freezeback and bond to the pile and itself become strong, safe, and stable permafrost.

A limitation of pile foundations is the skill set required for construction. While the basic concept and practices are not unfamiliar to people from warmer regions, it still requires a contractor familiar with pile installations with the equipment and operation skillset. It also often requires structural steel which is costly to ship. These two considerations make pile foundations relatively expensive compared with the other practices listed. It also requires permafrost thick enough to provide the required support. They are still, however, quite popular where post and pad foundations are not applicable being much cheaper than thermosyphons. They are also capable of supporting much larger loads than other design practices.

1.3: *Problem Statement*

Pile foundations are widely used in the permafrost region and dry augering over-sized holes and backfilling with a sand water slurry is the most common method of pile installation. One construction limitation in this set up is that project progress is halted until the slurry is completely frozen. However, there is little literature available that describes this process.

The current authority on freezeback time comes from a publication in the proceedings of the First International Conference on Permafrost in 1966 by Frederick Crory. Crory performed several tests in Fairbanks, Alaska on the freezeback time of piles of different material. He proposed equations that could be used in different areas that considered factors such as slurry density, energy released to freeze slurry, thermal conductivity, and heat capacity.

Crory's work has largely gone unchecked with no other major publication on the freezeback of slurry backfilled piles other than G.H. Johnston in 1981 who expands on Crory's publication. Some of the assumptions that he makes when creating his equation for the freezeback time are also overly simplified. At the time they were acceptable due to the limitations of the field of study at that time, however they can now be checked upon using modern techniques.

1.4: *Objective, Scope, and Limitations*

The goal of this research is to check evaluation of the freezeback time of slurry backfilled piles with that of Crory and Johnston using COMSOL® Multiphysics. COMSOL® is a finite element method (FEM) software that can handle multiple types of physics as they interact such as electrical, fluid, and heat flow as they happen simultaneously. For this work, only the physics of heat transfer will be used.

COMSOL® will also be used to measure freezeback times as different parameters change as well as modifying some of the original assumptions Crory made in his work. These results will be compared using standard benchmarks such as freezeback time and freezeback profiles showing the time it took for various points within the slurry to completely freeze.

The biggest limitation of this research is the lack of field verification. Ideally there would be physical tests to corroborate the model. In lieu of this, verification will be done with theoretical concepts by examining known and expected trends. Additionally, when thermal gradients are used in the model they are assumed to be linear despite the fact that ground temperatures follow non-linear patterns bounded by trumpet curves. Lastly, a limitation of the very comparison with Crory and Johnston is the lack of original data to compare to but rather just their published freezeback equations

Section 2: Literature Review

2.1: *Piles in Permafrost*

Piles have been used extensively in permafrost areas for decades being the main type of foundation in Alaska permafrost areas. Piles transfer the, typically large, loads through weaker soils that are susceptible to seasonal freeze-thaw cycles and into the stronger frozen soils. Piles are a good choice even in the ground where the temperature is near the freezing point and any surface disturbance could cause thermal settlement. While there is some point bearing support at the bottom of the pile most of the strength of the pile comes from the tangential adfreeze strength. They also provide a thermal break from the surface below by keeping the structure elevated several feet thus preventing heat from flowing downward into soil.

2.1.1: *Special Types of Piles*

There are several different types of special piles most of which attempt to either refreeze or keep the ground in a frozen state after installation. Some of them have similar names but with different designs and purposes. A thermal pile uses natural or forced convection to circulate a fluid medium through pipe piles to cool the ground. A thermosiphon, or thermosyphon, uses either a single-phase or two-phase system that uses natural convection to cool the ground. A single-phase thermosiphon uses a working fluid to absorb heat at the bottom of the pile, natural convection to take the less dense, heated fluid to the top of the pile, and radiates the heat out into the air usually with the aid of cooling fins. A two-phase thermosiphon, also called a thermopile, uses the latent energy associated with phase change to absorb heat and boil the working fluid, the vapor then carries to the top of the pile where it condensates and runs down the sides of the pile back to the bottom of the pile. A heat pipe is similar to a two-phase thermosiphon but with a wick to aid in returning the fluid to the bottom of the pile (Clarke, 2007; Johnston, 1981; Linell and Lobacz, 1980)

2.1.2: *Pile Design Considerations*

Pile foundation designs should consider several factors such as soil type and properties, the presence of massive ice, and the soil thermal profile. Considerations for pile determination should be chosen to maximize the adfreeze strength of the pile while reducing the thermal impact

on the permafrost and include the type of pile material, depth of embedment, and cross-sectional area. Ultimately, the main design points of a pile foundation are that the loads are transferred to the frozen soil below, pile embedment length is deep enough such that there will be no frost jacking and no drag down due to seasonal frost action, and that the soil thermal regime remains frozen. When considering pile support the main consideration is the adfreeze bond acting on the sides of the pile, which largely depends on the temperature of the permafrost and support nearly all of the pile loads (Heydinger, 1987; Johnston, 1981, Linell and Lobacz, 1980; U.S. Army Air Force, 1983; Weaver, 1979)

2.1.3: *Pile Materials*

Pile material is often a matter of availability and cost. Where wooden piles are used in remote areas due to material availability they degrade quicker than steel and concrete piles and are not capable of supporting large loads. Concrete piles are seldom used in the U.S. but are popular in Russia and China due to material availability and cost (Sanger, 1969). They often cannot be precast and shipped due to weight. Concrete piles require extra consideration due to the tension experienced when the active layer freezes in the fall. Over time small cracks in the concrete will develop allowing moisture to corrode the reinforcing steel. The heat of hydration from the concrete should also be considered to ensure that it does not thermally degrade the surrounding permafrost. Steel piles provide ample strength and corrosion resistance however they are expensive to purchase and ship.

2.1.4: *Pile Installation Methods*

2.1.4.1: *Driven Piles*

Another major consideration is the method of installation which is done by driving or using slurried piles both of which can be aided by steam thawing. Concrete piles are typically installed by precasting the pile and placing in an overdrilled hole or by injecting the concrete into a predrilled hole. Driven piles are convenient in that they use installation techniques similar to what would be seen in a more temperate region however they do not have adfreeze forces as large as slurry piles (Clarke, 2007). However, this difference in strength can easily be recovered if the pile is driven a few extra feet (Crory, 1967). A disadvantage of driving piles is that they do

not drive well into soils containing coarse grained material or large stones, or in cold permafrost. In order to get through the large stones it is common to use steam injection and then push the stones into the thawed, softened permafrost (Johnston, 1966). Driven piles are also limited in material types as wooden piles typically cannot be driven into the frozen ground without an aid like steam to soften the soil. Vibratory hammers can be used to aid in driving the piles (Johnston, 1981; Linell and Lobacz, 1980; U.S. Army Air Force, 1983).

2.1.4.2: *Slurried Piles*

Slurried piles add an additional element of heat to the when the permafrost freezes the slurry, known as back freezing. The energy released to freeze slurry depends on several factors however the largest is the amount of latent of phase change of the water in the soil.

Steam thawing can be incorporated in both of these installation methods however, due to the amount of energy introduced to the frozen soil, it should not be used in discontinuous permafrost where temperatures hover near the freezing point due to the amount of energy added to the permafrost (Crory, 1967; Johnston, 1966). Even in areas of continuous permafrost, the use of over-steaming can increase the time for the permafrost to return to thermal equilibrium, and to freezeback slurried piles, can increase in the order of weeks (Johnston, 1966).

Slurried piles also require special considerations. Oftentimes this method limits the type of pile to be an open-ended steel pile or an H-pile due to the fact that the water in the slurry will cause wooden and closed-end piles to float. This challenge can be overcome with anchoring and bracing but it is simpler to change the pile material and geometry to something more appropriate (Sanger, 1969).

The optimal mixture for the slurry is a sand-water mixture that's been vibrated in place (Crory, 1966). It can be mixed in portable concrete mixers and transported using small wheelbarrows on site. The use of sand for the slurry complicates the installation process if there is no such material on site and it has to be brought in from elsewhere. While silts and clays can be used, clays are very difficult to mix, place, and locate in Alaska and both silts and clays depress the

freezing point of water within the mixture leading to heavily reduced pile capacities especially in warm permafrost (Crory, 1966; Ladanyi, 1983). While cement grout over slurry will give higher adfreeze strengths than using a soil-water mixture, concrete should never be used due to its tendency to crack when experiencing tension in the fall when the active layer freezes. Also, the heat of hydration can melt ice within the permafrost and further delays the soil freezing back after pile installation (Linell and Lobacz, 1980; Ladanyi, 1983; Sanger, 1969; U.S. Army Air Force, 1983).

One unique nuance of slurried piles is monitoring the temperature of the slurry when it is placed. An apparent limitation of the temperature is that if it is too large, typically over 40°F (5°C), then there is too much energy being added to the permafrost. Some people have, however, tried to increase the freezeback time by using frozen chunks of soil, often times removed when the bore holes were drilled and then placed with the slurry. The optimum installation process involved mixing thawed materials prior to placement however it has been known to happen that frozen chunks will be placed and then a thawed slurry poured after. This leads to pockets of air being trapped in the annulus as the thawed slurry freezes around the frozen chunks. The use of frozen chunks of soil mixed above ground and then backfilling is another method that will lead to pile failure due to the fact that the slurry will not freezeback consistently and the adfreeze bond will not be uniform leading to decreased strengths (Clarke, 2007).

Another consideration is the thermal influence on the permafrost from the construction and installation methods. This is especially important in the discontinuous zone where the presence of permafrost is often determined by a balance between such factors as vegetation cover, terrain, winter snow cover, and presence of surface water (Shur and Osterkamp, 2007). While the heat added due to steam thawing and the heat required for slurry freezeback remain the largest considerations, the heavy machinery used to maneuver and install the pile can damage the surface vegetation reducing its ability to insulate the frozen soil below.

2.2: *Slurry Freezeback*

A majority of pile research has been focused on the strength of piles for a given installation method (Crory, 1967; Crory, 1968; Crory, 1975; Ladanyi, 1983; Luscher et al., 1984). A literature review of North American practices conducted by Ladanyi in 1983 describes slurried pile research focusing on pressure from ice expansion within the slurry and the dissipation of this pressure and concludes that is the area that required the most future research. However, there is little information on the freezeback of the slurry itself. The freezeback time is especially important in slurried piles because the pile has no strength or stability until the slurry completely freezes back.

2.2.1: *Natural Freezeback*

Natural freezeback relies on permafrost specific heat removing the latent heat of freezing slurry. The term freezeback can include the time required for the permafrost to return to the thermal equilibrium which was prior to pile installment however it largely refers to the time for the latent heat to be removed. This distinction is less important in colder soils due the fact that the sensible energy required to return the soil to equilibrium is relatively small compared with latent heat. However, in warmer soils or in soils that have been steam thawed this time can be several weeks which can affect the strength of the slurry (Crory, 1967; Heydinger, 1987; Johnston, 1966; Research Group on Pile Foundations in Permafrost, 1978).

2.2.2: *Artificial Freezeback*

Artificial freezeback uses a thermal pile of some sort to help in the initial freezeback of the slurry, help keep the soil frozen after installation, or a combination of both. Thermal piles are some of the oldest examples of artificial freezeback and often times used basic glycol lines to freeze the slurry around the pile. These lines were not maintained after construction, oftentimes the lines would be capped and left in place, and thus they were not designed to continually maintain the frozen ground temperatures (Crory, 1967). This is different from the thermosiphons used on the Trans Alaska Pipeline which continually remove heat from the ground maintaining the structural integrity of the vertical support members.

2.2.3: *Existing Methods of Evaluation of Freezeback Time*

An analytical solution, originally provided by Carslaw and Jaeger (1959) and expanded upon by Lee (1962), exists for the natural freezeback of slurry by considering it as a finite cylindrical heat source inside an infinite medium with the axis normal to the surface of the medium and heat only flowing radially, none from the bottom or top of the pile. This solution, presented below, only considers the heat required to be removed from the slurry, the size of the bore hole, and the thermal properties of the permafrost. For

α = Thermal diffusivity of the permafrost

r_b = Radius of the bore hole

Q = The amount of energy to remove from the slurry per unit length

ΔT = The difference between the permafrost temperature and the freezing point of the soil

K = Thermal conductivity of the permafrost

C = Volumetric heat capacity of the permafrost

t = Freezeback time of slurry

Using the dimensionless parameter τ as a dimensionless time parameter defined as

$$\tau = \frac{\alpha t}{{r_b}^2} \tag{2.1}$$

the equation for freezeback is expressed by the equality

$$Q\frac{\alpha}{K\,{r_b}^2} = \Delta T\left(14.50 + \frac{8}{\pi}\sum_{\tau_i=0.6}^{\tau} I(\tau_i)\Delta\tau_i\right) \tag{2.2}$$

$$\frac{Q}{C\,{r_b}^2} = \Delta T\left(14.50 + \frac{8}{\pi}\sum_{\tau_i=0.6}^{\tau} I(\tau_i)\Delta\tau_i\right) \tag{2.3}$$

The function I(x) is the modified Bessel function of the first kind with values that can be found in a 1943 publication by J.C. Jaeger and Martha Clarke.

The amount of energy to be removed can be a combination of latent and sensible heat however it is most commonly simply the latent heat required for freezing. In general, for

λ = Latent heat of fusion of water

A = Cross sectional area of slurry

w = Water content of slurry

γ_d = Dry unit weight of slurry

C_s = Volumetric heat capacity of slurry

ΔT_s = Temperature difference between the initial slurry temperature and the freezing temperature

the energy to be removed is

$$Q = LAw\gamma_d + AC_s\Delta T_s \tag{2.4}$$

Note that the first term is the energy from latent heat and the right term is the sensible heat. If sensible heat is being considered then the energy to cool the slurry to the freezing point and the energy to cool the frozen slurry to the ambient permafrost temperature should be considered. This is important to separate due to the change in the slurry volumetric heat capacity from the thawed to frozen state (Crory, 1966). **Figure 2.2.1** and **Figure 2.2.2** show a breakdown of how to calculate the latent heat in the slurry respectively and the freezeback time. **Figure 2.2.3** shows specific solutions to the analytic solution (Crory, 1966).

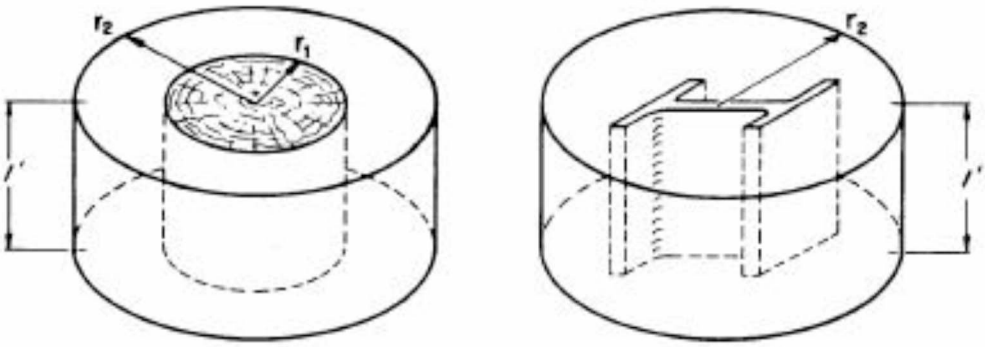

$Q = \pi L(r_2^2 - r_1^2)w\gamma_d$ or $Q = L(\pi r_2^2 - A)w\gamma_d$

where L = Latent heat of water

r_2 = Radius of hole

r_1 = Radius of pile

A = Cross sectional area of H-pile

w = Water content, percent dry weight/100

γ_d = Dry unit weight of slurry

Figure 2.2.1: *Evaluation of the latent heat required for the slurry to freezeback per length of pile (Crory, 1966).*

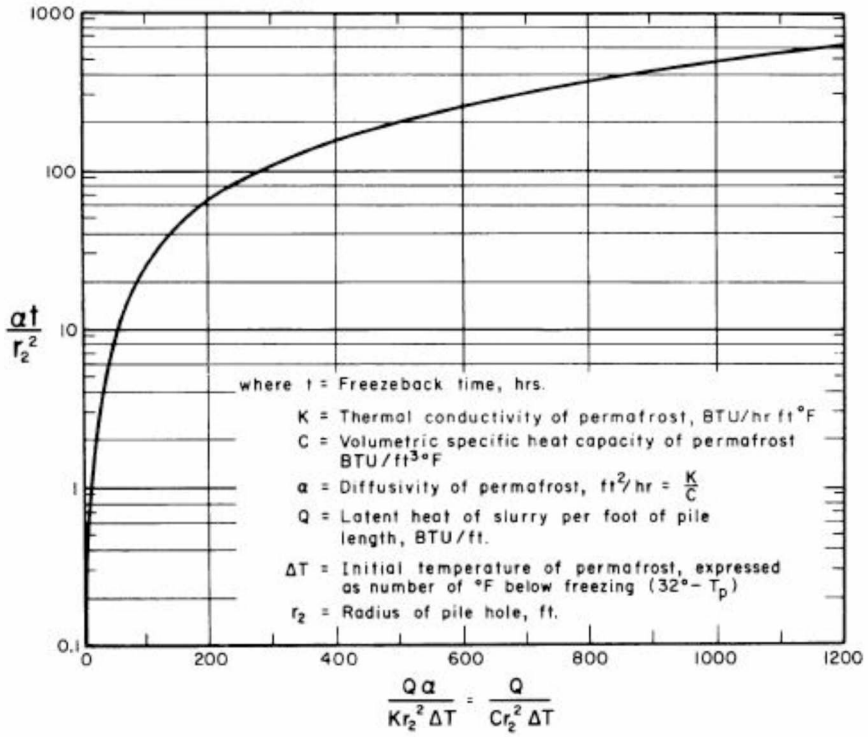

Figure 2.2.2: *Chart of slurry freezeback time (Crory, 1966).*

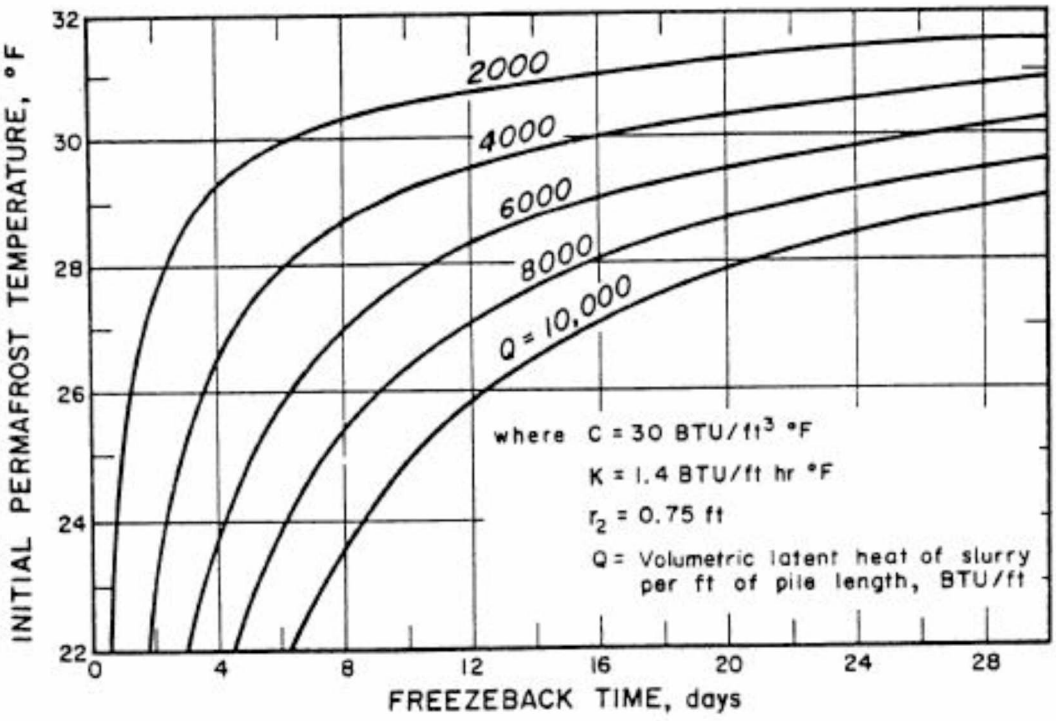

Figure 2.2.3: *Specific solution of slurry freezeback (Crory, 1966).*

2.2.4: *Crory's Work*

Frederick Crory, working for the Cold Regions Research and Engineering Laboratory, conducted extensive studies on pile installation and at Fairbanks and some other sites around Alaska (Crory, 1966; Crory, 1967; Crory, 1968; Crory, 1973; Crory, 1975). His most descriptive work on slurried piles was published in the Proceedings of the First International Conference on Permafrost in 1966. It was based on studies of 97 slurried piles installed at a test site in Fairbanks, Alaska. Crory reports the results of several tests including creep, freezeback time, load settlement, adfreeze strength, optimal slurry composition, and more. This paper remains the most comprehensive document available to describe slurried piles.

While the tests conducted in Fairbanks by Crory used silt- and clay-water slurries, Crory reports that saturated sand which has been vibrated and compacted in place has nearly 50% more

strength than silt-water slurries. Clay-water slurries, while difficult to mix and place, also have the lowest adfreeze strength with the strength increasing with particle diameter size up to vibrated sand.

Pile spacing can affect the freezeback time of slurried piles. Piles should be placed far enough apart such that there is no overlap in the radius of heat influence from the slurry of one pile with another. Pile spacing can be determined by setting the heat removed from the slurry equal the heat gained by the permafrost. Crory was the first to discuss the influence of pile spacing in his first 1966 publication which has been reproduced several times (Crory, 1966; Crory, 1967; Heydinger, 1987; Linell and Lobacz, 1980; Sanger, 1969; U.S. Army Air Force, 1988). The required spacing, S, is given below based on Crory's work. **Figure 2.2.4** shows the influence of pile spacing on freezeback time.

$$S = \sqrt{\frac{Q}{C\Delta T} + \pi {r_b}^2} \tag{2.5}$$

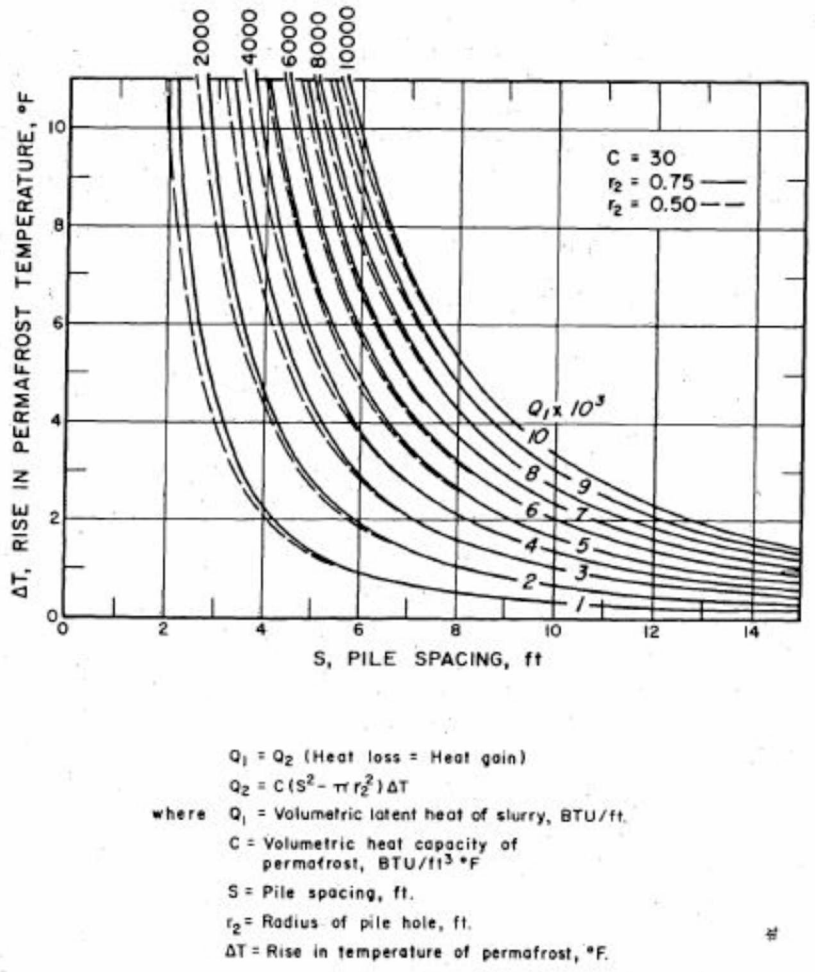

Figure 2.2.4: *The influence of pile spacing on freezeback time (Crory, 1966).*

Crory's work is largely referenced and stimulated much of the later work. Unfortunately, the data from the site in Fairbanks on which his original publication in International Conference on Permafrost was based have not been published and no longer available. According to we correspondence with the US Army Engineer Research and Development Center Library the technical report has never been published and their archives show it as deleted. However, there is a figure reproduced in a report by Sanger (1969) taken from an internal US Army Arctic Construction and Frost Effects Laboratory that shows the distribution of freezeback time for various pile types (**Figure 2.2.5**). Studied factors include the material of the pile, diameter of the hole, pounds of water per length of pile in the slurry, and the amount of latent energy per foot to be removed from the slurry. The original source is no longer available per correspondence with

CRREL. Note that the term "Degrees of Frost" refers to the number of degrees below the freezing point of water.

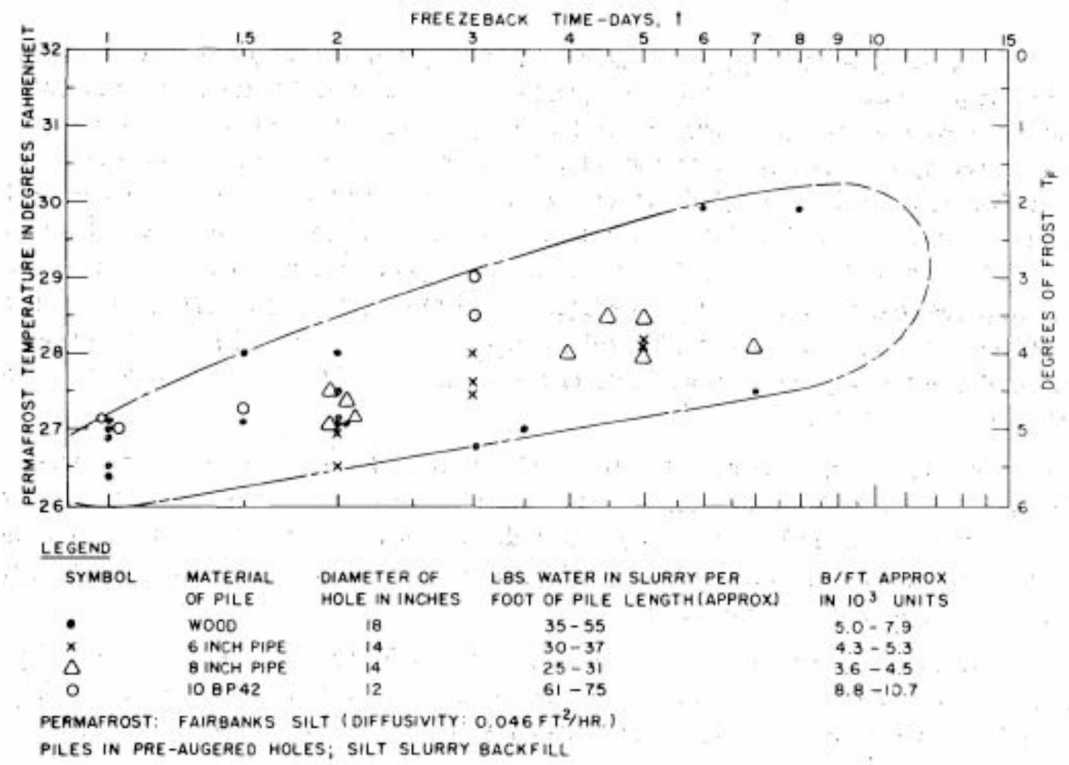

Figure 2.2.5: *Field data from Pile Site C in Fairbanks Alaska (Sanger, 1969).*

From the field data at Pile Site C Crory created an equation to try to fit the data. While it does consider the same parameters as the analytic solution the two are not related. Crory's equation for freezeback, using the same parameters as the analytical solution, is

$$t = \frac{1}{180}\left(\frac{C}{Kr_b}\right)\left(\frac{6Q}{C\pi\Delta T}\right)^{3/2} \tag{2.6}$$

The field results taken at Pile Site C are plotted against the equation in **Figure 2.2.6** for a heat capacity of 30 BTU/(ft^3·°F) and a thermal conductivity of 1.4 BTU/(ft·hr·°F).

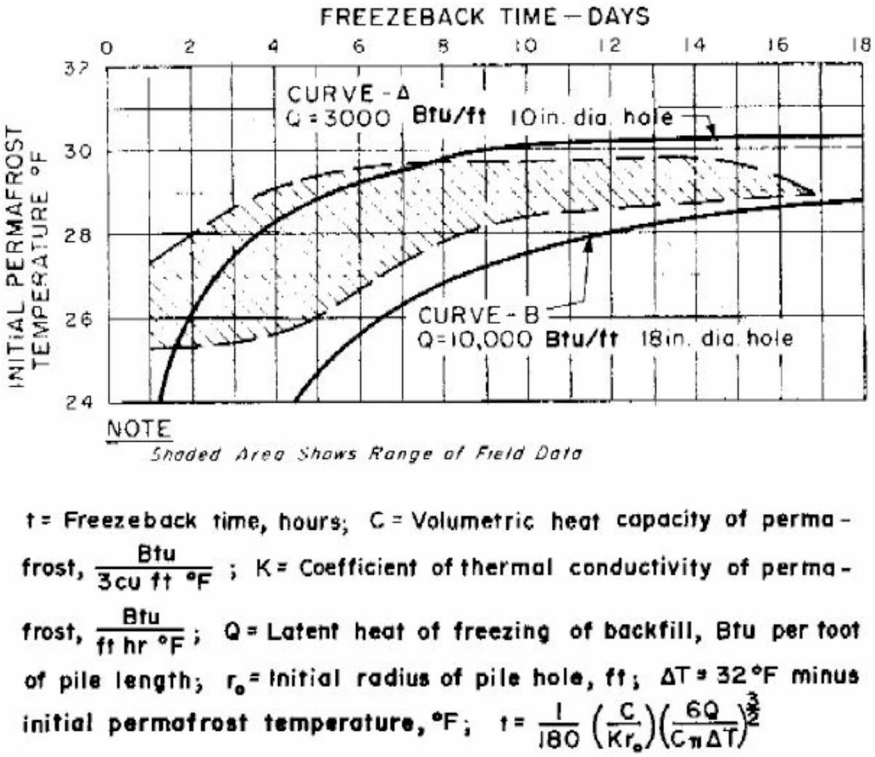

Figure 2.2.6: *A comparison of the field data taken at Pile Site C and the equation developed by Crory. Note that Curve A and Curve B have used C=3030 BTU/(ft^3·°F) and K=1.4 BTU/(ft·hr·°F) (Crory, 1966).*

An interesting and important detail is that in Crory's original publication of the equation the volumetric heat capacity of the permafrost used is actually one third of the actual heat capacity as seen in Figure 2.2.6. That is to say that while the heat capacity used for the specific solutions shown in Figure 2.2.3 is 30 BTU/(ft^3·°F), to calculate the points along the curves C/3 = 10 BTU/(ft·hr·°F) was used. For simplicity, the equation can be rewritten as

$$t = \frac{1}{180}\left(\frac{C}{3Kr_b}\right)\left(\frac{18Q}{C\pi\Delta T}\right)^{3/2} \tag{2.7}$$

2.2.5: *Johnston's Contribution*

A second equation for freezeback appearing in literature is from G.H. Johnston published in his flagship book "Permafrost Engineering Design and Construction" in 1981. Johnston references

Crory and says that the equation that he provides is modified from Crory's work published in the first International Conference on Permafrost. However, he does not say how he determined the equation, why he created one that is different from Crory's, nor does he give any comparison as to which would be more accurate for a given scenario. Johnson's equation is presented below and illustrated in **Figure 2.2.7**.

$$t = \frac{{r_b}^2}{\alpha}\left(\frac{Q}{9.3C{r_b}^2\Delta T}\right)^{4/3} \tag{2.8}$$

$$= \frac{{r_b}^2 C}{K}\left(\frac{Q}{9.3C{r_b}^2\Delta T}\right)^{4/3} \tag{2.9}$$

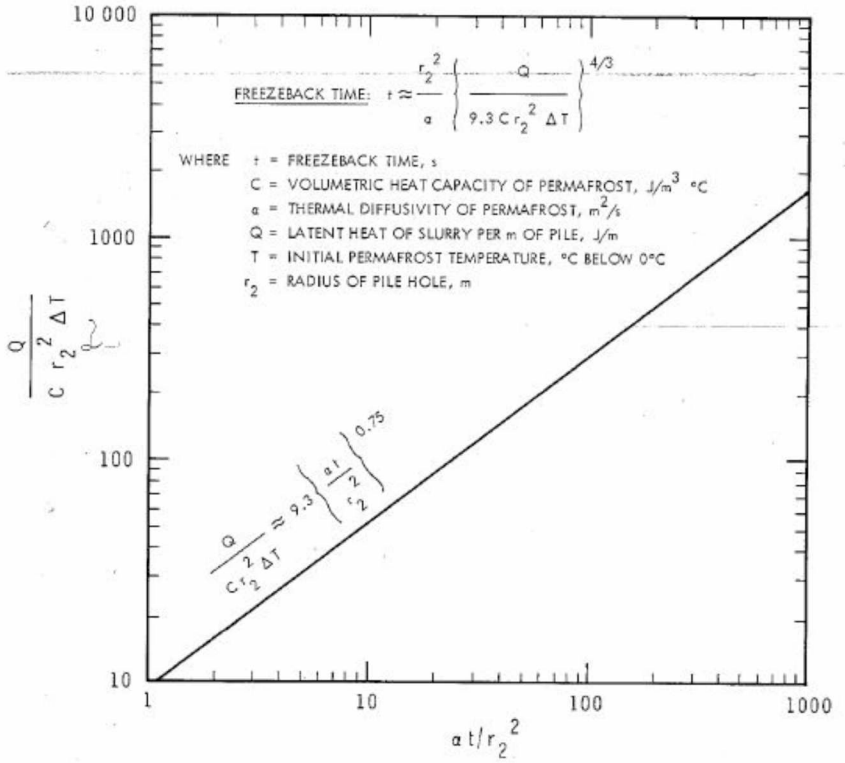

Figure 2.2.7: *Freezeback time according to Johnston's work (Johnston, 1981).*

Crory's and Johnston's freezeback equations show some similarities and differences. It is unclear how the authors arrived at their respective solutions because neither discuss how they developed their equations. The biggest difference is in how some terms are grouped. The radius of the bore hole is paired differently with terms within each equation and the group of terms with an exponent seem to have had that exponent chosen in such a way as to make the units work. An interesting point is the paring of the volumetric heat capacity with the square of the bore radius. Keeping this pair in mind it can be said that the largest difference between the approaches of the two is that, while based on the same data, Crory fit his equation to more closely represent the field data while Johnston chose to fit his according to the analytic solution. This can be seen in the fact that Johnston has two terms that can be directly seen in the analytic solution, those being

$$\frac{{r_b}^2 C}{K} \tag{2.10}$$

and

$$\frac{Q}{C{r_b}^2} \tag{2.11}$$

while Crory does not have any terms grouped as they were in the analytic solution.

Despite the differences in the two equations Johnston's is the one used more frequently today. This is supported by the fact that his equation is what is reproduced in the popular and widely used ASCE publication "Frozen Ground Engineering" by Andersland and Ladanyi (2004). In their text Andersland and Ladanyi show a comparison between Johnston's equation and the analytical solution which is reproduced below in **Figure 2.2.8**.

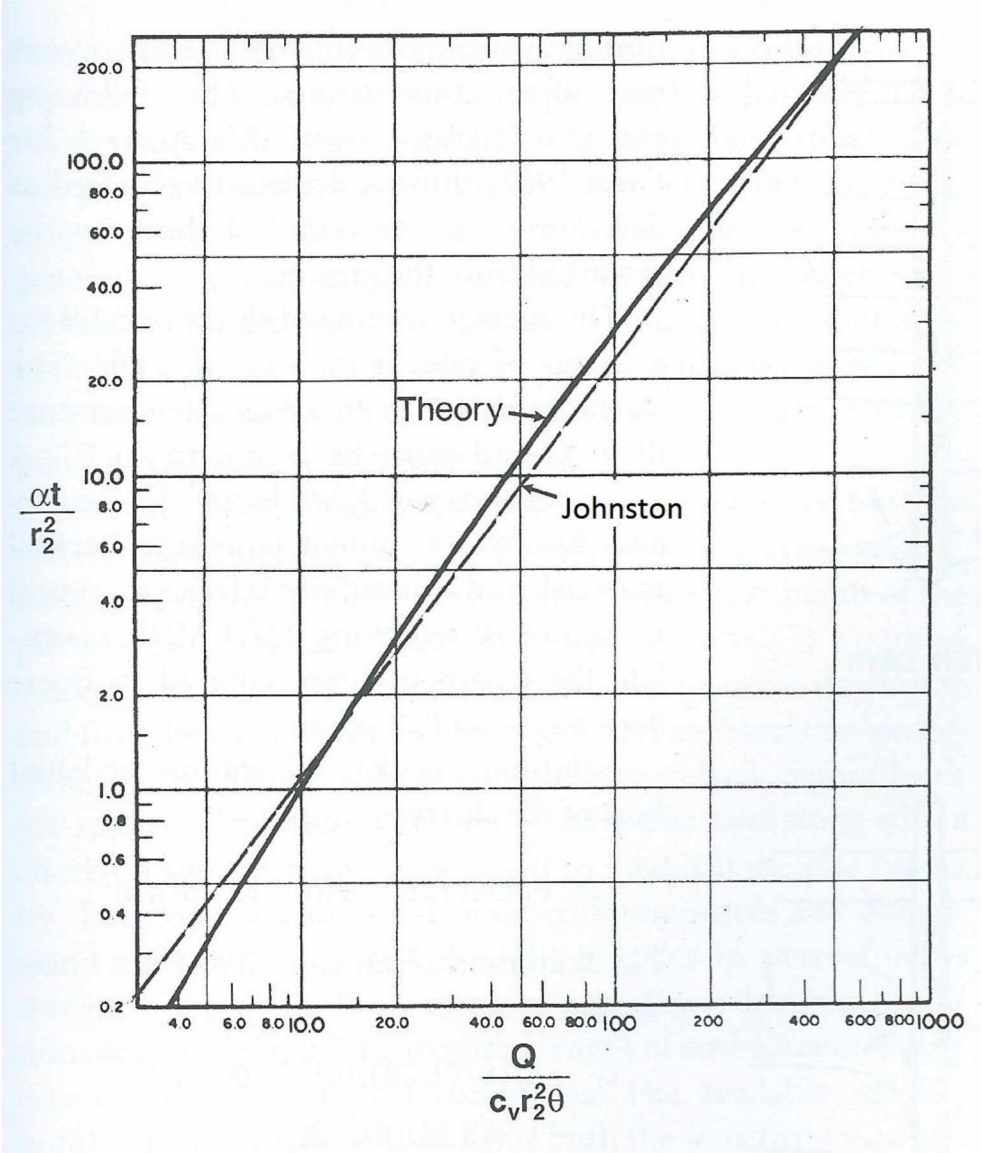

Figure 2.2.8: *Johnston's equation plotted against the analytical solution derived by Carslaw and Jaeger (1959). Modified from Andersland and Ladanyi (2004).*

2.3: *Modeling Permafrost*

Modeling has been used in permafrost for quite some time with Luk'yanov discussing the use of a hydraulic analog to simulate the depth of freeze two years before the first Turing machine (Luk'yanov, 1966). Modeling can be used to handle complicated problems including those with overlapping physics such as heat transfer, phase change, and moisture transport. While often

times only one of these processes is modeled at a time it is becoming more common to see overlapping physics as computational techniques and processing power increase.

2.3.1: *Material Properties*

Permafrost is a mixture of soil, liquid water, air, and ice. These four constituents influence how the permafrost matrix behaves. For a fully saturated soil there is no air present and for a fully thawed condition there is no ice. It is possible to have water present below the bulk freezing temperature if the soil is a fine silt or clay.

If no field data are present then assumptions have to be made about the permafrost properties. While having field data to use as inputs is the ideal scenario oftentimes models are used when field data are not present or too costly to obtain. The three basic things to start with are the soil type, density, and moisture content. From these the pertinent heat transfer characteristics can be determined.

Unfrozen water content plays an important role in modeling permafrost behavior due to the fact that it keeps the soil matrix being made up of four components, three if saturated. It also makes the soil structure less uniform making predicting how the soil will behave difficult. Unfrozen water content is not strongly related to the moisture content but rather the surface area of the soil. Hence, the biggest influence is the type and density of the soil where finer soils like silt and clay have more unfrozen water due to their high surface areas while sands and gravels have practically no unfrozen water (Lunardini, 1981). Anderson and Tice (1972) proposed a power law relationship between the unfrozen moisture content and temperature by

$$W_u = a\theta^b \tag{2.12}$$

where W_u is the unfrozen water content, θ is the number of degrees below 0°C, and a and b are parameters specific to the soil given in their same publication.

Another important heat transfer property is the thermal conductivity. The thermal conductivity is the amount of energy transferred through a unit length of soil, for a single degree in temperature difference, per second. It is a measure of a material's ability to transfer thermal energy. The higher the thermal conductivity the faster the material will conduct heat away from a heat source while the lower the thermal conductivity the better of an insulator it is.

While it is possible to consider the thermal conductivity as an average, geometric or otherwise, of the individual constituents in the permafrost this often requires knowing the specific mass percentages and geometric orientation of the permafrost matrix. This level of information requires extensive field and laboratory work and it may be easier to simply calculate the properties of a few whole samples than to consider each individual component. The most popular method for calculating thermal conductivity is through charts from Kersten (1949). Kersten conducted the earliest extensive studies of thermal conductivity of frozen and unfrozen soils and developed thermal conductivity charts as a function of the soil type, density, and moisture content. It is important to note that a soil will have a different thermal conductivity if it is frozen or thawed due to the difference in properties between liquid water and ice.

The heat capacity of the soil is the last component of concern for heat transfer within the soil. It describes the energy required to change either a unit mass or unit volume a single degree. Andersland and Ladanyi (2004) recommend equations to calculate the specific volumetric heat capacity of frozen and thawed soils reproduced respectively below

$$C_{vf} = \left(\frac{\rho_d}{\rho_w}\right)\left[\left(0.17 + \frac{1.0w_u}{100}\right) + 0.5\left(\frac{w-w_u}{100}\right)\right]c_{vw} \tag{2.13}$$

$$C_{vu} = \left(\frac{\rho_d}{\rho_w}\right)\left(0.17 + 1.0\frac{w}{100}\right)c_{vw} \tag{2.14}$$

Where c_{vf} and c_{vu} are the frozen and thawed volumetric heat capacities, w and w_u are the entire moisture and unfrozen water content, c_{vw} is the volumetric heat capacity of water equaling

(4.187 MJ/m^3), and the constants 0.17, 0.5, and 1.0 are the relative specific heat capacities of mineral soils, ice, and water respectively.

2.3.2: *Property Changes with Phase Change*

Phase change can significantly impact the properties of a soil due to ice and liquid water having significantly different properties. As such a model must be able to transition between frozen and thawed properties as the water within the soil changes phase. This can be done by basing the properties of the soil as being dependent on the proportion of each constituent in the permafrost matrix with the moisture and unfrozen water content being functions of temperature. A simpler way can be to use a transition function over a specified temperature range to change from frozen to thawed properties and vice versa. If this transition range is not present then there is essentially a step function being used to transition the properties.

It is more common to use a linear transition over a small temperature range where it is assumed that all of the water in the soil freezes (Dagher et al., 2014; Gornov et al., 2014; Qin et. al., 2013). This is effectively done using piecewise functions where the property in question is constant outside of the transition range and a linear function within the range. The use of functions like this create non-differentiable points at the ends of the transition range which can create issues for models and programs. Komle and Feng (2009) used the transition from one state to another as reproduced below for thermal conductivity. The use of a function that is differentiable and integrable allows for fewer errors and smoother performance by the model.

$$k(T) = \frac{1}{2}\left(k_f + k_u\right) + \left(k_f - k_u\right)\frac{1}{\pi}\arctan[b_m(T - T_m)] \tag{2.15}$$

Note that T_m is the melting temperature and b_m is a constant describes the sharpness of the transition between frozen and thawed states.

2.3.3: *Apparent Heat Capacity*

The heat capacity of a soil only considers the energy required to change a substance's temperature (sensible energy). It does not take into account the energy required for phase change known as the latent energy. This latent energy is typically substantially larger than the sensible energy with the latent heat of fusion of water, the energy required to change from a solid to a liquid is λ_w=333.4 kJ/kg while the same energy could change the temperature of 1 kg of water 79.6 °C (Ladanyi, 1984). Because the latent energy is only released or absorbed during phase change it can be difficult to predict or model and is highly related to the unfrozen moisture content.

Contemporary models of the phase change at the freezing point use what is known as an apparent heat capacity (Andersland and Ladanyi, 2004; Dagher et. al., 2014; Kömle and Feng, 2009; Noetzli et. al., 2007; Qin et. al., 2013; Sheppard et. al., 1978; Wan and Booshehrian, 2015). Andersland and Ladanyi (2004) describe this as

$$c_a = c_s + c_i(w - w_u) + c_w w_u + \frac{1}{\Delta T}\int_{T_1}^{T_2} \lambda_w \frac{\partial w_u}{\partial T} dT \qquad (2.16)$$

The reason for using the apparent heat capacity is that it allows numerical models to treat heat transfer as a simple heat conduction situation without directly taking into consideration attributes of phase change. Instead the latent heat is added as another term to the heat capacity by limiting the range it's applied over. The end result is that as the water in the soil approaches the freezing point the heat capacity of the soil will increase significantly to account for the latent energy. This will cause the soil to appear to have the same temperature profile as if the latent heat were directly accounted for.

2.3.4: *Boundary Conditions*

There are two types of boundary conditions that are applied in first-order differential. Dirichlet boundary conditions prescribe a value of a potential at a boundary. In a heat transfer model this is analogous to assigning a temperature boundary condition where within the model the Dirichlet boundary will always remain at the prescribed temperature, which may be a function of time. Isothermal boundary conditions are when a Dirichlet boundary is set to be constant, singular temperature over time. Neumann boundary conditions involve setting a constant derivative at a boundary. In heat transfer this equates to a specified heat flux at a boundary. Adiabatic conditions are when the heat flux at a boundary is set to zero.

Typically permafrost models will set adiabatic boundary conditions for lateral boundaries. This is applicable when the model is wide enough such that the influence from anything in the center of the model will not reach the outer lateral boundaries. The more specific boundaries are typically the upper and lower boundaries. A common combination is to use measured air temperature data to impose a Dirichlet boundary condition at the top and a Neumann boundary at the bottom based on a geothermal heat flux. Marchenko et. al. (2008) used this method and their work was expanded on by Darrow et. al. (2013). Using the work of Marchenko et. al., Darrow et. al. used a lower Neumann boundary condition of 0.008 BTU/(hr·ft^2) to be an average value for the geothermal heat flux across Alaska. This varies from Dagher et. al. (2014) who used a lower boundary condition of 0.0565 W/m^2 (0.0179 BTU/(hr·ft^2)) and Noetzli et. al. (2007) who used 0.08W/m^2 (0.0254 BTU/(hr·ft^2)). Gornov et. al. (2014) used an adiabatic lower boundary condition essentially ignoring the geothermal heat flux.

Dirichlet upper boundary conditions are common for permafrost models. Air temperature data is one of the easiest things to measure and is often available online from various sources. Qin et. al. (2013) proposes that using Dirichlet upper boundary conditions is, however, less optimal than Neumann boundary conditions. Using measured air temperature data to create a fitted sinusoidal mean annual soil surface temperature for several years of data they noticed that there is no zero curtain effect, when the temperature of the permafrost appears isothermal as latent energy is being released or absorbed. When they compared this with a Neumann boundary condition

where they calculated the heat flux over the same time period based on surface air convection, solar radiation, and geothermal conduction this issue was no longer present. The Neumann boundary simulations matched the measured field data with a statistical coefficient of determination of R^2=0.97 while the Dirichlet boundary condition simulations matched the data with an R^2=0.89.

2.3.5: *Use of COMSOL to Model Thermal Processes*

COMSOL® is a multi-physics software that can account for multiple types of physics and boundary conditions. It is marketed as a modeling software capable of handling heat transfer, mass transfer, electricity, allowing for users to account for as many different types of physics simultaneously. It allows users to define materials, geometries, meshes, boundary conditions, customized formulas, and more (COMSOL, 2011).

COMSOL has been used previously in several permafrost simulations. Darrow et. al. (2013) used COMSOL to model groundwater flow and heat transfer beneath a road embankment. Wan and Booshehrian (2015) used it to model permafrost degradation, frost heave, and fluid flow at a mining operation. Noetzli et al. (2007) used an imported surface topography to model heat transfer in alpine permafrost. Komle and Feng (2009) combined gas flow and heat transfer to simulate ways to protect road and railway embankments. Dagher et. al. (2014) compared COMSOL's effectiveness in modeling heat transfer under shallow thaw lakes with previous work done that used other finite element method (FEM) software. Each of these studies has shown that COMSOL efficiently and accurately models the various types of physics observed in permafrost regions.

Section 3: Model Description

3.01 *Initialization and Inputs*

The model was initiated using the model wizard. The *Space Dimension* is 2D Axisymmetric, the *Physics* selected is Heat Transfer in Solids, and it is a time dependent study. 2D axisymmetric means that COMSOL treats a 3D volume with radial symmetry as a 2D object. Similarly for this work, a cylindrical shape is represented in a 2D axisymmetric manner by rotating a user defined rectangle about the longitudinal center of the cylinder 360°.

In the initial stages of planning how to compare COMSOL modeling results with Crory's results it was the intention to use British Gravitational Units (BGU) with BTU, feet, and degrees Fahrenheit. However, COMSOL did not have an option for selecting the appropriate units needed within the model so it was decided to use metric units. Because of this many of the basic parameters appear arbitrary with around 4 significant figures however they have typically been converted from round values in BGU. **Table 3.01.1** shows a list of the geometry and boundary condition parameters while **Table 3.01.2** shows the various properties of the slurry and the permafrost in BGU and metric units. The determination for each parameter is described the following sections.

Table 3.01.1: *Geometry and boundary condition parameters used in the model presented in SI and BGU. Note that calculated parameters only show the resulting value. Determination of the parameters, including equations, are listed in the following sections.*

Parameter	SI Units	British Gravitational Units	Description
h_p	6 [m]	19.7 [ft]	Depth of pile
h_s	18 [m]	59.1 [ft]	Depth of sample
r_b	0.2286 [m]	0.750 [ft]	Radius of bore hole
r_p	0.0814 [m]	0.267 [ft]	Radius of pile
r_s	2.286 [m]	7.50 [ft]	Radius of sample area ($r_s = 10 \cdot r_b$)
T_{PT}	-5 [°C]	23.0 [°F]	Temperature at Permafrost Table
T_{bot}	2 [°C]	35.6 [°F]	Temperature at Bottom of Model
T_s	3 [°C]	37.4 [°F]	Initial Slurry Temperature

Table 3.01.2: *Properties of the slurry and permafrost used in the model. Note that calculated parameters only show the resulting value. Determination of the parameters, including equations, are listed in the following sections.*

Parameter	SI Units	British Gravitational Units	Description
γ_{PF}	1922 [kg/m^3]	120.0 [lb/ft^3]	Density of Permafrost
γ_{sand}	1922 [kg/m^3]	120.0 [lb/ft^3]	Density of Sand
γ_{water}	1000 [kg/m^3]	62.4 [lb/ft^3]	Density of Water
w_s	0.15 []	0.15 []	Moisture Content of Slurry
W_{pf}	0.13 []	0.13 []	Moisture Content of Permafrost
$C_{p,w}$	4.179 kJ/(kg·k)	0.9982 BTU/(lb·°F)	Heat Capacity of Water
$C_{v,pf,f}$	1891 [kJ/(m^3·K)]	28.2 [BTU/(ft^3·°F)]	Heat Capacity of Frozen Permafrost
$C_{v,pf,t}$	2414 [kJ/(m^3·K)]	36.0 [BTU/(ft^3·°F)]	Heat Capacity of Thawed Permafrost
$C_{v,s,f}$	1972 [kJ/(m^3·K)]	29.4 [BTU/(ft^3·°F)]	Heat Capacity of Frozen Slurry
$C_{v,s,t}$	2575 [kJ/(m^3·K)]	38.4 [BTU/(ft^3·°F)]	Heat Capacity of Thawed Slurry
$k_{p,f}$	2.08 [W/(m·k)]	1.20 [BTU/(ft·hr·°F)]	Thermal Conductivity of Frozen Permafrost
$k_{p,t}$	1.92 [W/(m·k)]	1.11 [BTU/(ft·hr·°F)]	Thermal Conductivity of Thawed Permafrost
$k_{s,f}$	2.25 [W/(m·k)]	1.30 [BTU/(ft·hr·°F)]	Thermal Conductivity of Frozen Slurry
$k_{s,t}$	1.92 [W/(m·k)]	1.11 [BTU/(ft·hr·°F)]	Thermal Conductivity of Thawed Slurry
λ_w	333.4 [kJ/kg]	143.4 [BTU/lbm]	Latent Heat of Fusion of Water

3.01.1 *Density, Moisture Content, and Thermal Conductivity*

The first parameters defined were the density, moisture content, and thermal conductivity of the soil. Both the slurry and the permafrost were chosen to be saturated soils with a dry density of 120 lb/ft^3 while the slurry was a granular sand and the permafrost was silty-clay. From these two components the thermal conductivities were determined using charts redrawn from Kersten (1949) and the Department of the Air Force (1966) provided by Pavement Interactive. **Figures**

3.01.1 and **3.01.2** show this below for the permafrost and slurry respectively. From these charts moisture contents were chosen to be

$$w_{pf} = 0.13$$
$$w_s = 0.15$$

and the frozen and thawed thermal conductivities, converted to W/(m·K), are

$$k_{pf,f} = 2.08$$
$$k_{pf,t} = 1.92$$
$$k_{s,f} = 2.25$$
$$k_{s,t} = 1.92$$

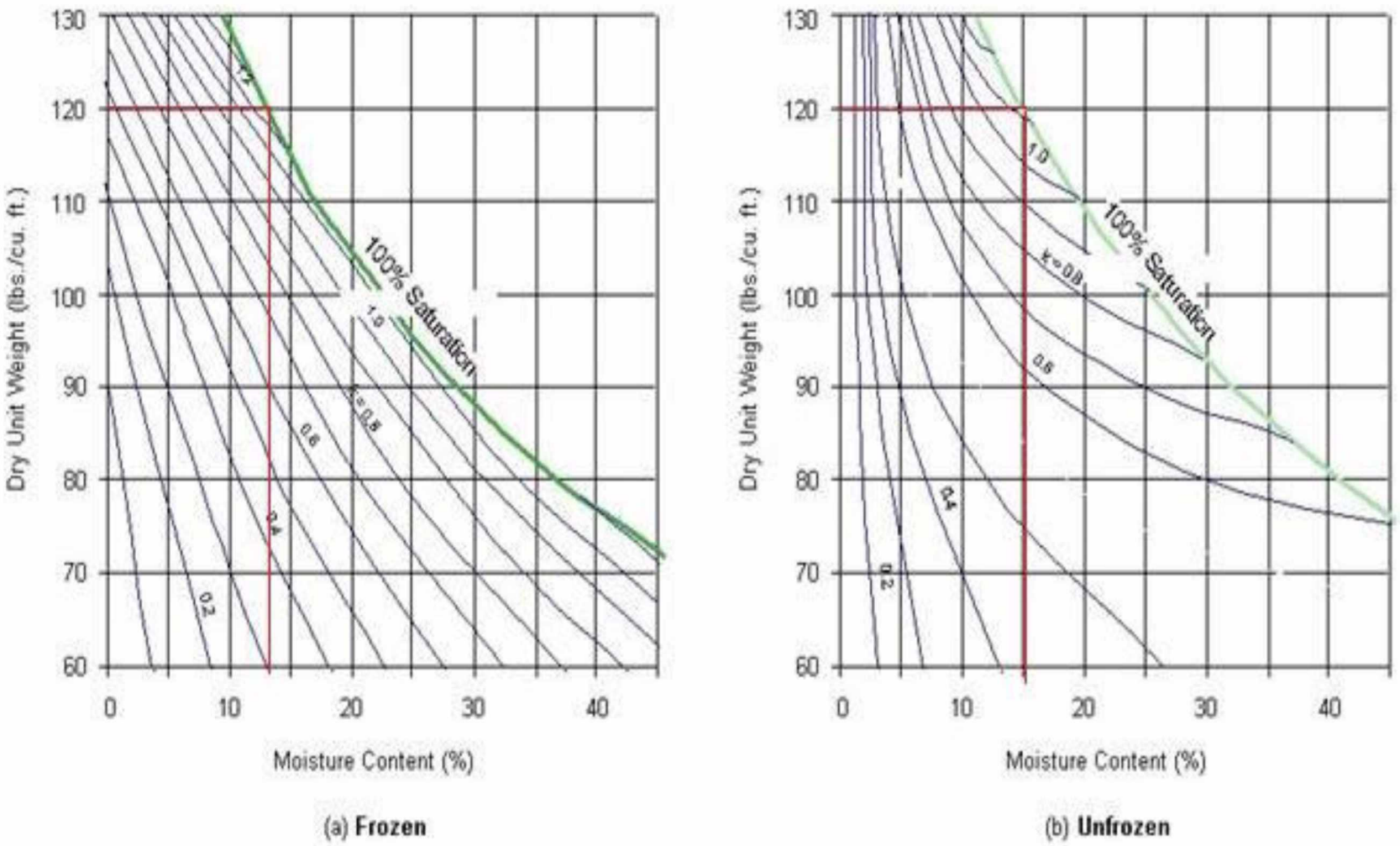

Figure 3.01.1: *Redrawn Kersten charts for the permafrost, a silty-clay, used to find the frozen and thawed thermal conductivities (Pavement Interactive, 2012).*

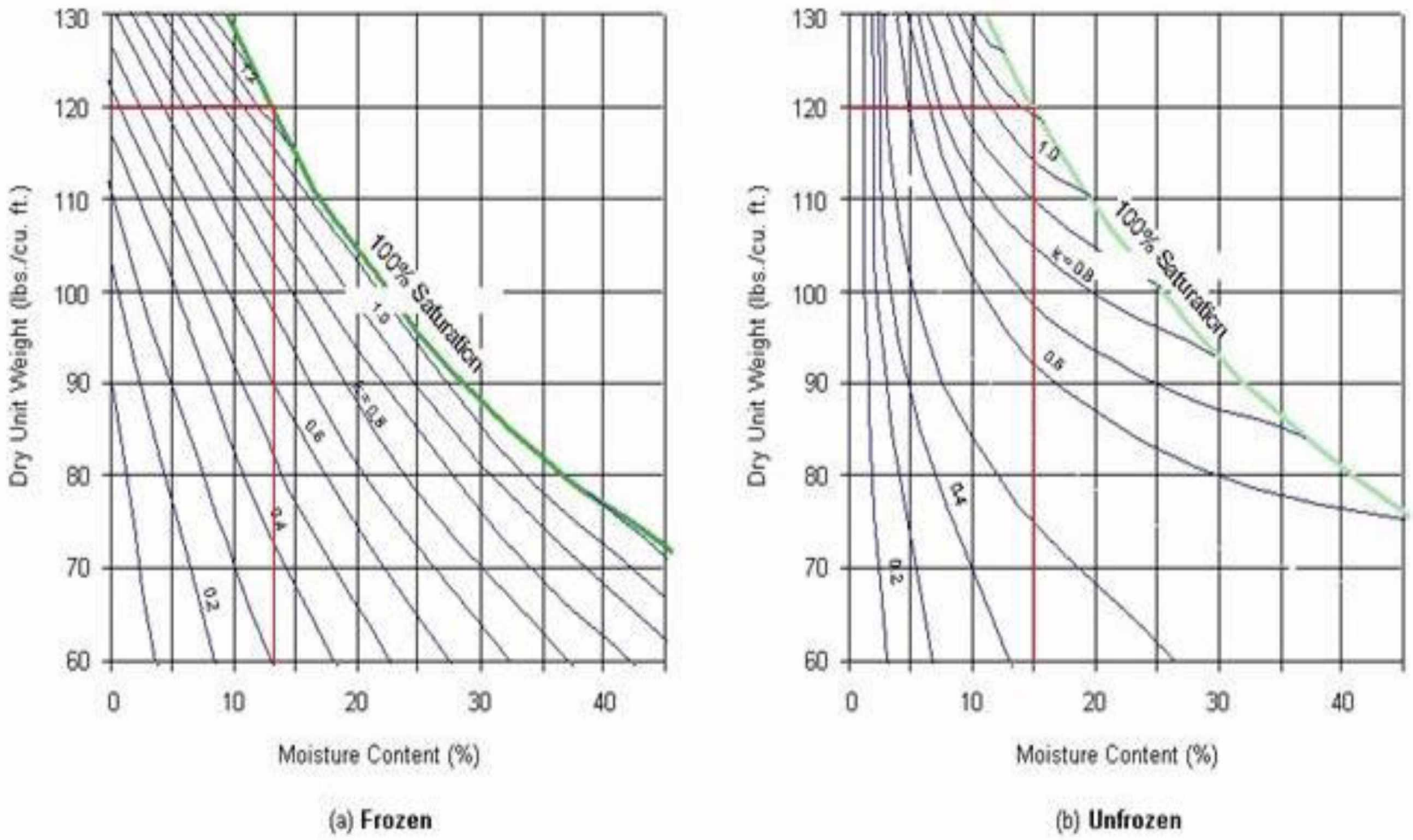

Figure 3.01.2: *Redrawn Kersten charts for the sand-slurry used to find the frozen and thawed thermal conductivities (Pavement Interactive, 2012).*

3.01.2 *Heat Capacity*

Volumetric heat capacity is the material property that determines the rate of sensible heat transfer. It describes the energy required to change the temperature of a unit volume of material a single degree. This does not take into account latent heat which is associated with phase change. Volumetric heat capacities were determined using methods described in Andersland and Ladanyi (2004) where the thawed and frozen heat capacities are defined as

$$C_{v,t} = \rho_d \cdot \left(0.17 + \frac{w}{100}\right) \cdot c_{p,w} \tag{3.1}$$

$$C_{v,f} = \rho_d \cdot \left(0.17 + 0.5 * \frac{w}{100}\right) \cdot c_{p,w} \tag{3.2}$$

where $c_{v,w}$ is the volumetric heat capacity of water, 4.187 kJ/kg, and moisture content w is a percentage. From this the thawed and frozen volumetric heat capacities for the permafrost and slurry are

$$C_{v,pft} = 2.414\ {}^{MJ}/_{m^3 \cdot K}$$

$$C_{v,pff} = 1.891\ {}^{MJ}/_{m^3 \cdot K}$$

$$C_{v,st} = 2.575\ {}^{MJ}/_{m^3 \cdot K}$$

$$C_{v,sf} = 1.972\ {}^{MJ}/_{m^3 \cdot K}$$

3.01.3 *Pile, Bore and Sample Area Dimensions*

The bore radius was chosen to be 0.75 ft (0.2286 m) which corresponds to the value used by Crory in 1966. From that dimension, the pile radius was chosen in such a manner as to allow for 4000 BTU/ft of latent energy required per pile length in the slurry per Crory's equation

$$Q = \pi \cdot L \cdot \left({r_d}^2 - {r_p}^2\right) \cdot w_s \cdot \gamma_{d,s} \tag{3.3}$$

where L is the latent heat of vaporization for water, 333.4 kJ/kg. When solved for the pile radius and taking the positive root it is shown that

$$r_p = \sqrt{{r_d}^2 - \frac{Q}{\pi \cdot L \cdot w_s \cdot \gamma_{d,s}}} \tag{3.4}$$

This methodology was used to define the standard pile radius. When the pile radius sweep was performed this method was not followed. For the parameters listed the standard pile radius is

$$r_p = 0.0814\, m$$

The pile and bore depths were considered equal and that the pile was not resting on anything at the bottom of the bore hole. An arbitrarily long pile length of 6 m was chosen as an adequate representation of modern practices as well as being sufficiently long enough to allow for special freezeback effects experienced at the top and bottom of the sample to not influence the overall freezeback time significantly.

The sample area was chosen to be wide enough such that any influence from the slurry being poured into the permafrost would be negligible at the outermost boundaries. This was accomplished by setting the sample radius and depths to be ten times as wide as the bore radius and three times as long as the pile length as represented by

$$r_s = 10 \cdot r_b \tag{3.5}$$

$$h_s = 3 \cdot h_p \tag{3.6}$$

3.01.4 *Gaussian Pulse and Sigmoid Function*

The largest consideration when considering a heat transfer problem in permafrost is the latent energy associated with phase change. Latent energy is the energy required to change the physical state of a material between phases. The amount of energy is different depending on whether the change is between a solid and a liquid, a solid and a gas, or a liquid and a gas. This is different from sensible heat which is the heat required to change the temperature of a substance. The latent heat of fusion required for water to change phase between a liquid and a solid is substantially larger than the heat required to change the temperature of liquid water or

ice. Sensible heat losses are frequently ignored in many models and only the latent energy required is considered. The latent heat of fusion for water is listed in Table 3.01.2.

Latent heat is difficult to simulate in many numerical models because they focus solely on the sensible heat component described by the standard heat conduction equation shown below in equation 3.7. Note that F if the energy per length of pile required to change the temperature, ΔT, with thermal conductivity k between the inner and outer radius, r_1 and r_2 respectively. This is true in COMSOL where phase change energy is not considered in its heat conduction physics. However, it is possible to include the latent heat in models by using what is known as an apparent heat capacity. The apparent heat capacity essentially uses a step or pulse type of function to distribute the latent energy over a small temperature range. This energy is then added to the volumetric heat capacity so that when the model approaches the freezing point the volumetric heat capacity drastically increases causing the rate of temperature change to slow down. While there are different methods that have been implemented to create the apparent heat capacity, the method used in this research involves the Gaussian Pulse.

$$F = \frac{2\pi k \Delta T}{ln\left(r_2/r_1\right)} \tag{3.7}$$

The Gaussian Pulse function, described below, is a bell shaped curve with the property that the integral from (-∞,∞) is one. Its shape and position are controlled by two variables a and σ being the phase shift and the standard deviation, respectively. The phase shift determines where the pulse is centered at while the standard deviation determines the width of the curve.

$$pulse(x) = \frac{1}{\sigma\sqrt{2\pi}} \cdot e^{\frac{(x-a)^2}{2\cdot\sigma^2}} \tag{3.8}$$

$$\int_{-\infty}^{\infty} pulse(x) = 1 \tag{3.9}$$

For the model, the pulse was a function of temperature and related to the phase change temperature. The soils in the model are non-saline therefore the phase change temperature is

0°C. However, due to the symmetry of the pulse if it were centered right at 0°C there would be some material that froze at temperatures slightly above the freezing point. Therefore the pulse was shifted such that slightly more than 99% of the pulse, and thus latent energy, occurs below the freezing point, resulting in a phase shift of

$$a = -3\,\sigma \tag{3.10}$$

The standard deviation requires more consideration in order to make the model representative of real world scenarios. If the standard deviation, and thus the width, of the pulse is too small in an attempt to make the latent heat be applied as closely to the freezing point as possible, then the numerical model may skip the temperature range entirely during its time-stepping computation. However, if the temperature range is too large then the model is no longer representative of the real world. After some basic test runs to see how the freezeback time was affected a standard deviation of 0.1°C was chosen thus

$$\sigma = 0.1°C$$

This can be combined with statistics to describe the 95 and 99% confidence intervals which are described as the ranges where 95 and 99% of the values, in this case the area and consequently the latent heat, lies. They are defined as 2.0 and 2.6 standard deviations away from the mean. Because the pulse is an even function centered at 0°C the ranges are

$$CI(95\%) = (-0.5°C, -0.1°C)$$

$$CI(99\%) = (-0.56°C, -0.04°C)$$

Figure 3.04.1 shows the resulting Gaussian Pulse. One of the drawbacks of using the pulse is that the freezing taking place below the known freezing point is not related to the unfrozen moisture content present in the soil. For the purposes of this model, however, the pulse almost exclusively applies to the slurry which is comprised of sand which has a very small amount of unfrozen water content that dissipates quickly due to its large pore sizes.

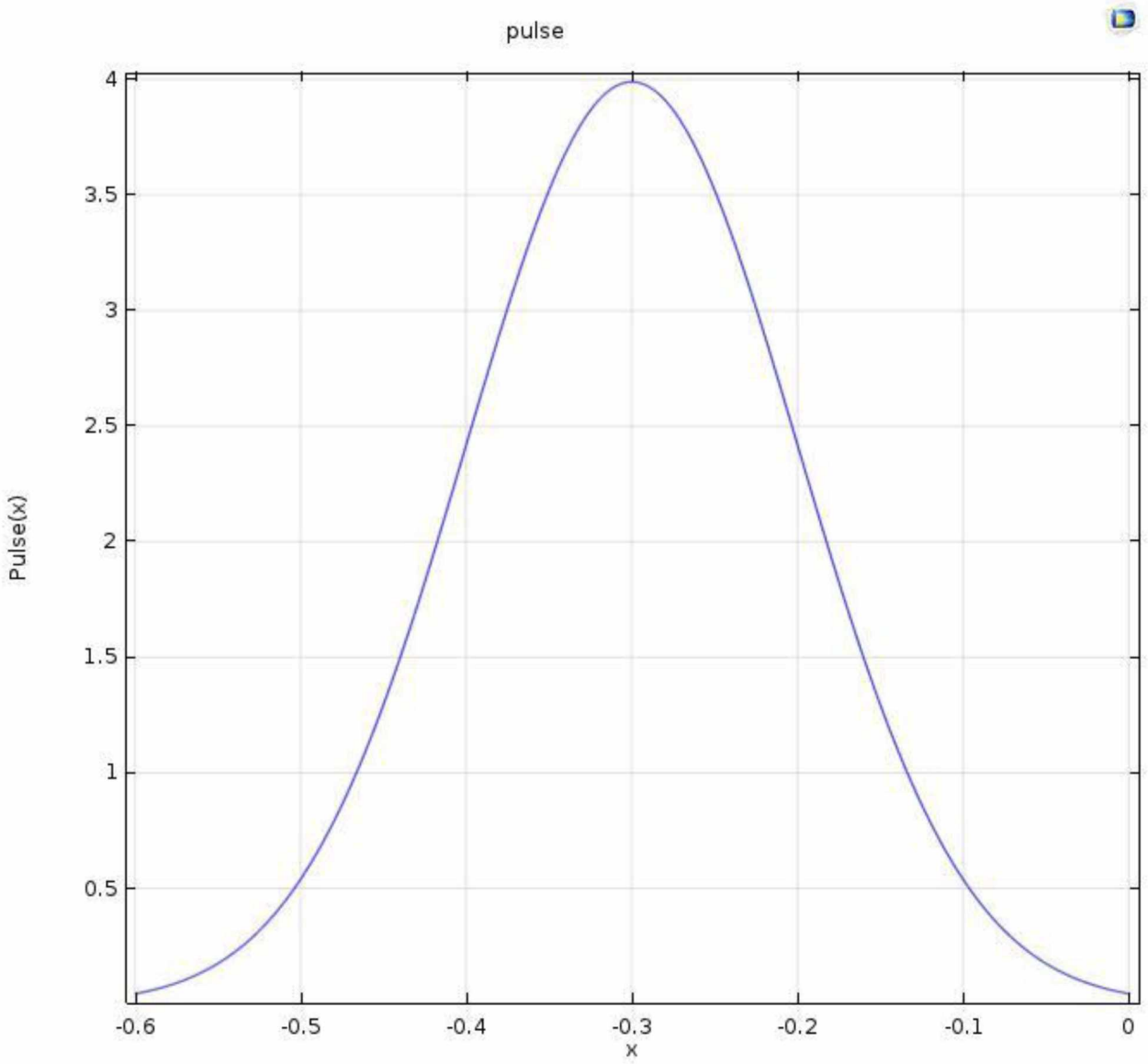

Figure 3.01.3: *The Gaussian Pulse used to distribute the latent heat over a small temperature range.*

Another challenge when using COMSOL is the transition from frozen to thawed permafrost. It is well established that permafrost and frozen soils behave significantly differently depending on whether or not they are thawed or frozen. In order to incorporate the change between frozen and thawed properties a transition function is required. Many models simply use a piecewise function with a linear transition between the two states while others use more complicated

methods such as incorporating the arctangent function. Piecewise functions are not ideal because they are not differentiable at the transition points which can cause numerical instabilities near those points. This model uses the Sigmoid function.

The Sigmoid function is defined as

$$sig(x) = \frac{1}{1 + e^{-a\cdot(x+3\sigma)}} \tag{3.11}$$

The function has asymptotes at zero and 1 as x approaches $-\infty$ and ∞ respectively. That is to say

$$\lim_{x\to-\infty} sig(x) = 0$$

$$\lim_{x\to\infty} sig(x) = 1$$

The variable a controls the steepness of the transition between zero and one. It was chosen in such a way as to align with the Gaussian Pulse so that after all of the pulse was consumed the properties will have fully transitioned from thawed to frozen values. In this case the Sigmoid transitions material properties between the temperature extremes of (-0.6°C, 0°C). That is to say that a was chosen such that for

$$dsig(x)/_{dx} = sig(x)\cdot(1 - sig(x)) \tag{3.12}$$

the slope of the sigmoid function at the end of the desired range is near zero. For calculation purposes this was chosen to be 0.0001 represented by

$$dsig(0)/_{dx} = sig(0)\cdot\big(1 - sig(0)\big) = 0.01$$

This yields

$$a = 15.28\,°C^{-1}$$

The results of this are plotted in **Figure 3.04.2**. An interesting note is that

$$sig(0) = 0.5$$

Thus after half of the latent heat has been consumed with the Gaussian Pulse, the Sigmoid function averages the values between the frozen and thawed state.

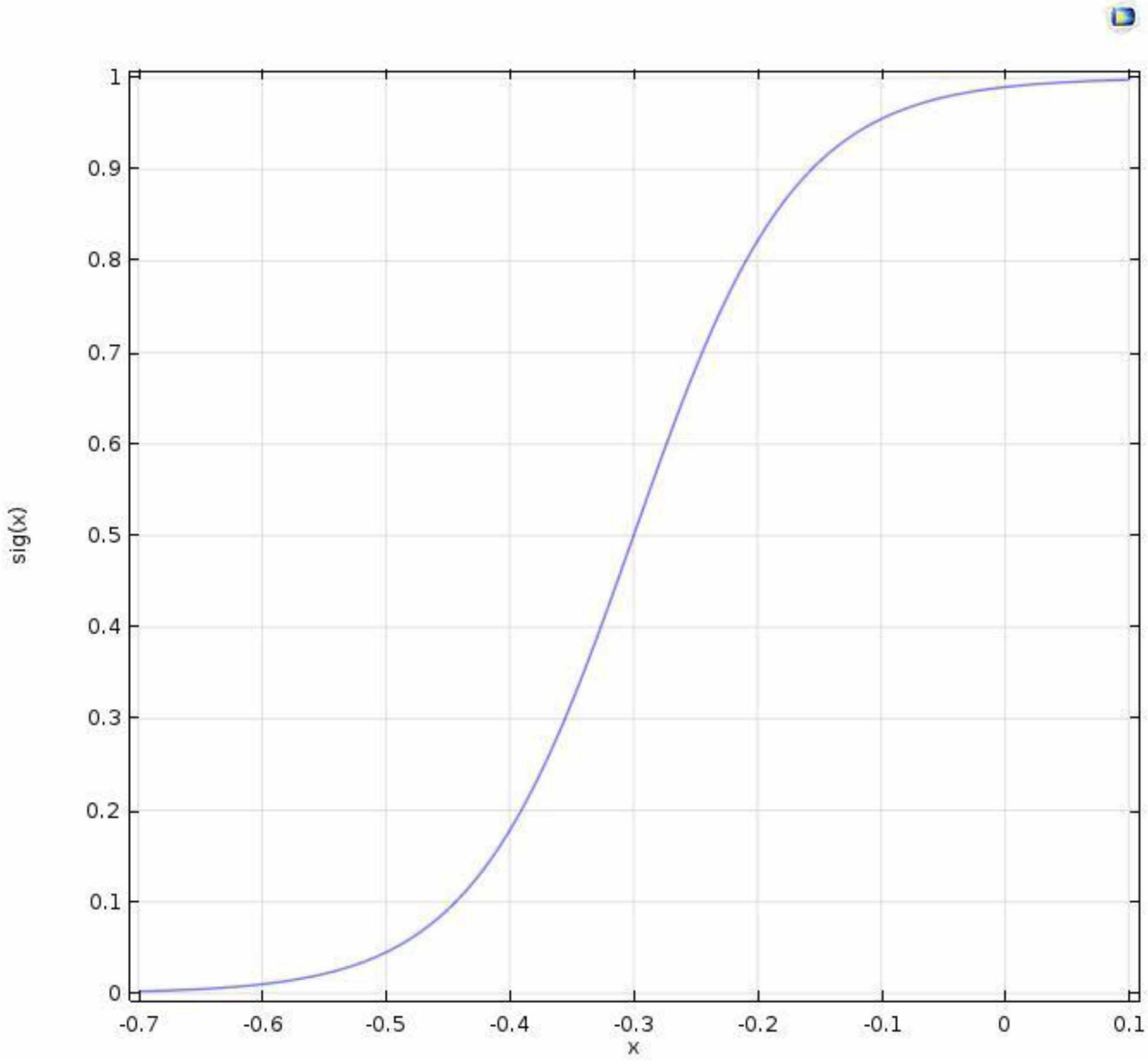

Figure 3.01.4: *The Sigmoid function fitted to coincide with the prescribed Gaussian Pulse.*

Both the Gaussian Pulse and the Sigmoid function were combined with the volumetric heat capacity, while only the sigmoid function was used with the thermal conductivity, of the slurry and permafrost. These are represented by

$$C_{v,pf} = C_{v,pff} + sig(T) \cdot \left(C_{v,pft} - C_{v,pff}\right) + w_{pf} \cdot \gamma_w \cdot (C_{p,w} + pulse(T) \cdot \lambda_w) \tag{3.13}$$

$$C_{v,s} = C_{v,sf} + sig(T) \cdot \left(C_{v,st} - C_{v,sf}\right) + w_{sf} \cdot \gamma_w \cdot (C_{p,w} + pulse(T) \cdot \lambda_w) \quad (3.14)$$

$$k_{pf} = k_{pff} + sig(T) \cdot \left(k_{pft} - k_{pff}\right) \quad (3.15)$$

$$k_s = k_{sf} + sig(T) \cdot (k_{st} - k_{sf}) \quad (3.16)$$

While in the model only the slurry goes through any significant freezeback, the pulse was applied to the permafrost as well to account for any minute, temporary phase change that might happen when the slurry is heating up the permafrost before freezing.

3.02 *Model Geometry*

The axisymmetric model is based on a circular pile being placed into an over-drilled hole and backfilled with a sand-water slurry. This means that all results are symmetric when rotated about the z axis so it is only necessary to view a 2D cut of the pile installation going out from the z axis radially and so a cylindrical geometry can be represented by rectangles on the COMSOL screen. When creating the geometries the order they are listed in COMSOL matters as certain geometries are built from previously defined shapes.

The geometry begins by creating a rectangle that will represent part of the permafrost area having a *(width, height)* of $(r_s\text{-}r_b,\ h_s\text{-}h_p)$ located at an *(r,z)* of $(r_b,0)$ with r_s, h_s, r_b, and h_p being defined in section 3.01 as the sample radius, sample height, bore radius, and pile length respectively. The next geometry is the permafrost located below the slurry defined spatially as $(r_b\text{-}r_p, hs\text{-}hp)$ with a base at $(r_p,0)$. The next step is creating the permafrost below the pile defined as $(r_p,\ h_s\text{-}h_p)$ located at $(0,0)$. The last section of the permafrost is defined as $(r_s\text{-}r_b,\ h_p)$ with a base at $(r_b, h_s\text{-}h_p)$. The final component is the slurry which is added by creating another rectangle with dimensions $(r_b\text{-}r_p, h_p)$ and a base at $(r_p, h_s\text{-}h_p)$. The last step is to use *Form Union* to finalize the geometries within COMSOL. In this model there is no difference between *Form Union* and *Form Assembly* however typically *Form Assembly* is not used. Note that with this geometry the

pile and corresponding space within the circular, hollow pile are not specifically introduced. By assuming that heat flow out of the pile is negligible the pile-slurry boundary is assumed to be adiabatic. **Figures 3.02.1** and **3.02.2** show the geometry as a whole and up close at the slurry respectively.

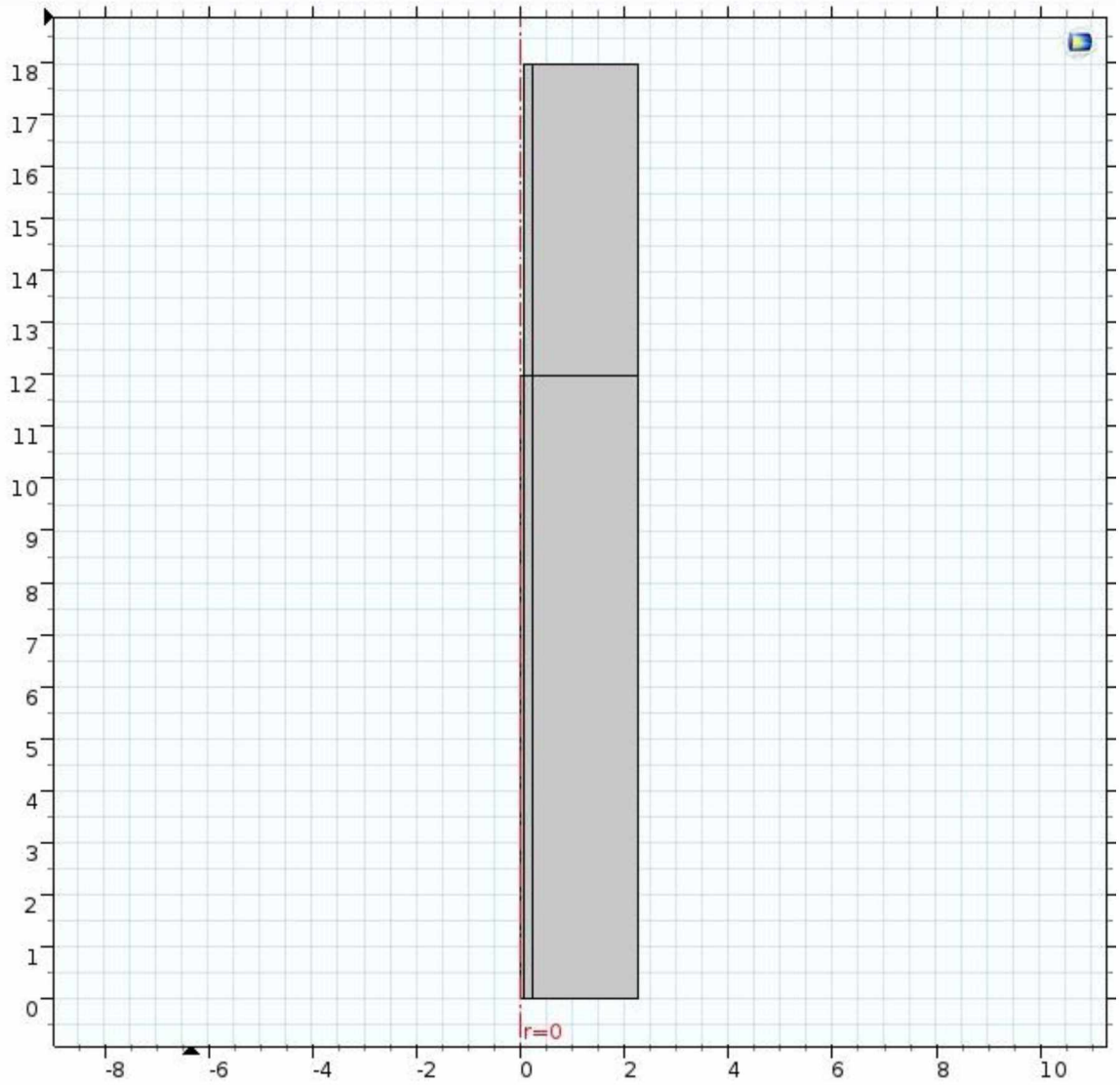

Figure 3.02.1: *Model geometry in its entirety. The vertical axis is the elevation with the top of the geometry representing the bottom of the active layer. The r-axis is the radius measuring out from the center of the pile.*

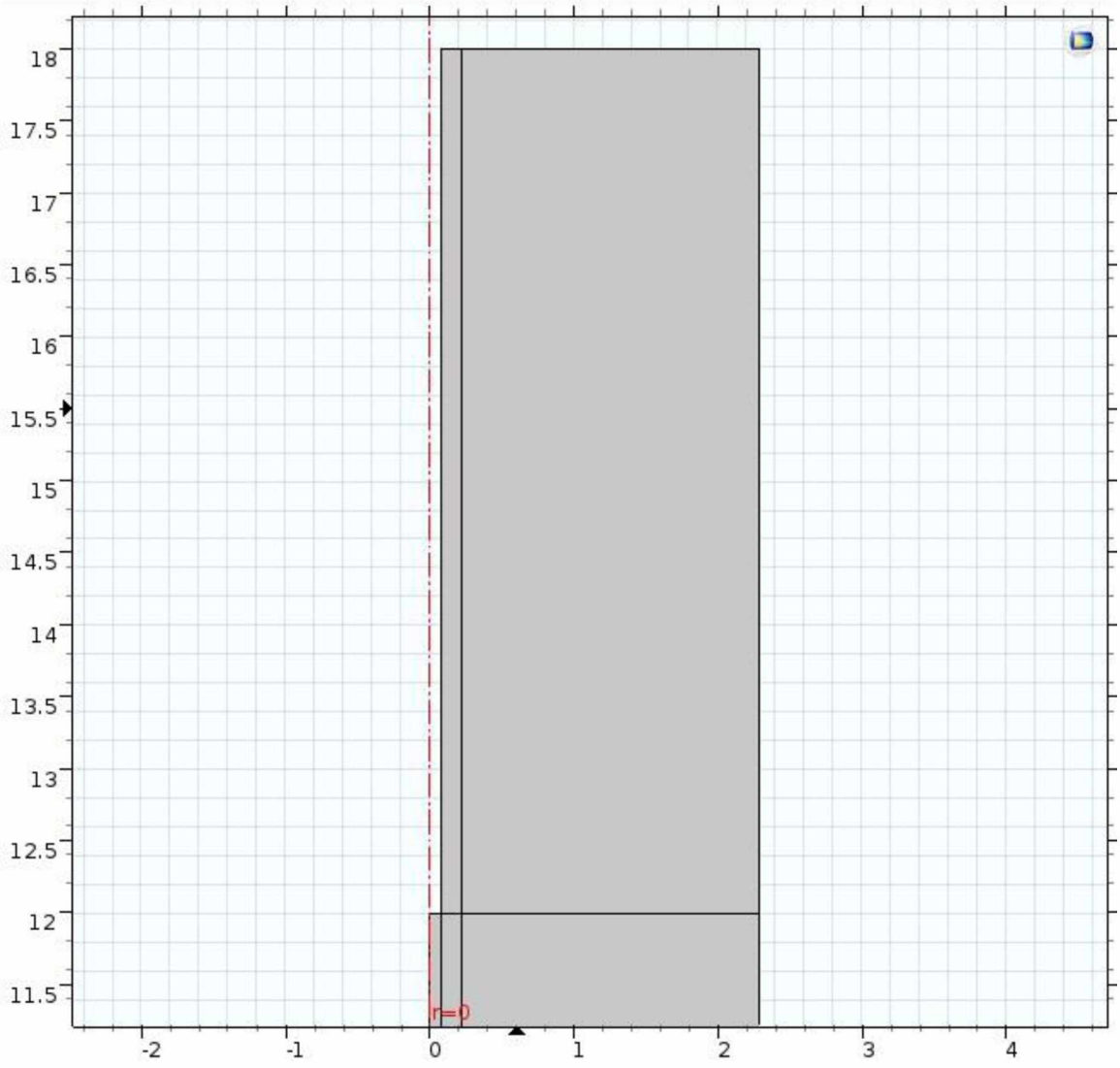

Figure 3.02.2: *Model geometry up close. The small rectangle on the left represents the slurry. The encompassing geometry is the permafrost. The gap between the center of the geometry, r=0, and the left slurry boundary represents the center to the outside of the pile which is not modeled.*

3.03 *Mesh*

The mesh for the model was kept as a simple *Mapped Mesh* for both the slurry and the permafrost. The mapped mesh creates a relatively uniform rectangular grid that matches rectangular geometries that the slurry and permafrost are based on. The use of a different type of mesh, such as free triangular, would not efficiently handle the corners, edges, and shapes associated with rectangular geometries. Also, there was a negligible difference in computation time or file size for creating a less dense mesh in the permafrost therefore it was decided to keep the permafrost mesh at the more rigid level required for the slurry. The mesh was set to have a maximum element Size of 0.07m which for a standard simulation consisted of 8,858 domain elements and 1,049 boundary elements.

Figure 3.03.1 shows the mesh system for the entire system while **Figure 3.03.2** shows the mesh for the slurry. The blue highlighted boxes are the slurry.

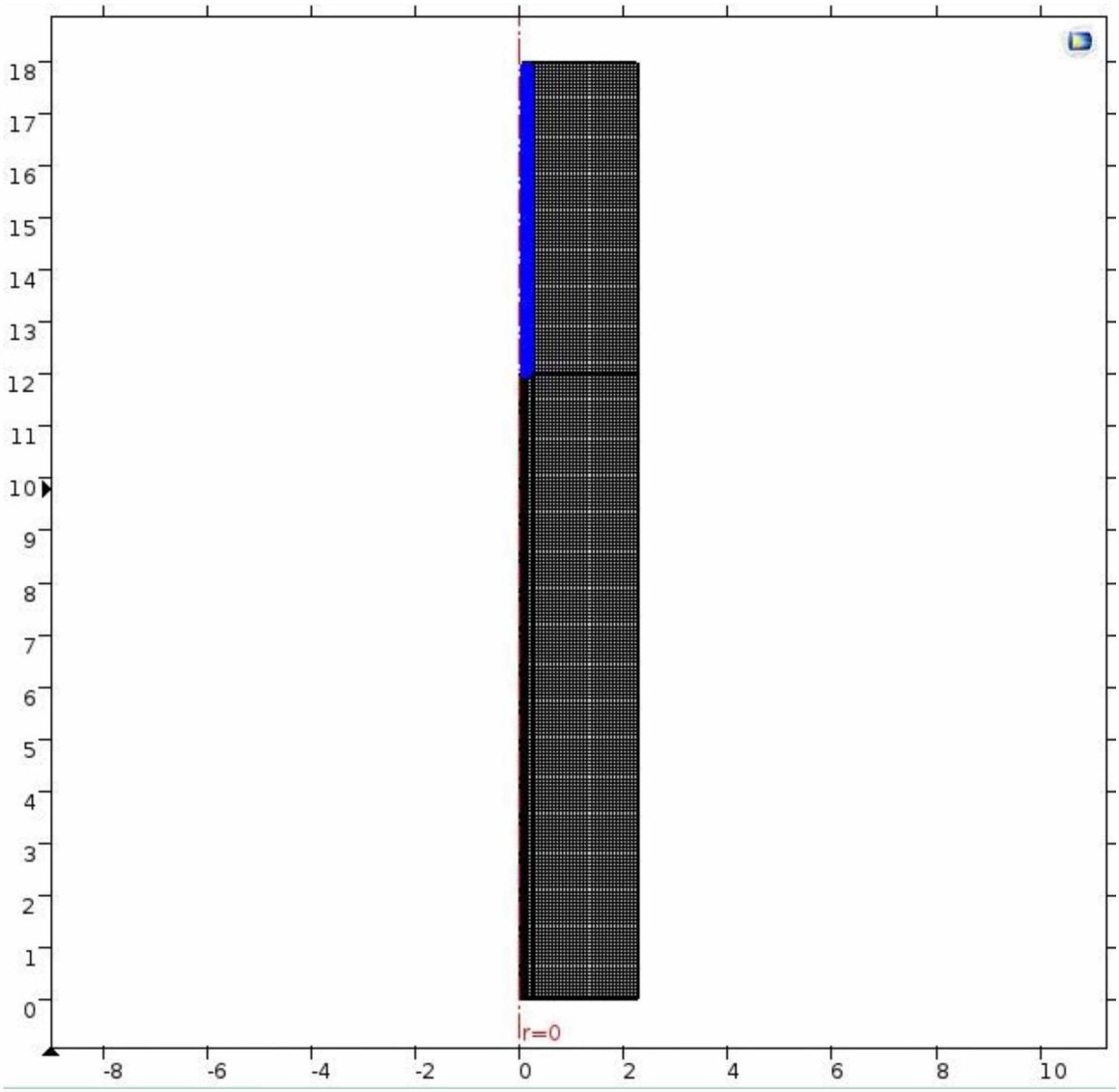

Figure 3.03.1: *Mesh of the entire geometry with the y- and x-axis displaying the z and r components respectively.*

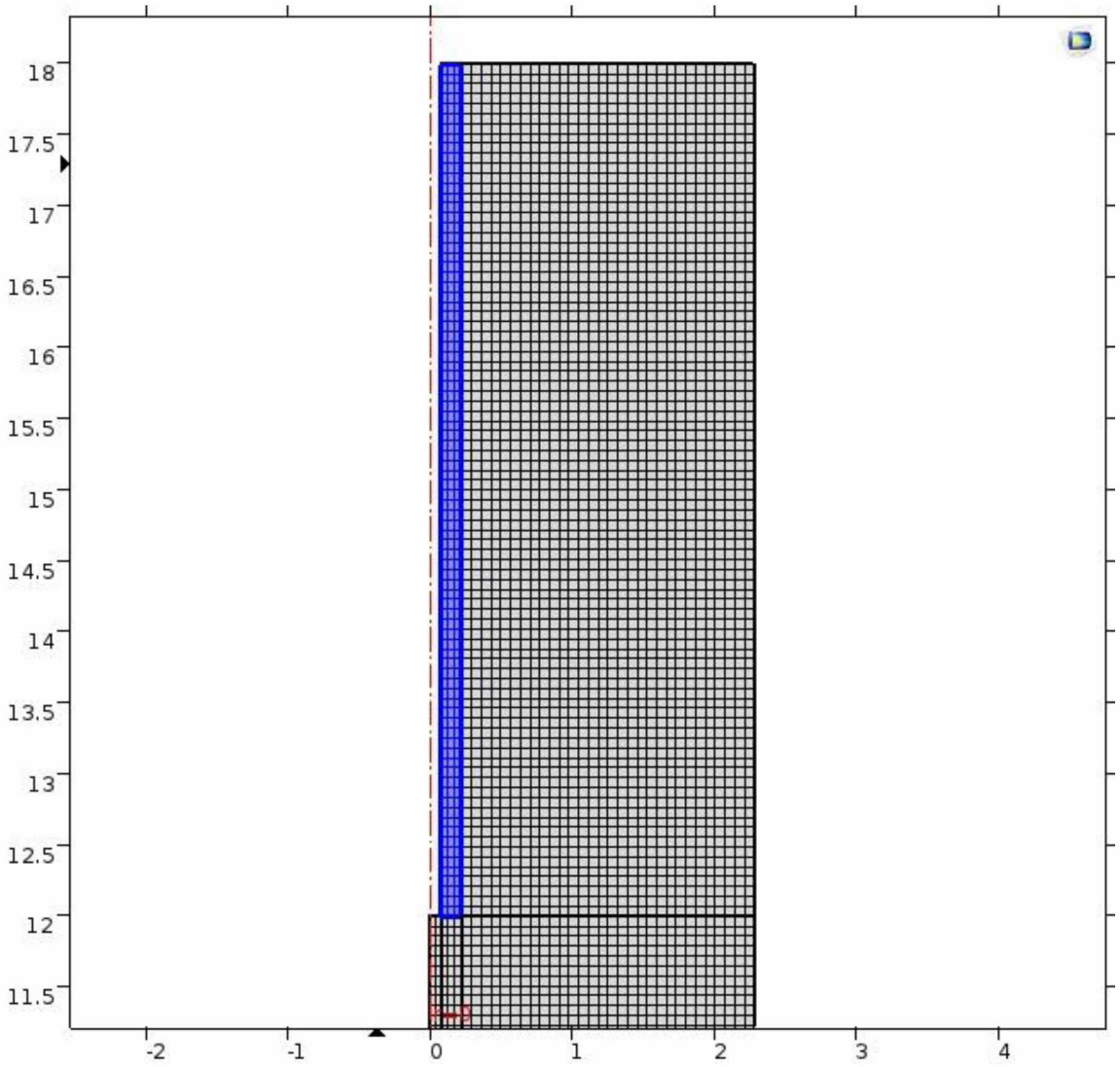

Figure 3.03.2: *Mesh where the pile and slurry meet the permafrost. The y- and x-axis display the z and r components respectively.*

3.04 *Heat Transfer in Solids*

The portion of the model *Heat Transfer in Solids* represents which physics are applied to which geometries as well as boundary conditions. For all runs heat transfer in solids in the slurry and permafrost, axial symmetry about $r=0$, thermal insulation or adiabatic boundary conditions applied at the pile-slurry interface as well as at the $r = r_s$ boundary, and an initially slurry temperature of 3°C or 37.4°F are used. The slurry temperature was chosen to be cold enough not to significantly thaw the permafrost upon placement but not so cold as to prevent uniform

freezing as might be seen if chunks of ice or glacial melt water were used. A linear temperature profile was applied over the range of the permafrost and is defined below. Note that the geothermal gradient was not directly included in the model.

$$T(z) = T_{Bot} + \frac{T_{PT} - T_{Bot}}{h_s} z \tag{3.18}$$

3.05 *Data Acquisition (Probes)*

Probes are a way of extracting certain data from specific locations within COMSOL®. Probes can be over a domain, boundary, point, and other more complicated definitions. A domain probe takes data from a region. In a 2D axisymmetric model the domain probe would be represented as an area rotated around the z-axis meaning that it examines data within a volume. A boundary probe can be used at the edges of defined geometries. In a 2D axisymmetric model a boundary probe would be seen as a line at the edge of a single geometry or between two adjoining geometries. When considering the fact that this line is rotated 360° about the z-axis it becomes apparent that a boundary probe represents data being extracted from an area. The last probe to be discussed is a domain point probe. This is a probe that examines a single point location within the model. Just as an area and line in a 2D axisymmetric model represent a volume and area in when rotated about the z-axis so does a point represent a line.

This model primarily uses 2 types of probes; boundary and point. A boundary probe was set up along the pile-slurry interface as this is the final location that will freeze back. By placing a boundary probe at the interface and extracting the maximum temperature over time data, the freezeback time for the entire slurry can be determined. When creating a boundary probe a variable name will automatically be assigned that can be changed by the user. It is important that the user define that variable in the parameters to initialize the value as COMSOL® is unable to complete a simulation otherwise.

Point probes were used to examine the temperatures at specific points along the pile. Several different locations were examined along the pile-slurry interface. Points were defined at different percentages of the pile embedment depth within the permafrost where 0% is at the top of the model, the boundary between the permafrost and active layer, and 100% is the bottom of

the pile. The points were defined at *(r_p. h_s-Percent/100*h_p)* where *Percent* is the percent of pile embedment. **Figure 3.03.4** shows a point probe at 100% of the pile embedment length.

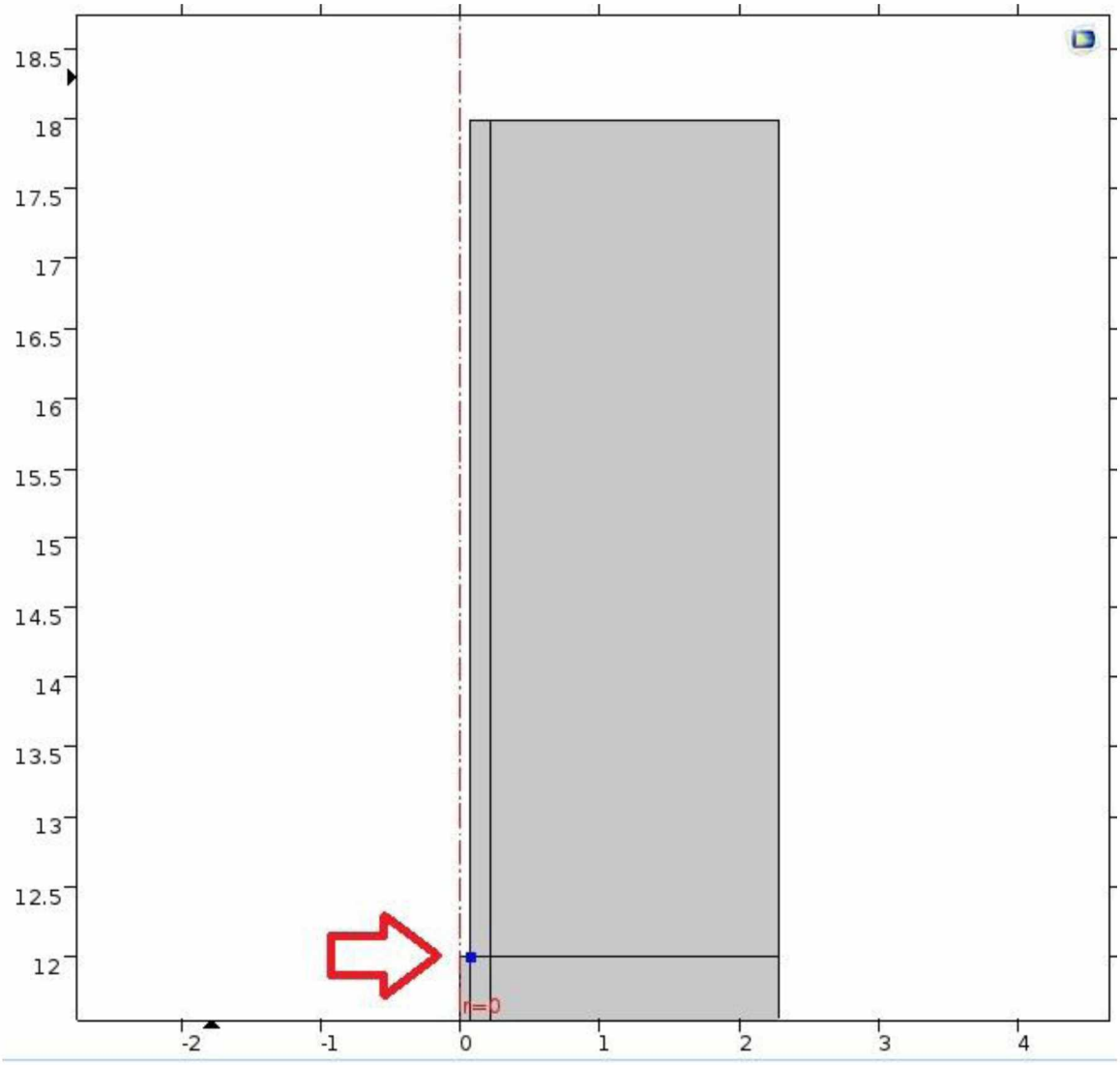

Figure 3.05.1: *Location of the probe at 100% of the pile embedment length. The point is represented by the blue dot at the bottom left corner of the slurry.*

Section 4: Results

4.1: *Model Baseline*

Several different parameters were varied within the model using a technique called a parameter sweep in COMSOL. A parameter sweep describes the influence of each parameter on the freezeback time of the slurry. In order to have a clear significance there must be a baseline or standard to which all simulations can be compared against. The standard parameters are defined in **Table 4.1.1.** All sweeps done will use the standard parameters unless otherwise noted. Table 4.1.1 introduces the term T_p which is the temperature at the bottom of the pile. For sweeps where the bottom sample temperature is warmer than the permafrost table temperature this represents the warmest temperature in the permafrost directly adjacent to the pile.

Table 4.1.1: *Standard parameters used as a baseline for parameter sweeps.*

Standard Inputs		
Inputs	Value	Units
r_b	0.2286	m
r_p	0.0814	m
h_p	6	m
w	0.15	-
γ_d	1922	kg/m^3
L	334	kJ/kg
Q	1.38E+04	kJ/m
C	1891	kJ/kg·K
C/3	630	kJ/kg·K
K	0.00208	kW/m·K
T_{PT}	-5	°C
T_{bot}	2	°C
T_p	-2.67	°C

To determine the freezeback time a boundary probe was set to measure the maximum temperature along the pile-slurry interface. The freezeback time was determined by linearly interpolating the temperature data for when the maximum temperature drops below -0.6°C which corresponds to all of the latent energy in the pulse being consumed. At this time all of the slurry will be below the freezing point and completely frozen. Point probes were set up at various points along the pile embedment length to determine the freezeback profile along the pile. Additional attention was given at the upper and lower 10% of the pile length to capture any special freezeback patterns as the gradient was changed in certain sweeps. The freezeback time for points along the pile for the standard conditions as well as the maximum temperature are shown in **Table 4.1.2** and **Figure 04.1.1**. This is used as a baseline for all other simulations where certain variables were changed to determine their influence.

Table 4.1.2: *Freezeback time for various points along the pile. Note that 0% of the pile length corresponds to the location of the pile at the permafrost table while 100% corresponds to the bottom of the pile.*

Percentage of Pile Length [%]	Freezeback Time [days]
0	4.3
1	4.3
5	4.4
10	4.6
20	4.9
30	5.1
40	5.6
50	6.1
60	6.6
70	7.3
80	8.0
90	8.0
95	6.6
99	3.4

100	1.3
Max	8.3

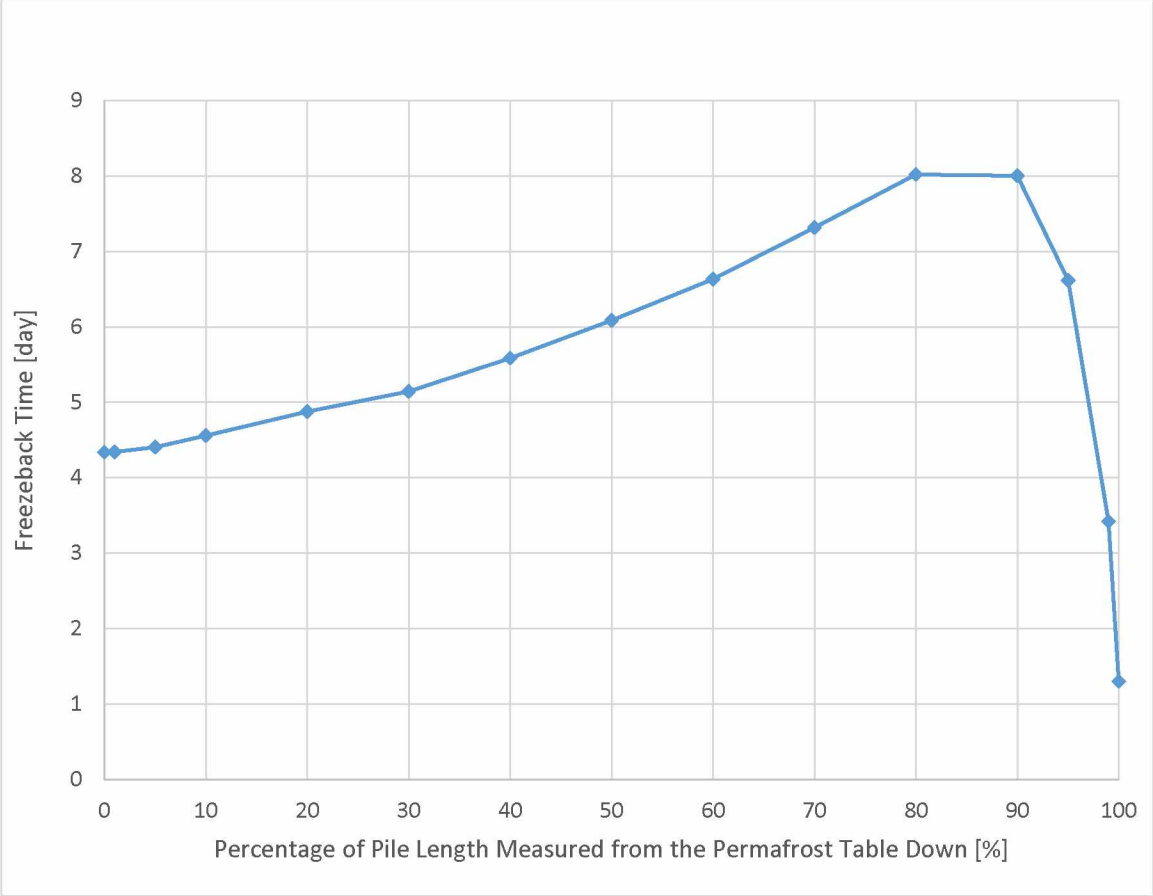

Figure 4.1.1: *Freezeback time for various points along the pile under standard assumptions.*

An important feature of the freezeback profile shows a distinct drop in the freezeback time at 90-100% of the pile embedment length, a layer of slurry with a thickness of 60 cm. This is due to the downward heat flow from the slurry into the permafrost at the bottom of the pile. While most of the energy travels radially outward from the slurry there is a small percentage that flows from the bottom. A freezeback time of 0 hours at the bottom of the pile occurs because the moment the slurry touches the cold permafrost a thin molecular layer of the slurry freezes due to the thermal discontinuity of the thawed and frozen material coming in contact. As the slurry starts to freeze from the bottom up. The rate of freezeback slows as the frozen material begins to act as an insulator to the advancing freezing front.

The freezeback time at 100% embedment length is 0 for most simulations. This is due to the fact that the point itself is on a boundary between the slurry and permafrost. While the slurry and permafrost have user defined initial temperatures, the boundaries where these materials meet do not. COMSOL takes a weighted average of the temperatures surrounding the boundary and uses that as an initial condition. For the case of the 100% probe, considering a circular area of influence around the point, the bottom two quadrants are at the temperature T_p, one quadrant is at the initial slurry temperature T_s, and one quadrant is undefined representing the pile. Averaging these temperatures it can be seen that

$$T_{100\%} = {}^{2}/_{3}\, T_p + {}^{1}/_{3}\, T_s \tag{4.1}$$

Thus

$$T_{100\%} = {}^{2}/_{3}\,(-2.67°\text{C}) + {}^{1}/_{3}\,(3°\text{C})$$
$$= -0.78°\text{C}$$

This correlates well with the value at time $t = 0$ of -0.77°C.

4.2: *Validating the Model*

It is important to ensure that a numerical model is producing accurate results. This is often done by validating or ground-truthing the model against a set of known data or values. Because there are no field tests to compare with the model there can be no straight-forward calidation. In lieu of having comparable data the model will be validated by looking for known trends and patterns that occur in permafrost heat transfer.

4.2.1: *Zero Curtain Effect*

When modeling the freezeback of saturated soils, there are two distinct phases that control the temperature of the soil. Sensible heat loss, the heat loss associated with a change in temperature, happens before and after the phase change occurs. The latent heat loss, the energy associated with phase change, takes much longer than the sensible heat to dissipate because there is significantly more energy required to cause phase change than to change temperature. This causes a distinct halt in the decreasing temperature often called a zero curtain effect. If the

model is performing correctly by accounting for all latent heat effects, there is a distinct and prolonged pause in the decreasing temperature profile at the freezing point (Qin et al, 2013). **Figure 4.2.1.1** shows the temperature profiles of various points along the pile for the standard conditions.

Zero curtains are present at each point except at the bottom of the pile. Also noticeable is that each point approaches a different asymptotic temperature. These asymptotes, which decrease in temperature as the points move closer to the permafrost table, correspond to the temperature gradient modeled within the permafrost where, for this simulation, the permafrost table is significantly colder than the bottom of the pile. The presence of both a zero curtain effect and the asymptotic temperatures are indications that the model is behaving correctly.

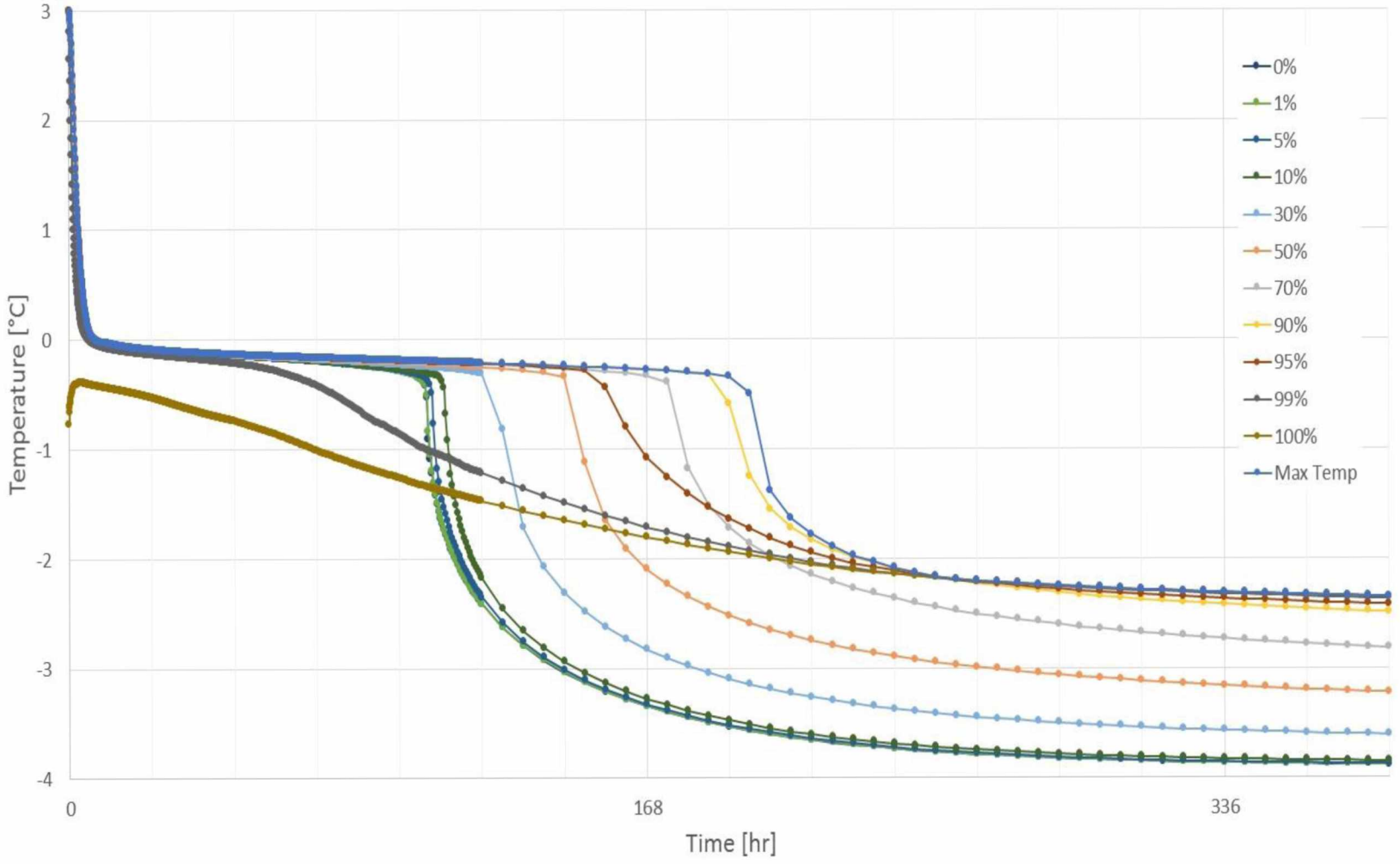

Figure 4.2.1.1: *Temperature curves for various points along the pile for standard model conditions. The zero curtain effect is apparent at the freezing point. The percentages correspond to percentage of pile embedment length in the permafrost*

4.2.2: *Impact of Pile Radius*

The pile radius simulations were done using standard conditions, varying the radius of the pile, and keeping the radius of the bore constant. This creates a relationship where a decrease in pile radius caused an increase in the slurry volume and thus an increase in the amount of latent heat. This increase in slurry volume is what causes the increase in the freezeback time, which can be seen in **Figure 4.2.2.1**. Figure 4.2.2.1 plots the maximum freezeback time for each simulation in the sweep. **Figure 4.2.2.2** shows the freezeback profile for each simulation in the sweep. This sweep is the equivalent of keeping the surface area of the slurry in contact with the frozen permafrost constant while changing the volume.

The freezeback profiles match the shape from the standard simulation. Also, the results show a decrease in freezeback time as the pile radius increases and, consequently, the volume of slurry decreases. Both of these characteristics further support the contention that the model is behaving correctly.

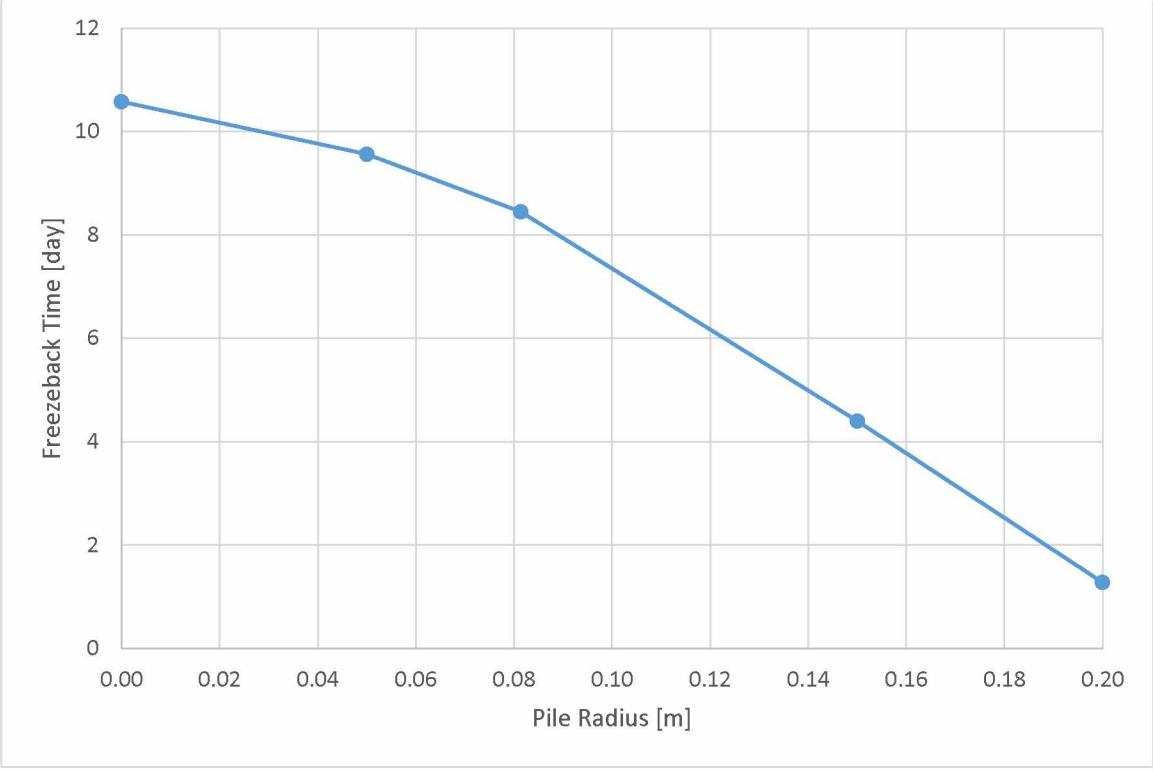

Figure 4.2.2.1: *Freezeback time for a varying pile radius.*

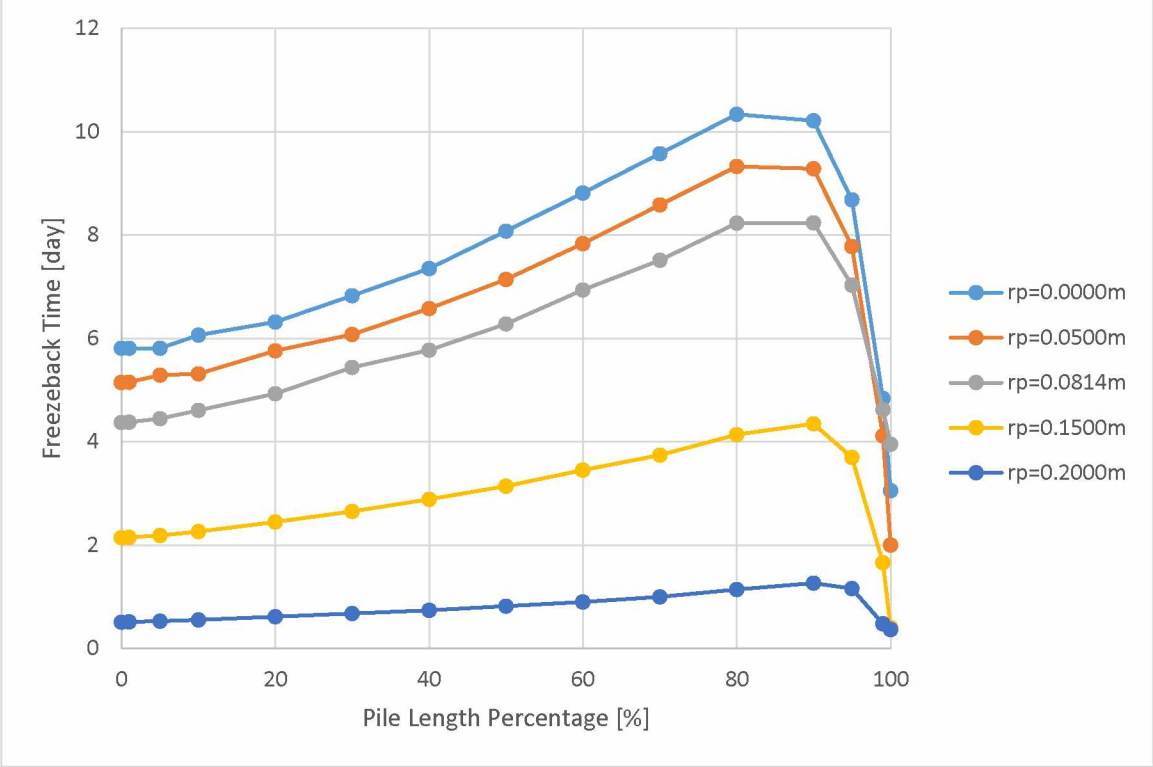

Figure 4.2.2.2: *Freezeback time profiles of each simulation in the pile radius sweep.*

4.2.3: *Impact of Bore Radius*

The bore radius simulations were done using standard conditions, varying the radius of the bore, and keeping the radius of the pile constant. Like the pile radius sweep, an increase in the bore radius causes a direct increase on the volume of the slurry freezing, however it also causes an increase in the surface area of the initial freezing interface. This effect can be seen in **Figure 4.2.3.1**. **Figure 4.2.3.2** shows the freezeback profiles of the sweeps.

Figure 4.2.3.1 shows a strong linear correlation with an increase in the bore radius causing an increase in the freezeback time. This differs from the simulations of varying the pile radius where the relationship between the pile radius, effectively the slurry volume, and the freezeback time was nonlinear. One interesting aspect of the freezeback profiles is that the location of the maximum freezeback time moves up the pile as the drill radius increases. This confirms that the drop at the bottom is related to the heat flow through the bottom of the pile as indicated by the fact that as the bore radius increases the radial thickness of the slurry increases. The freezing

front from the bottom can move farther up the pile before the freezing front from the radial direction reaches the pile-slurry interface.

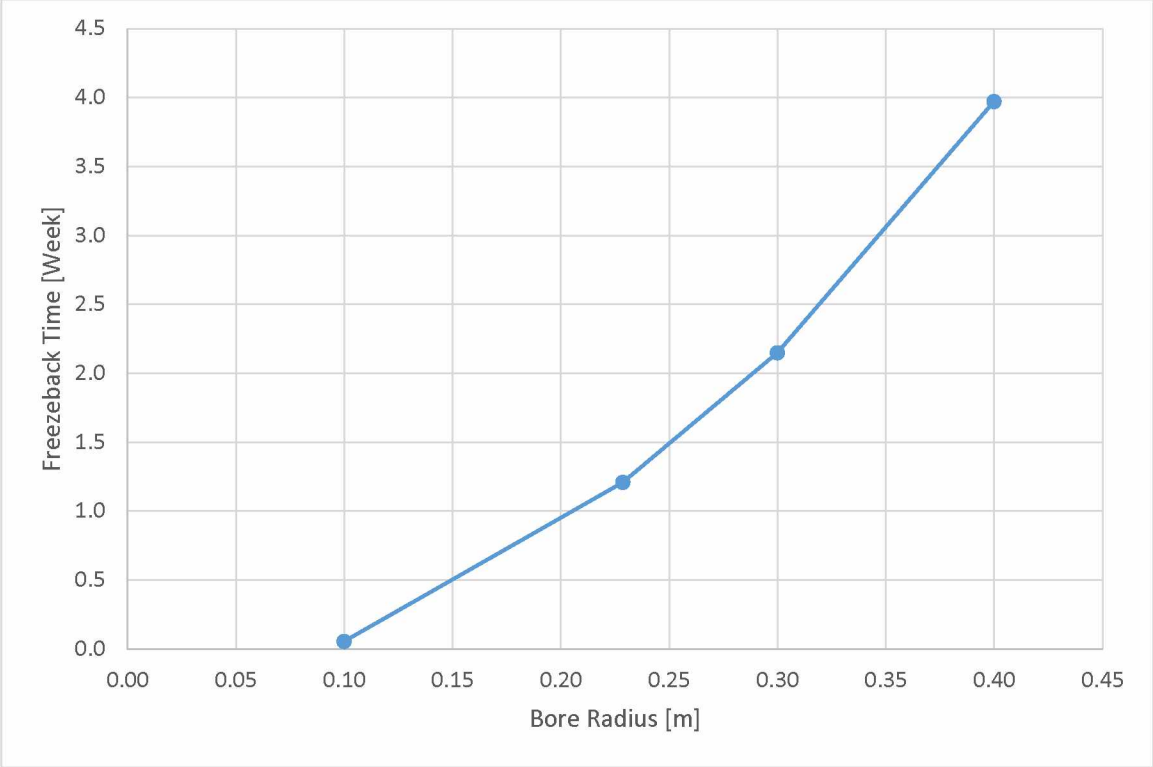

Figure 4.2.3.1: *Freezeback time for a varying bore radius.*

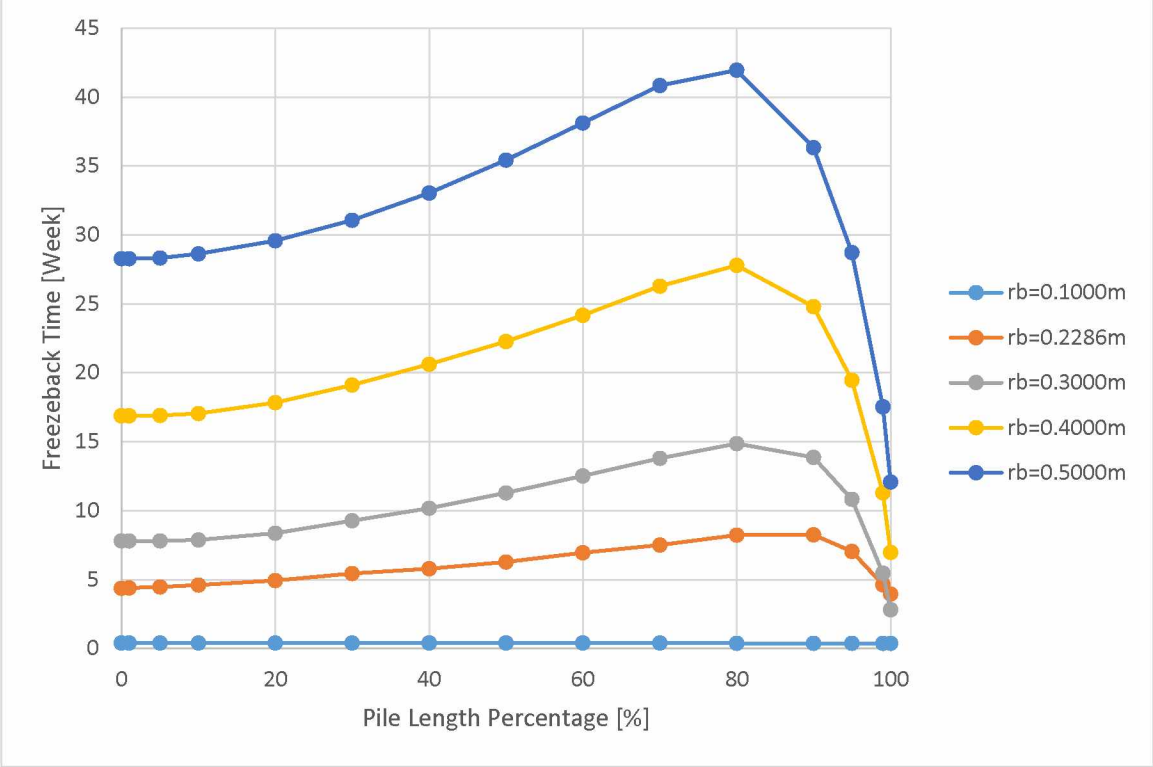

Figure 4.2.3.2: *Freezeback profiles for each simulation in the bore radius sweep.*

4.2.4: *Impact of Pile Embedment*

Simulations were done to determine the effect of the pile length on freezeback time. Due to the way the model geometry was defined, this kept the temperature at the bottom of the pile constant regardless of pile length but decreased the slope of the linear temperature profile in the permafrost. This can be shown by knowing that at height $z = 0$, $T = T_{bot}$ and at $z = h_s = 3 \cdot h_p$, $T = T_{PT}$. Thus

$$T(z) = T_{Bot} + z\frac{T_{PT} - T_{Bot}}{h_s} \tag{4.2}$$

Knowing that the bottom of the pile is at $z = h_s - h_p = 2 \cdot h_p$ and corresponds to temperature $T = T_p$ it can be shown that

$$T(2h_p) = T_p = T_{Bot} + (2h_p)\frac{T_{PT} - T_{Bot}}{3h_p} \tag{4.3}$$

$$T_p = T_{Bot} + {}^2/_3\,(T_{PT} - T_{Bot}) \tag{4.4}$$

$$T_p = {}^1/_3\,T_{Bot} + {}^2/_3\,T_{PT} \tag{4.5}$$

Figure 4.2.4.1 shows the freezeback time versus pile embedment length and **Figure 4.2.4.2** shows the freezeback time profiles of each run. There is a slight linear trend showing increasing freezeback time with increasing pile length. This is due to the shallower temperature gradient in the model caused by fixing the temperature at the top and bottom of the model but changing the pile length, which is proportional to the sample length. As can be seen in Figure 4.2.4.2, the freezeback profiles for each simulation are identical until the 90% point where the larger pile embedment lengths continue to take longer to freezeback. This is due to the relationship between the heat flow through the bottom of the slurry and in the radial direction which is effected by the change in the permafrost temperature gradient.

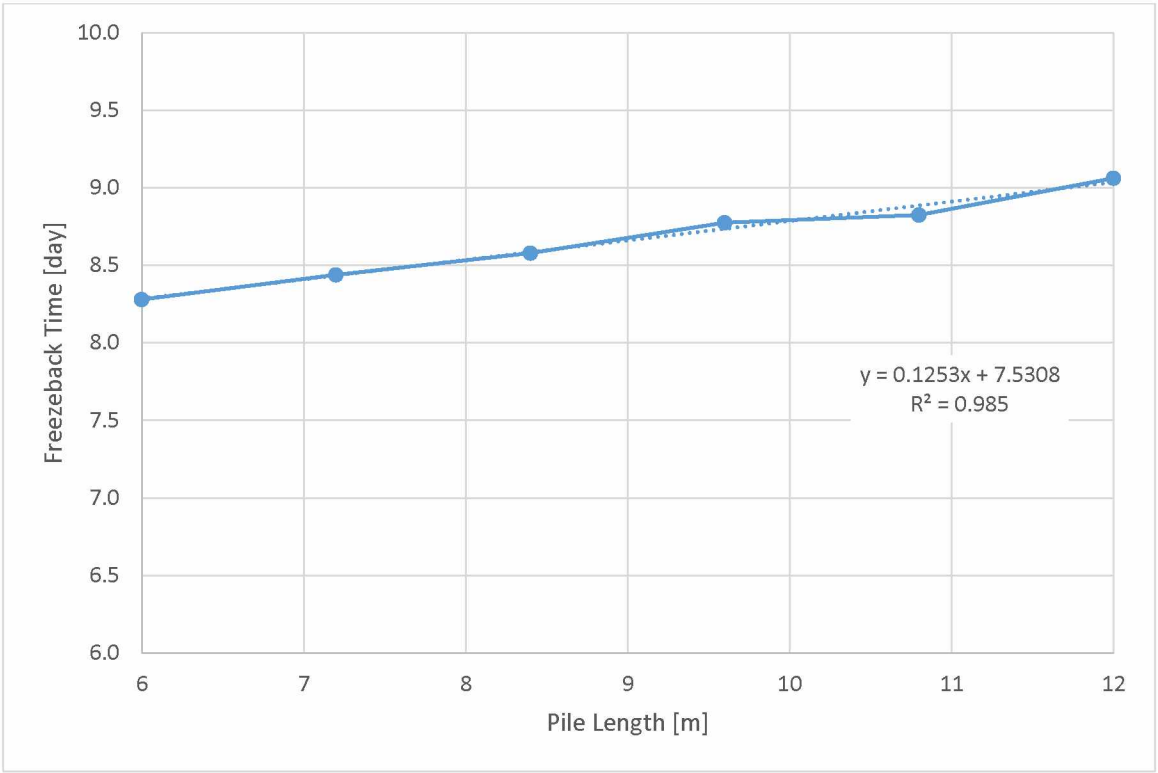

Figure 4.2.4.1: *Freezeback time as a function of pile length.*

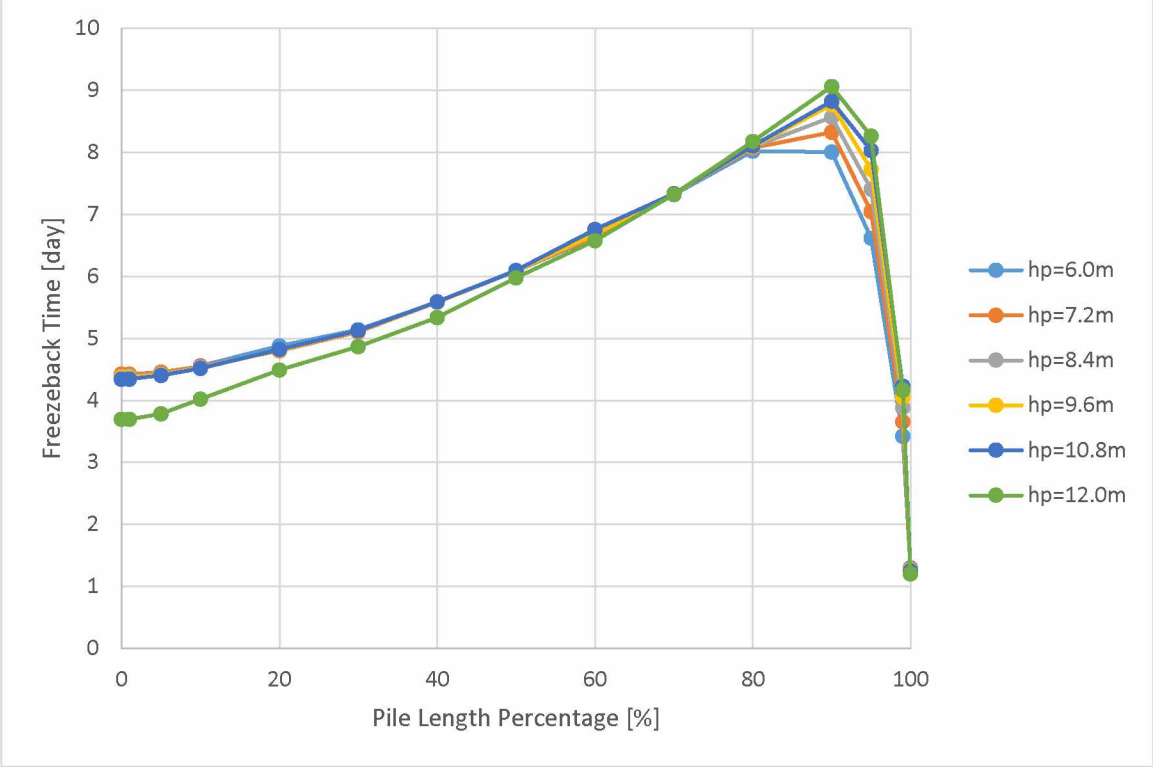

Figure 4.2.4.2: *Freezeback profiles for varying pile embedment lengths.*

Figure 4.2.4.3 shows the simulation results when a constant temperature profile in the permafrost of -2.67°C. This reduces the issue of a changing gradient as the pile length changes allowing for a clearer examination of the accuracy of the model. The numerical results are fairly similar as demonstrated by the low slope and coefficient of determination values. **Figure 4.2.4.4** shows the freezeback time profile for the isothermal permafrost simulations for varying pile length. It is worth noting that in both the standard and the isothermal permafrost temperature scenarios the simulations noticeably vary considerably between 80 and 100%. This is because the location that these points are measuring changed with each simulation because the pile length changed.

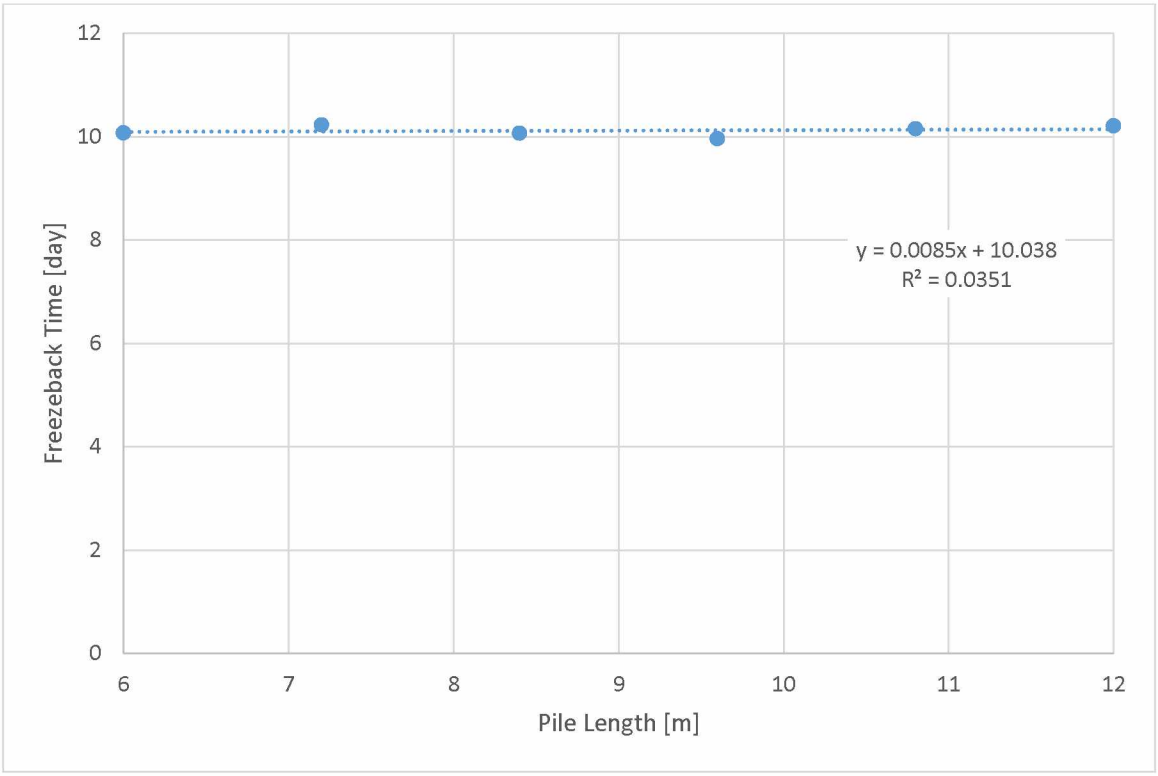

Figure 4.2.4.3: *Freezeback time for varying pile length with isothermal permafrost.*

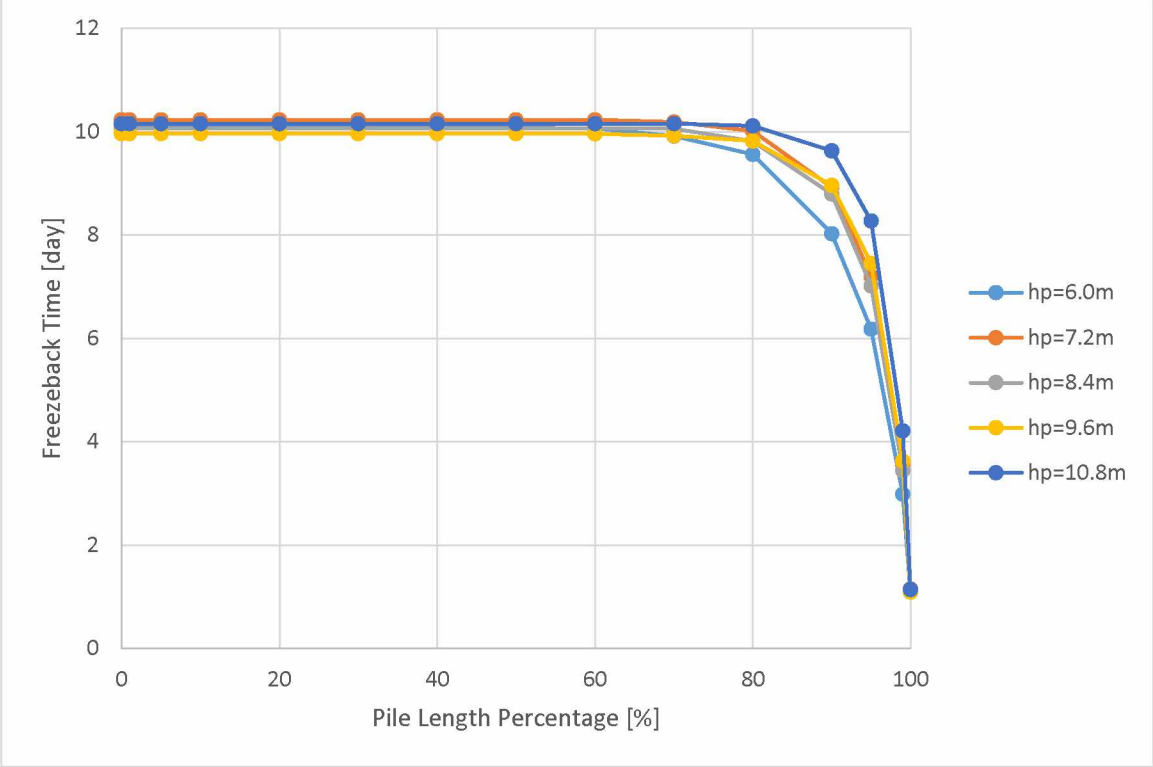

Figure 4.2.4.4: *Freezeback profiles for varying pile length with isothermal permafrost.*

4.2.5: *Maximum Element Size*

The size of the numerical mesh is not something that should effect the model results such as freezeback times. However it is important to analyze in order to help determine the accuracy of the model. The mesh size is a characteristic of the numerical model. A smaller the mesh size corresponds to a more dense grid of nodes, and thus more points where numerical data is being recorded. While a smaller mesh size typically leads to more accurate simulations, it also often leads to significantly larger data files and longer computation times. Because of these factors, the goal when determining the size of the mesh is to make it as large as possible without losing significant accuracy. **Figure 4.2.5.1** shows the maximum freezeback time for a varying max element size while **Figure 4.2.5.2** shows freezeback profiles of each simulation. It is clear from Figure 4.2.5.1 that there is little effect of to the maximum element size for the range tested. Based on these results, the maximum element size was set at 0.070 m.

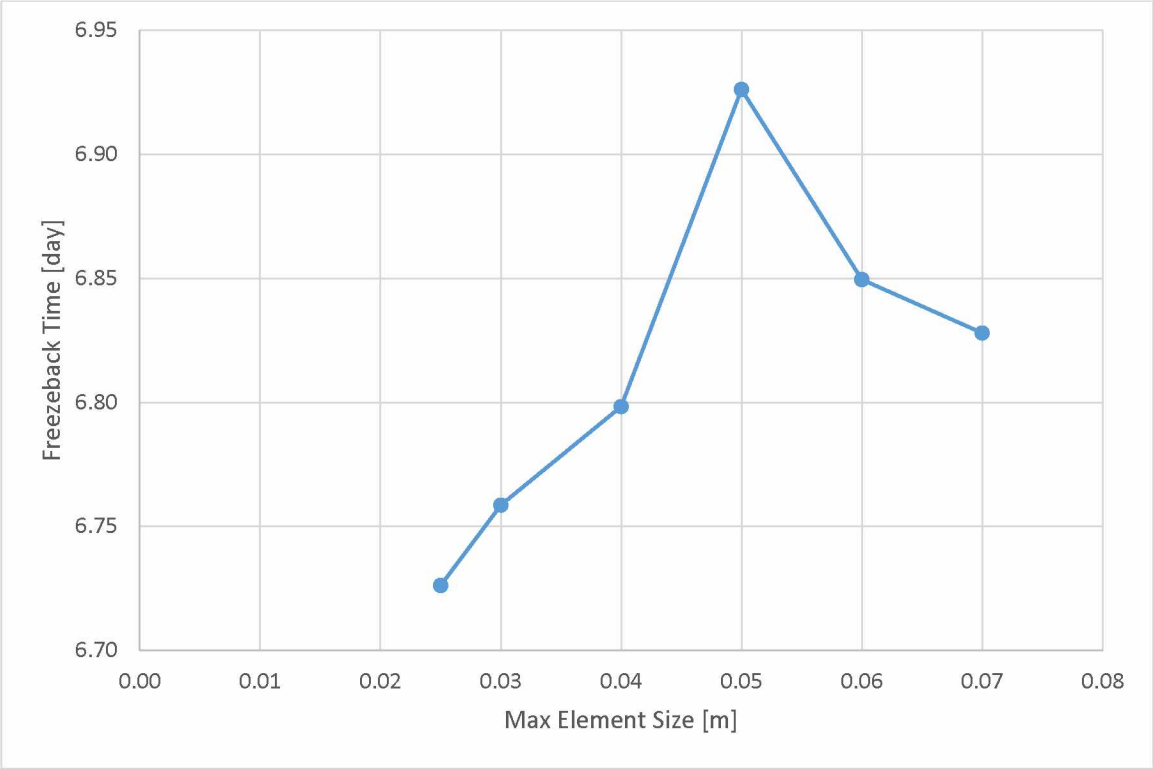

Figure 4.2.5.1: *Freezeback time for the max element size of the mesh used in both the slurry and the permafrost.*

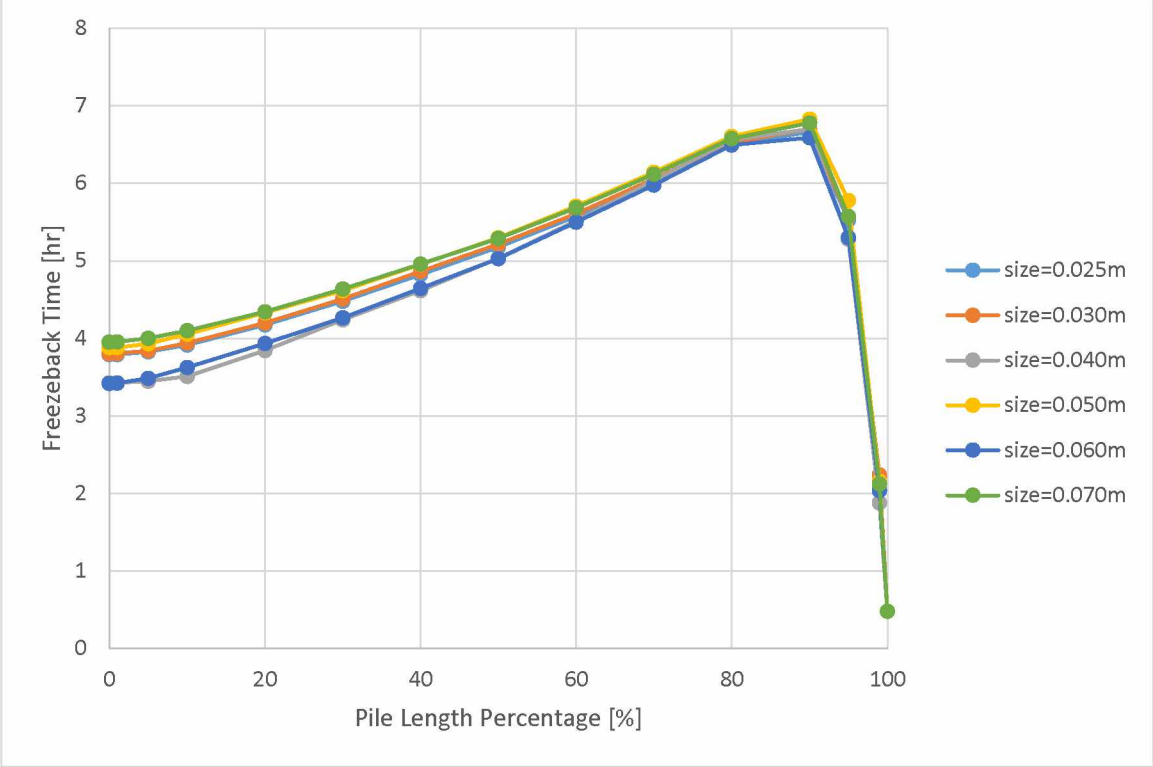

Figure 4.2.5.2: *Freezeback profiles for each simulation when varying the maximum element size of the permafrost and slurry mesh.*

4.2.6: *Gaussian Pulse Range*

The Gaussian Pulse is the function used to distribute the latent energy from a single temperature to a temperature range. Ideally this range is very small to represent a coarse grained material having little to no unfrozen moisture. Thus a smaller range corresponds more closely to reality. A wide range will also hinder the occurrence of a zero curtain effect because the apparent heat capacity will be distributed over a larger temperature range. However, if the range is too small then the model may miss portions of the latent heat because the latent heat is only accounted for if the model calculates several temperatures within the pulse range. If this range is too small then the model will miss large portions or the entire pulse and thus not account for any of the latent energy. This pulse range is determined by the standard deviation of the pulse. 99% of the pulse range is ±3 standard deviations from the pulse center while 95% is ±2 standard deviations from the pulse center. Thus the smaller the pulse standard deviation the smaller the range that

the latent heat is applied over. **Figure 4.2.6.1** shows the freezeback times for varying pulse standard deviations while **Figure 4.2.6.2** shows the freezeback profiles for these simulations.

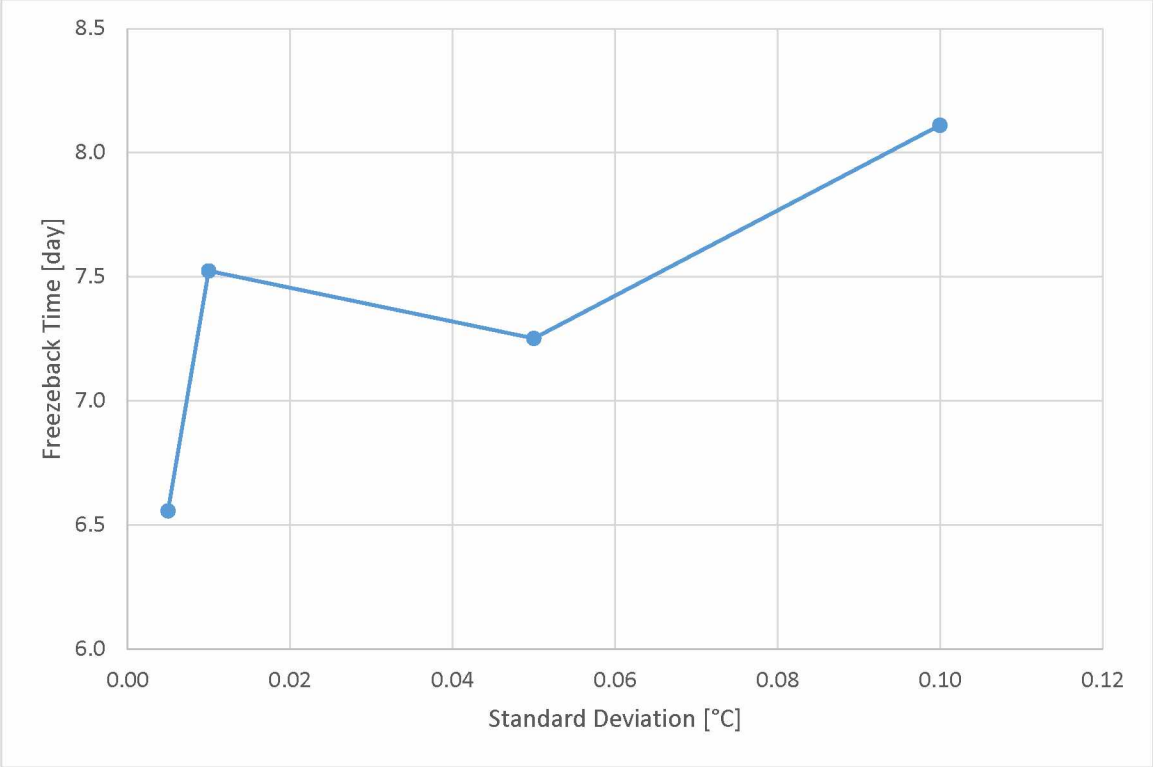

Figure 4.2.6.1: *Freezeback time for a varying Gaussian Pulse standard deviation.*

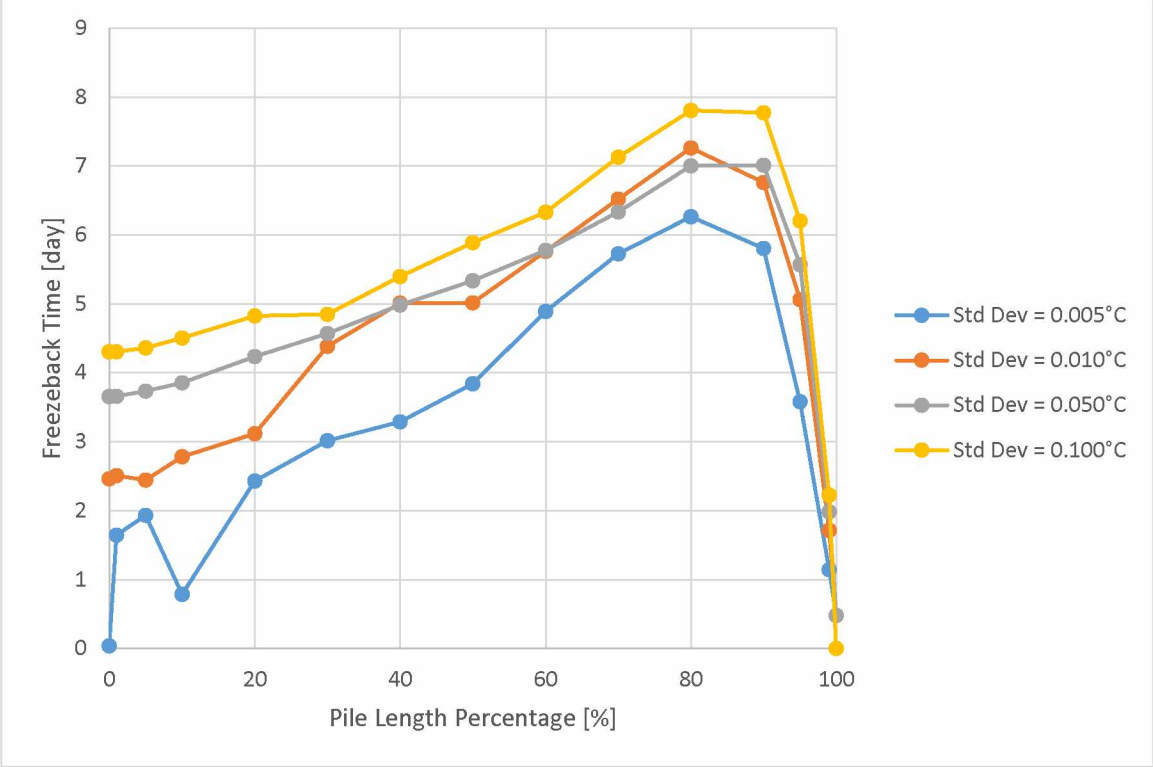

Figure 4.2.6.2: *Freezeback profiles for the Gaussian Pulse simulations.*

The sharp decrease in freezeback time shown in Figure 4.2.6.1 combined with the instability demonstrated in Figure 4.2.6.2 shows that a standard deviation of 0.005°C creates a pulse range that is too small. The instability shown in Figure 4.05.2 for a standard deviation of 0.01°C is on the border of a range that is too small. **Figures 4.2.6.3**, **4.2.6.4**, and **4.2.6.5** show the maximum temperature over time for a standard deviation of 0.01, 0.05, and 0.10°C respectively. It is clear from the large variations near the freezing point for 0.01°C makes it unsuitable for simulations. While the variation associated with the standard deviation of 0.05°C is much smaller, it is still not as smooth as 0.10°C. For these reasons the standard deviation was kept at 0.10°C.

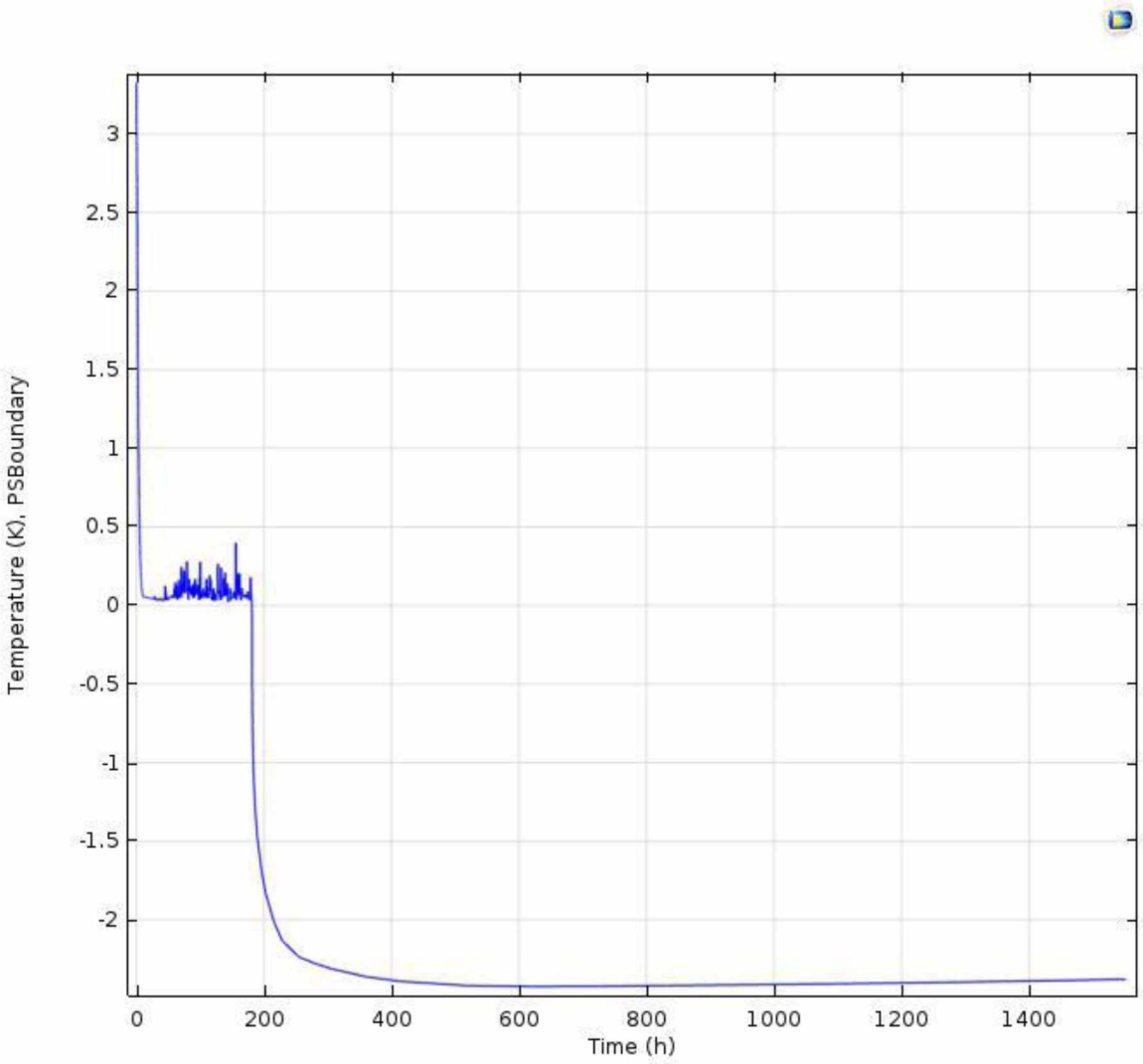

Figure 4.2.6.3: *Maximum temperature along slurry pile interface for a Gaussian Pulse standard deviation of 0.01°C.*

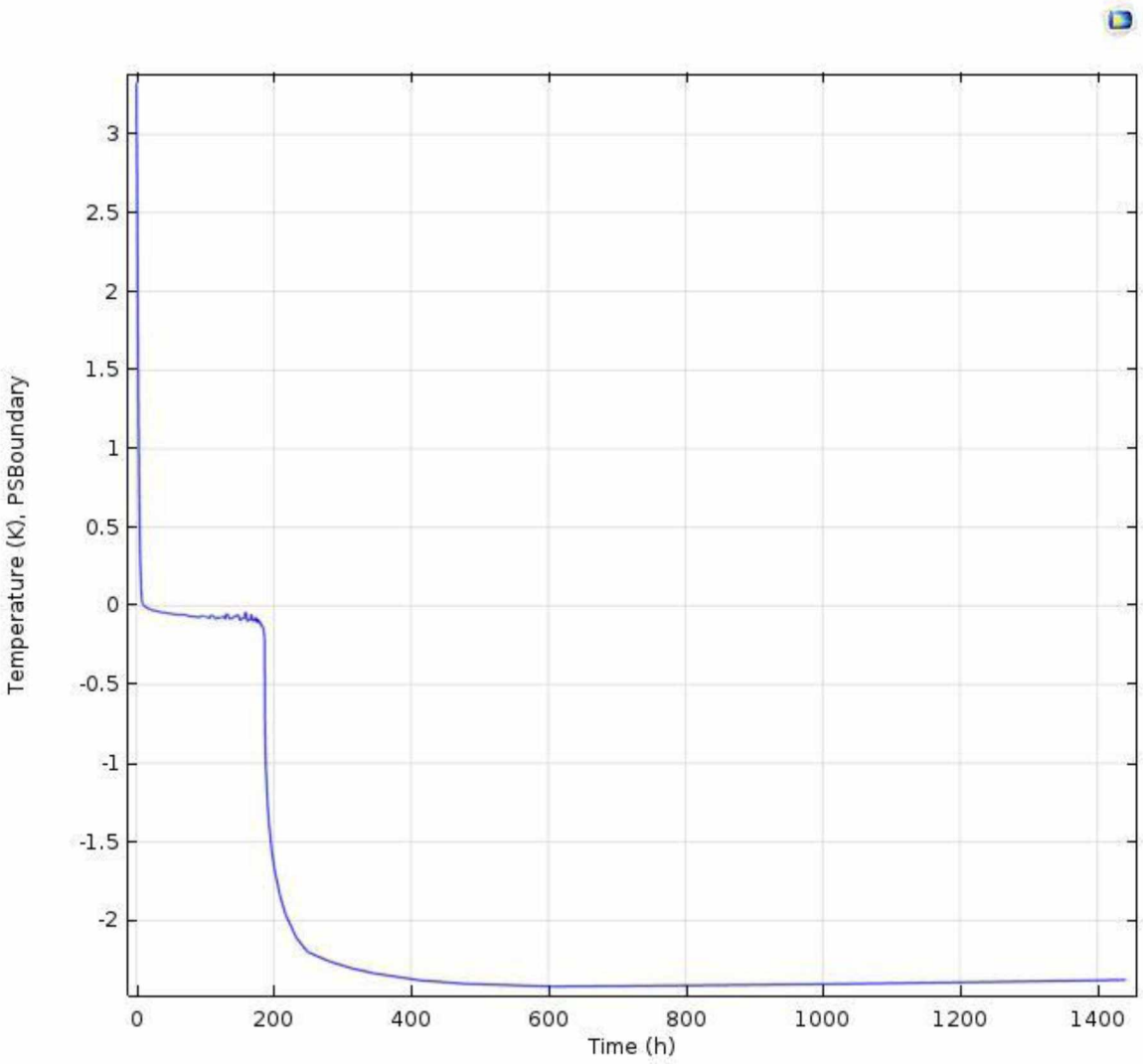

Figure 4.2.6.4: *Maximum temperature along slurry pile interface for a Gaussian Pulse standard deviation of 0.05°C.*

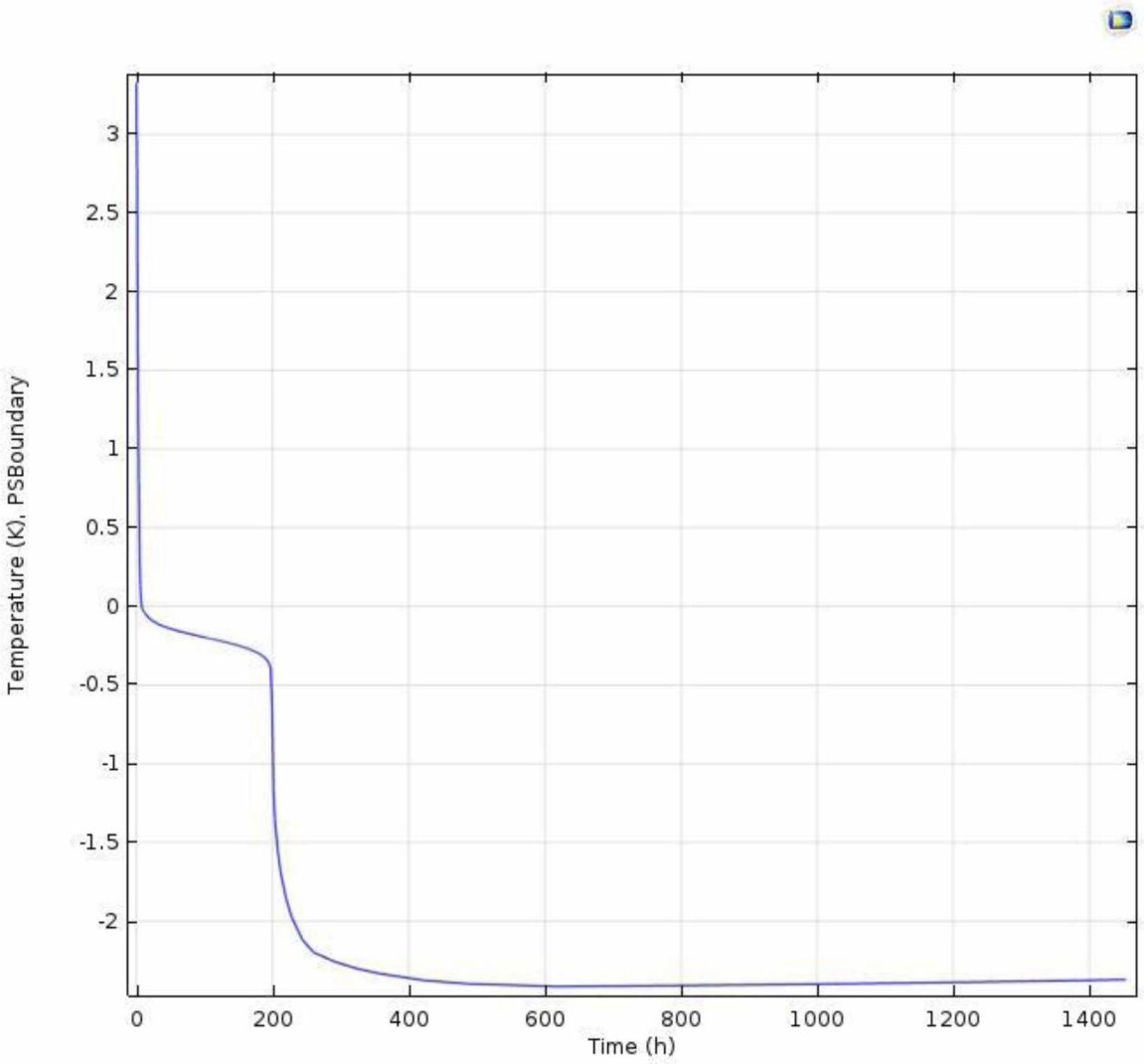

Figure 4.2.6.5: *Maximum temperature along slurry pile interface for a Gaussian Pulse standard deviation of 0.01°C.*

4.3: *Constant Active Layer Temperature*

One of the preliminary assumptions in the model was that the active layer covering the permafrost acted as a perfect insulator and thus the atmospheric temperature above had no influence on the temperatures below. This parametric sweep examines the effect of removing this assumption by computing the same values for when the upper boundary at the permafrost table is adiabatic and isothermal. An adiabatic boundary condition is when there no heat flux through the boundary and an isothermal boundary condition when the boundary is set to a

constant temperature. **Figure 4.3.1** shows the freezeback times for the two conditions. The results show that the two simulations closely overlap. **Table 4.3.1** shows the freezeback times as well as the percent difference between the two simulations. The data show that the difference between the two simulations is negligible in terms of the slurry freezeback until the temperature at the bottom of the pile, T_p, becomes small. Note that because freezeback is not complete until the temperature is below -0.6°C that a T_p = -0.9°C is only 0.3°C below the temperature required to fully freeze the slurry. It is worth noting that simulations were done where T_p = -0.7 and -0.8°C however for the adiabatic boundary condition the slurry never froze back even when the simulation time was allowed to go on for several years. The isothermal boundary condition results did not have this issue.

Figure 4.3.2 shows the freezeback profiles for the isothermal boundary while **Figure 4.3.3** shows the adiabatic condition. An interesting note that both of these figures show is that the bottom of the pile, at 100% of the embedment length, is not immediately frozen. This is due to the fact that for some of the runs the temperature at the bottom of the pile was significantly warmer than other simulations. Thus when the temperature at the boundary was averaged the result was above the freezing point. Another interesting factor is that for the isothermal condition all of the freezeback times at the top of the pile, 0% embedment length, were 0. This is because the temperature along the permafrost table was defined to be below zero. Thus the temperature was already below the freezing point when the simulation began. This is not the case for an adiabatic boundary where the initial temperature is that of the slurry and must dissipate heat into the permafrost in order to freeze.

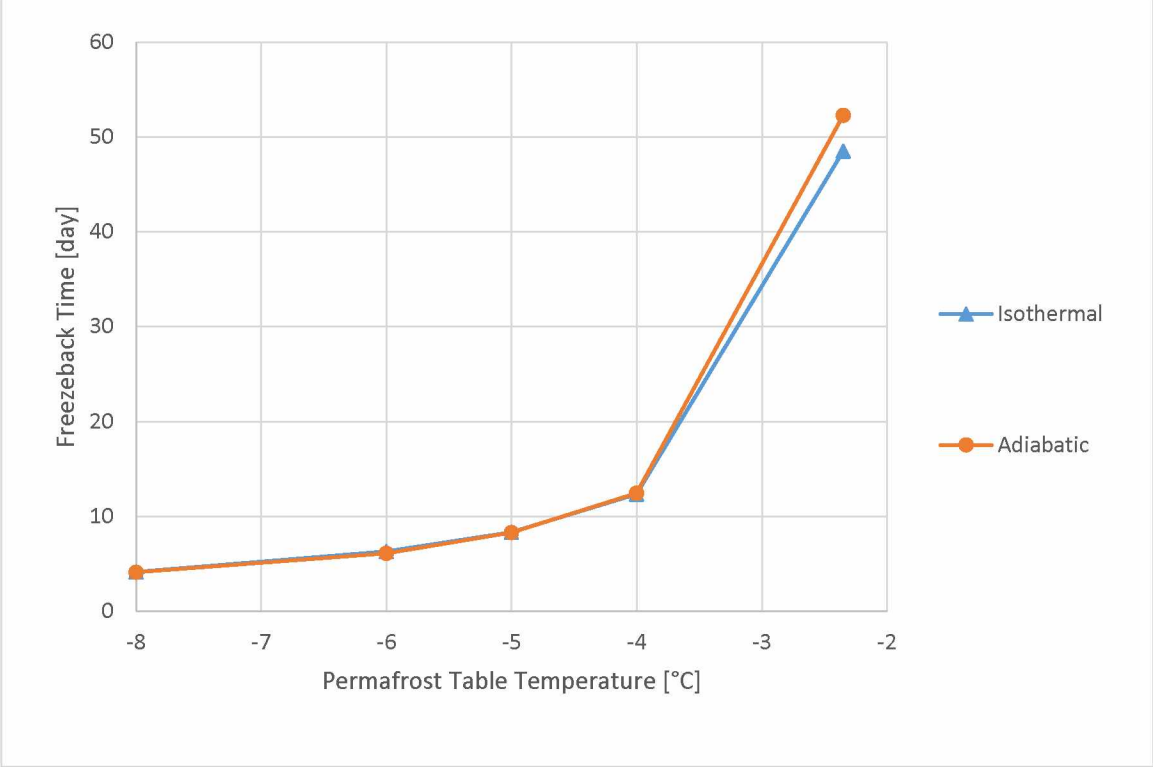

Figure 4.3.1: *Effect on freezeback time when the active layer is not considered a perfect insulator and a constant temperature is applied at the permafrost table compared with when there is no heat flow through the permafrost table into the active layer.*

Table 4.3.1: *Freezeback time and percent difference for adiabatic and isothermal permafrost table boundary conditions.*

T_{PT} [°C]	T_p [°C]	Freezeback Time [day]		Percent Difference
		Isothermal	Adiabatic	
-2.35	-0.9	48.5	52.3	7.82%
-4.00	-2.0	12.3	12.4	0.68%
-5.00	-2.7	8.3	8.3	0.30%
-6.00	-3.3	6.3	6.1	3.49%
-8.00	-4.7	4.1	4.1	1.16%

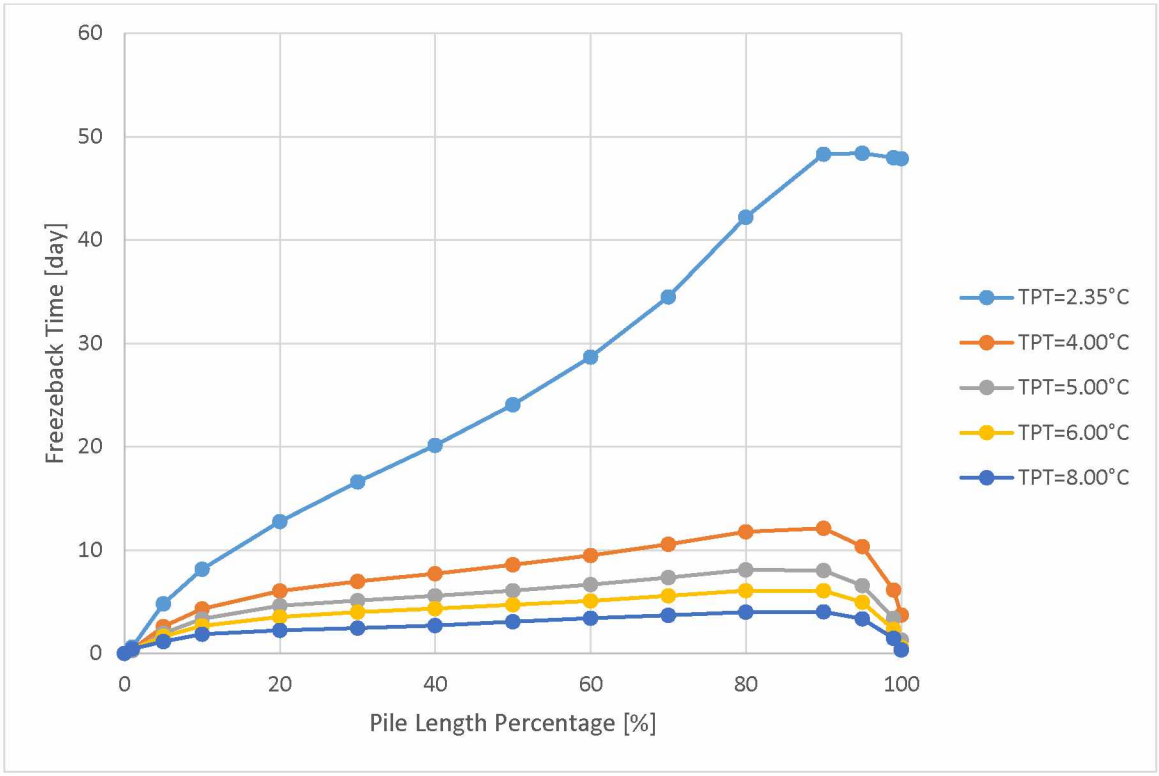

Figure 4.3.1.2 *Freezeback profiles for an isothermal boundary condition at the permafrost table boundary and varying the permafrost table temperature,* T_{PT},

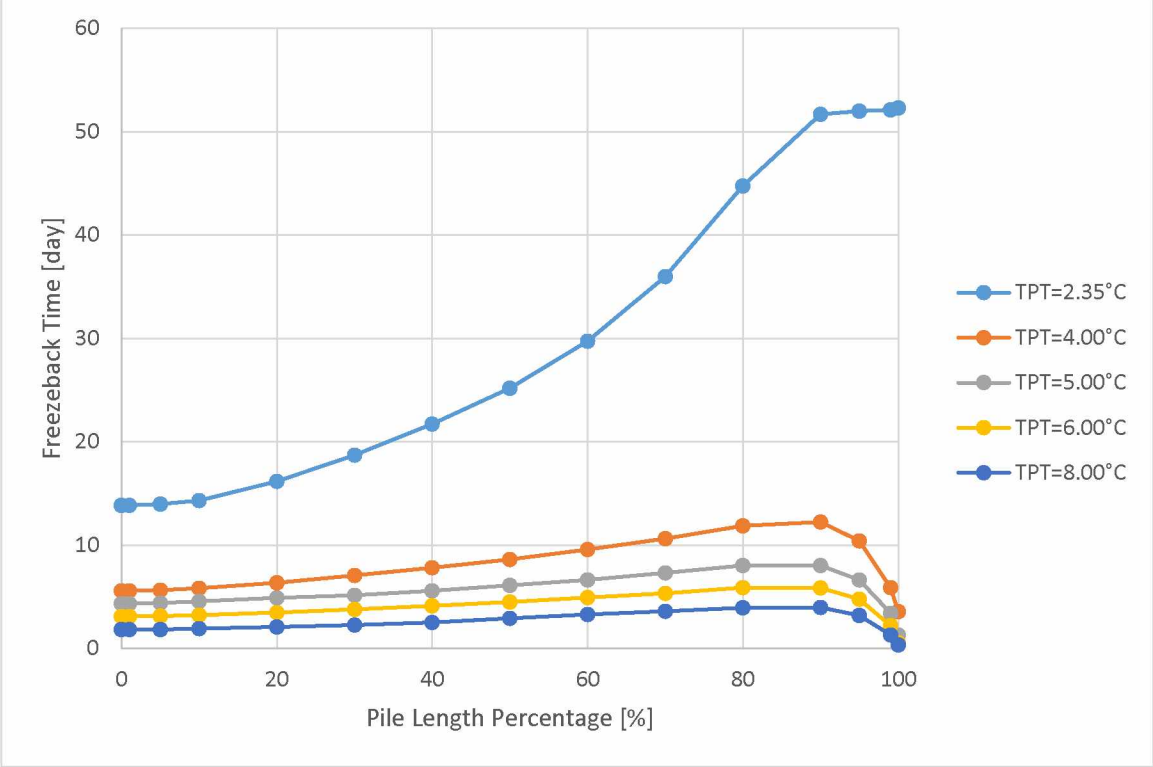

Figure 4.3.3: *Freezeback profiles for an adiabatic boundary condition at the permafrost table boundary while varying the permafrost table temperature.*

4.4: *Impact of Temperature Gradient*

The influence of a varying temperature gradient on freezeback time was also studied. To vary the gradient a parametric sweep was done of the bottom temperature for each temperature at the permafrost table creating a much larger and representative field of data than what was done in the other sweeps. For all temperature gradient sweeps the standard conditions were used and the top and bottom boundaries were considered adiabatic but the permafrost table and bottom temperature were varied. Due to the fact that the pile length remained constant, the depth of the sample remained constant and the initial temperature profile of the permafrost can be written as

$$T(z) = T_{Bot} + \frac{T_{PT} - T_{Bot}}{h_s} z$$
$$= T_{Bot} + \frac{T_{PT} - T_{Bot}}{18m} z \tag{4.6}$$

The thermal gradient can be taken from this definition as

$$T_{grad} = \frac{T_{PT} - T_{Bot}}{18m} \tag{4.7}$$

Figure 4.4.1 shows the freezeback time of the slurry as a function of the bottom temperature and the active layer temperature. **Figure 4.4.2** presents the same results in a different manner by showing the freezeback time as a function of the thermal gradient and the permafrost table temperature while **Figure 4.4.3** shows the data as a function of permafrost table temperature and the temperature at the bottom of the pile. Each simulation includes a set of conditions such that the temperature at the bottom of the pile, T_p, is -0.9°C. This is 0.3°C colder than when 99% of the latent energy is consumed. This temperature was chosen to see what happened in simulations when the warmest part of the permafrost near the pile is near the thaw temperature. Due to some simulations never freezing at -0.7 and -0.8°C the warmest temperature that could be consistently simulated was -0.9°C.

Each of these figures show that freezeback time increases significantly in warm permafrost. As the permafrost gets colder the differences become negligible as is seen in Figure 4.4.3 where the freezeback time somewhat converge as the temperatures decrease.

Figure 4.4.2 shows the same data but with emphasis placed on the temperature profile of the permafrost. By recognizing that a thermal gradient of 0 implies that the temperature is constant throughout the permafrost the data can be broken up into two groups. For positive thermal gradients the permafrost temperature is warming with an increase in depth and for negative thermal gradients the permafrost is cooling with depth. This is representative of different construction seasons where the upper portion of permafrost is cold in the spring and warm in the fall.

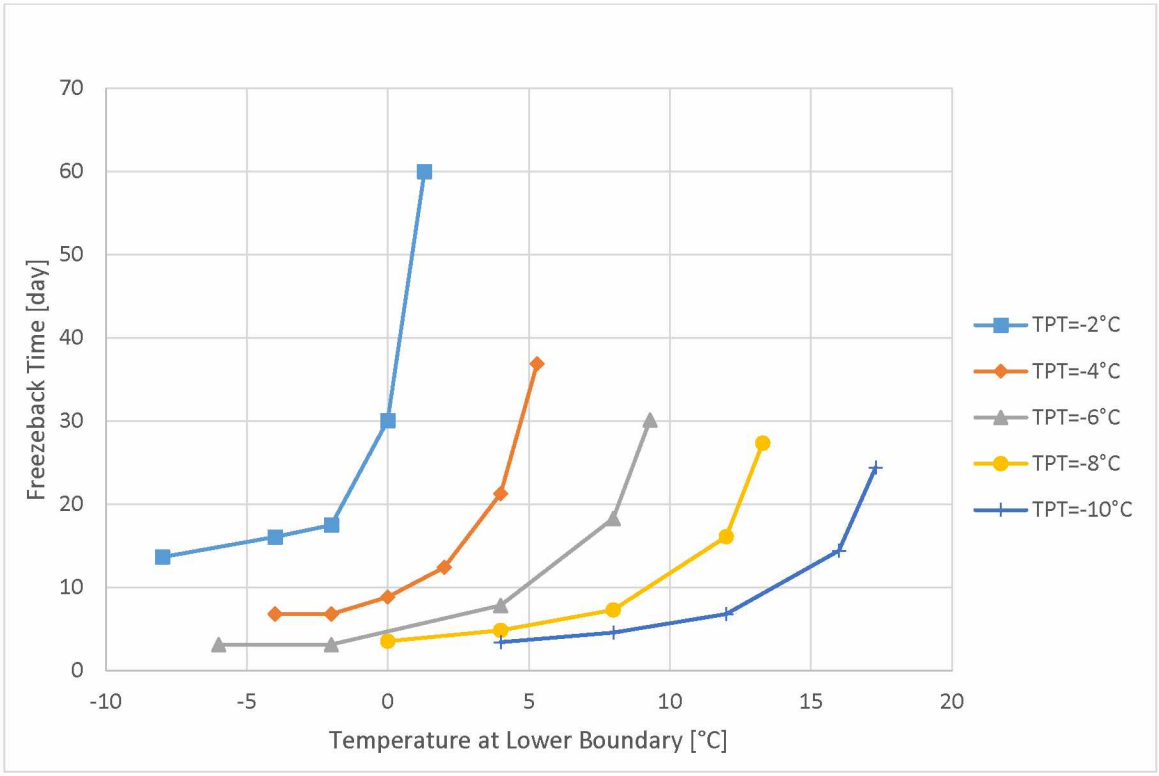

Figure 4.4.1: *Influence of varying the temperature at the permafrost table and bottom of the sample on the freezeback time as a function of the two temperatures.*

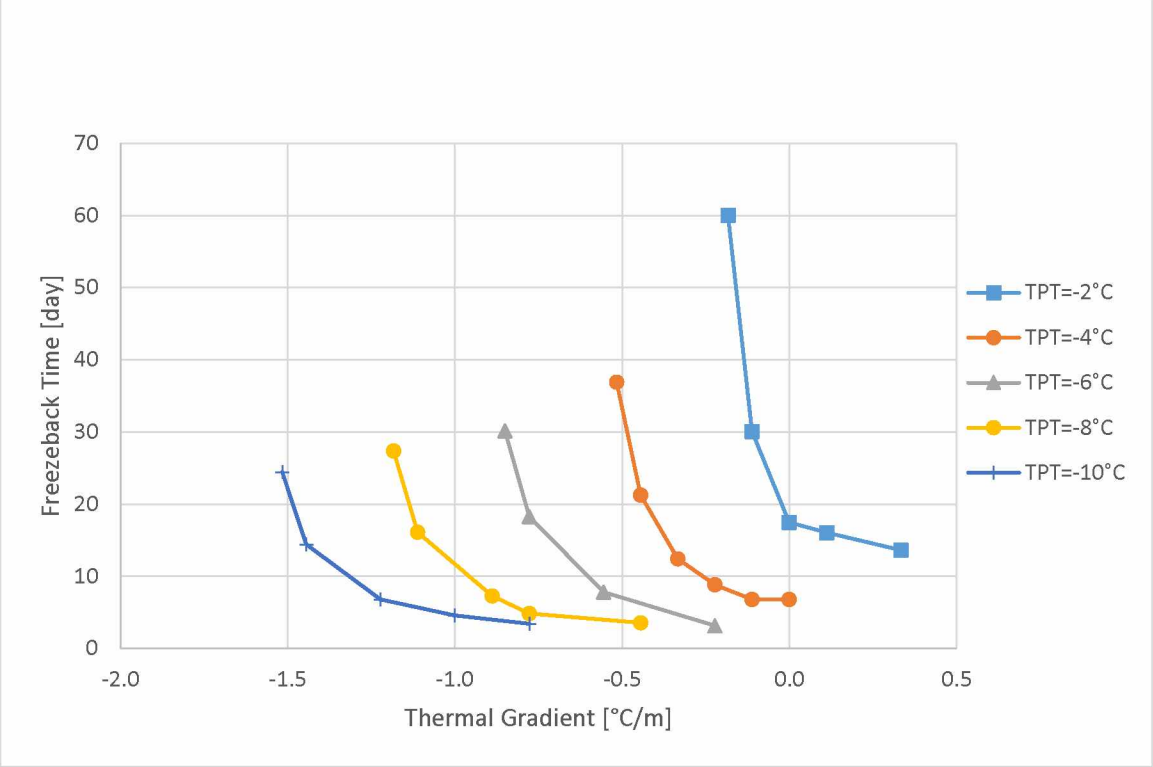

Figure 4.4.2: *Influence of varying the temperature at the permafrost table and bottom of the sample on the freezeback time as a function of the linear gradient and the permafrost table temperature.*

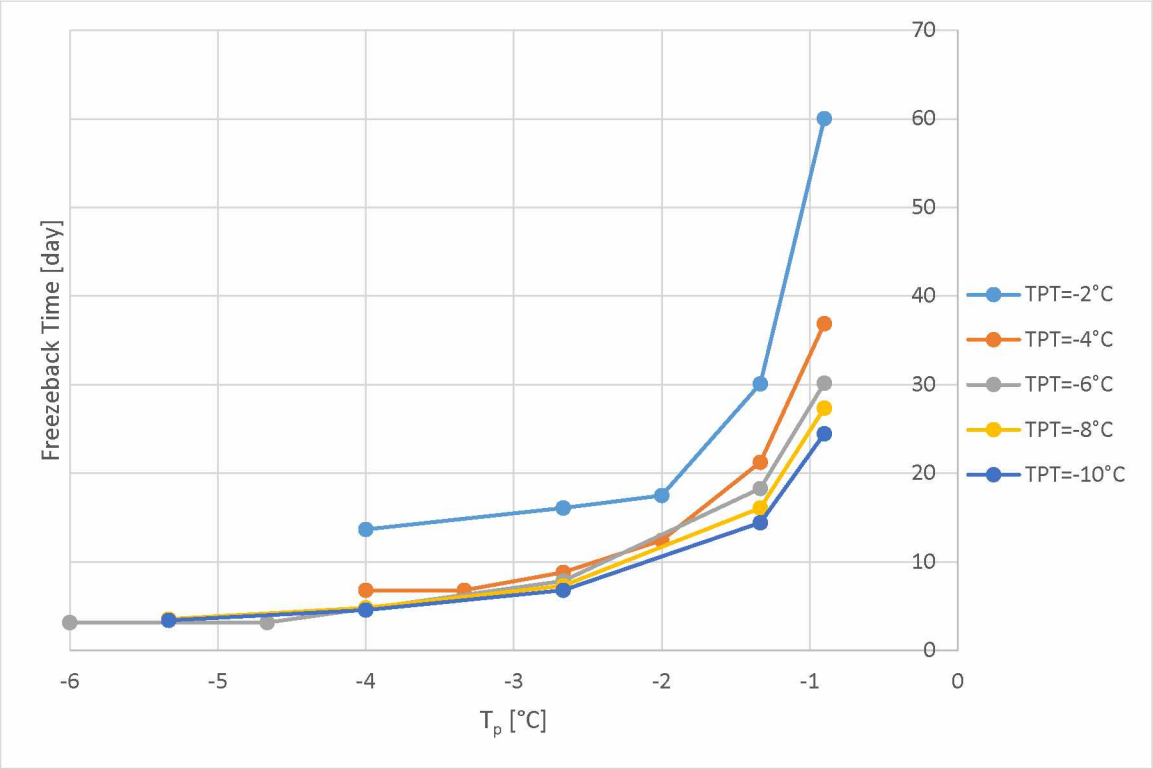

Figure 4.4.3: *Influence of varying the temperature at the permafrost table and bottom of the sample on the freezeback time as a function of the temperature at the bottom of the pile.*

4.5: *Slurry Density*

Slurry density is related to several different parameters. When the slurry is placed in the bore hole it is saturated with water and has an associated frozen and thawed thermal conductivity. If the density of the sand changes so does the moisture content required to saturate it as well as the frozen and thawed thermal conductivities. Thus changing the density of the sand in the slurry actually influences four separate parameters. Of each of the four parameters the moisture content is the most important because it is directly related to the latent heat of the slurry while the density and both conductivities are related to sensible energy. Because of this two separate sets of simulations were done. One set where the sand density varied and was kept fully saturated and a set where, for the same densities and thermal conductivities from the saturated simulations, the moisture content was kept at a constant value. The constant was a value of 24%, the average of the moisture contents from the saturated simulations. **Figure 4.5.1** shows the

freezeback times for both the saturated and constant moisture content while **Figure 4.5.2** and **Figure 4.5.3** show the freezeback profiles for each set of simulations. **Table 4.5.1** shows the sand desnsities, moisture contents, and thermal conductivities used.. The thermal conductivities were taken from Kersten's charts shown in **Figures 4.5.4**.

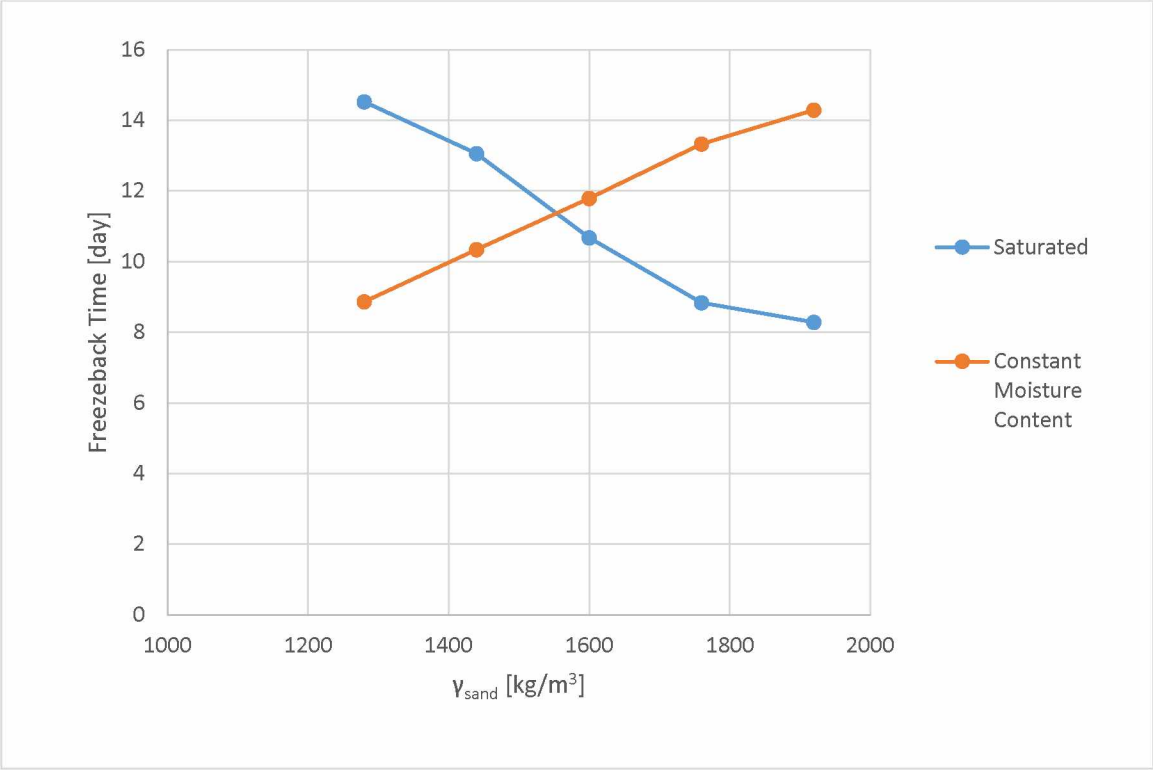

Figure 4.5.1: *Effect of a varying sand density under saturated and constant moisture conditions.*

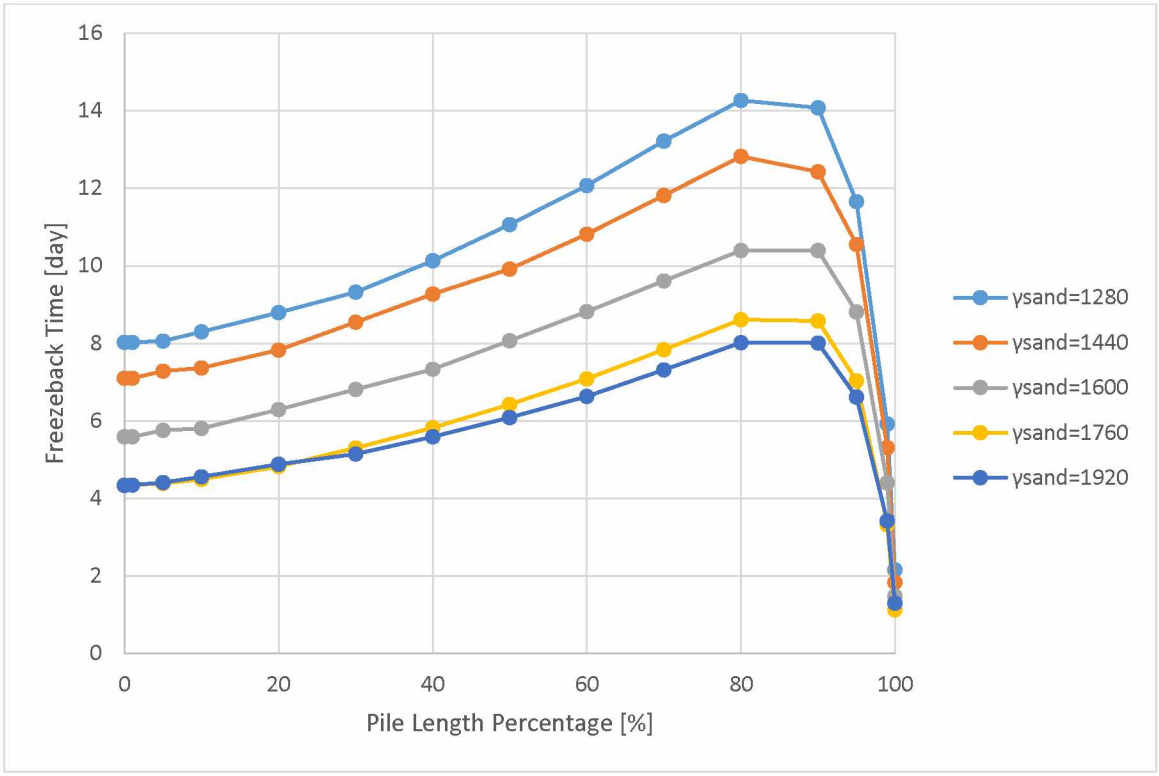

Figure 4.5.2: *Freezeback profiles for a varying sand density kept saturated.*

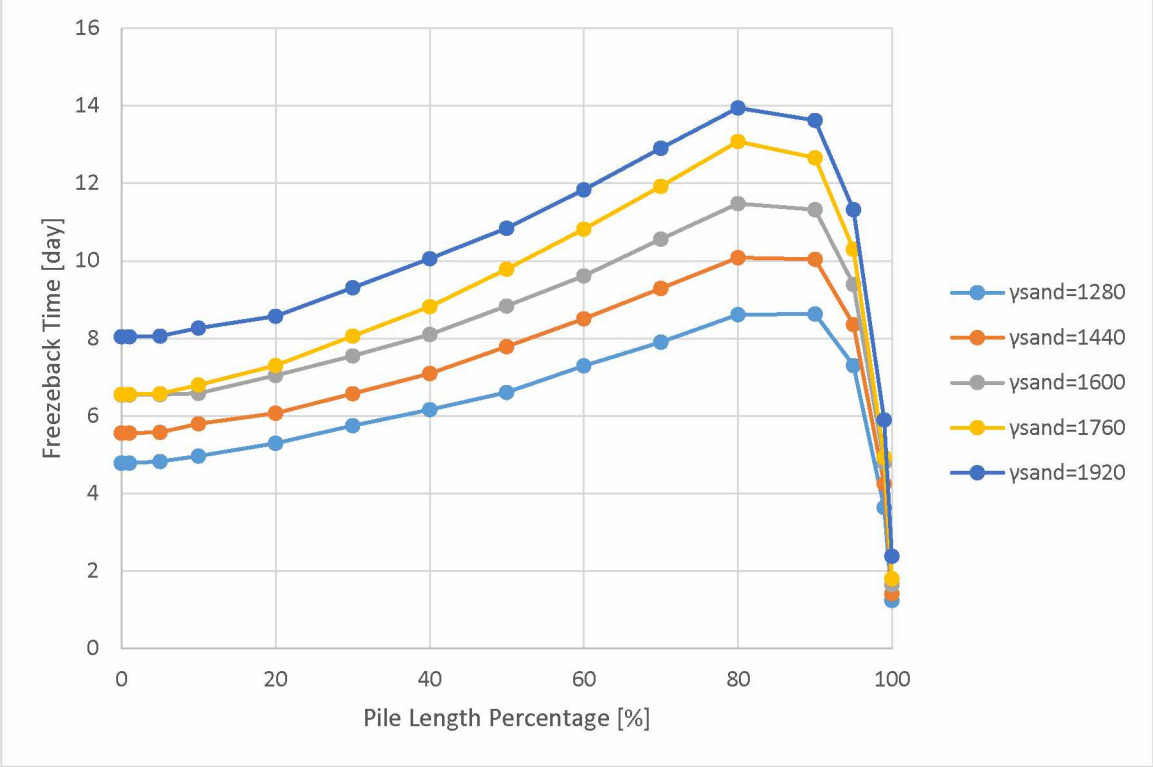

Figure 4.5.3: *Freezeback profiles for a varying sand density with a constant moisture content. The frozen and thawed thermal conductivities were taken from the saturated simulations.*

Table 4.5.1: *Input values for a varying slurry density with moisture content corresponding to a saturated mix and thermal conductivities taken from Kersten's charts.*

γ_{sand} [kg/m^3]	w_s	k_f [W/(m·K)]	k_t [W/(m·K)]
1280	0.36	2.08	1.12
1440	0.29	1.99	1.30
1600	0.22	1.99	1.56
1760	0.17	1.99	1.73
1920	0.15	2.25	1.92

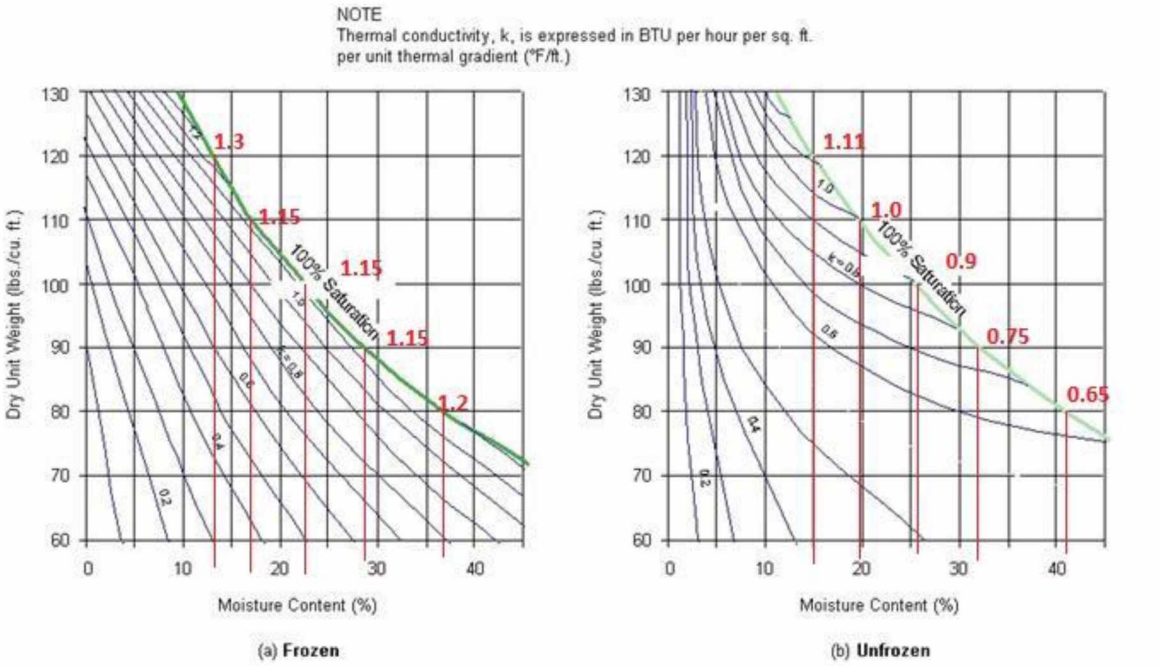

Figure 4.5.4: *Diagram of thermal conductivities for sand. The red lines and numbers correspond to values that were used in the slurry density sweep (Pavement Interactive, 2012).*

It is apparent from Figure 4.5.1 that the effect of the thermal conductivities and the effect of the moisture content are both nearly linear and opposite in magnitude from each other. For the case of the constant moisture content, the thawed thermal conductivity steadily increases with the increase in sand density. This reduces the time it takes to remove the heat from the slurry. For the saturated simulations where the moisture content it is clear that an increase in density, and decrease in moisture content, leads to shorter due to the fact that the more dense a material is the less void space there is and consequently the smaller the moisture content. The higher the density the closer the slurry is to a complete solid and freezeback time decreases. The smaller the density the more water that is present in the slurry and thus the freezeback time increases.

Section 5: Analysis

5.01: *Comparison of Modeling with Crory and Johnston*

The work done by Crory and expanded upon by Johnston is the only work available on the natural freezeback time of slurried piles. Using the equations provided by each of them it is possible to calculate and compare the freezeback time of the simulations presented here with their work. When calculating the freezeback time using Crory and Johnston's equations there are two things that should be kept in mind. First, neither considered a temperature gradient within the permafrost. Therefore when calculating their freezeback time the warmest temperature along the slurry permafrost boundary was used which was either T_{PT} at the permafrost table or T_p at the bottom of the pile. Second, both sources consider the energy per linear foot of pile, Q, required to freeze the slurry. To give a better comparison with Crory and Johnston these values are reproduced, when changing within a simulation, in the tables below. **Table 5.01.01** and **Table 5.01.02** show the freezeback times for the bore and pile radius sweeps compared with Crory and Johnston's equations while **Figure 5.01.01** and **Figure 5.01.02** graphically show the correlating information. **Table 5.01.03** and **Figure 5.01.3** compare the results of the pile length simulations with the calculated values of Crory and Johnston.

Table 5.01.01: *Results from the bore radius simulations.*

r_b (m)	Q (kJ/m)	t_{Crory} (days)	$t_{Johnston}$ (days)	t_{Model} (days)
0.1000	1.02E+03	0.24	0.30	0.36
0.2286	1.38E+04	5.29	5.51	8.45
0.3000	2.52E+04	9.96	10.27	15.04
0.4000	4.64E+04	18.65	19.11	27.79
0.5000	7.36E+04	29.82	30.48	42.12

Table 5.01.02: *Results from the pile radius simulations.*

r_p (m)	Q (kJ/m)	t_{Crory} (days)	$t_{Johnston}$ (days)	t_{Model} (days)
0.0000	1.58E+04	6.49	6.60	10.58
0.0500	1.51E+04	6.03	6.19	9.56
0.0814	1.38E+04	5.29	5.51	8.45
0.1500	9.00E+03	2.79	3.12	4.40
0.2000	3.71E+03	0.74	0.96	1.28

Table 5.01.03: *Results from the pile length simulations.*

h_p (m)	Q (kJ/m)	t_{Crory} (days)	$t_{Johnston}$ (days)	t_{Model} (days)	$t_{Model,const}$ (days)
6.0	1.38E+04	5.29	5.51	8.28	10.07
7.2	1.38E+04	5.29	5.51	8.44	10.23
8.4	1.38E+04	5.29	5.51	8.58	10.07
9.6	1.38E+04	5.29	5.51	8.77	9.96
10.8	1.38E+04	5.29	5.51	8.82	10.15
12.0	1.38E+04	5.29	5.51	9.06	10.21

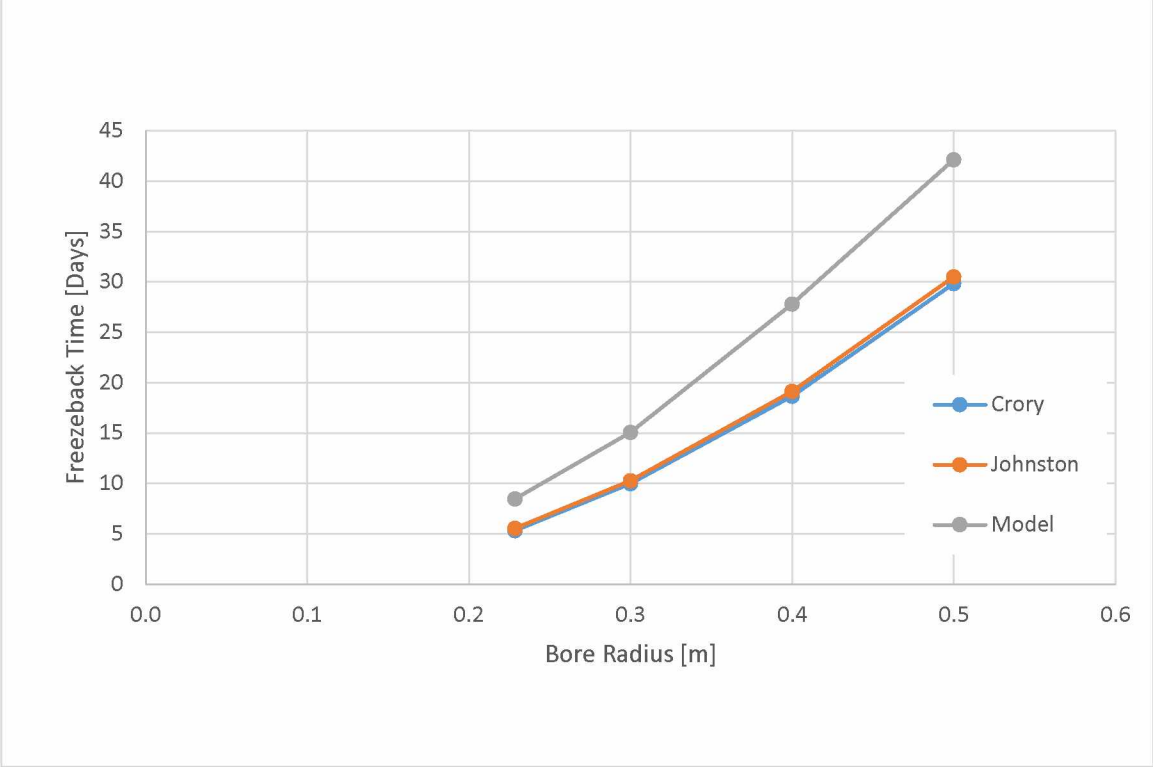

Figure 5.01.01: *Comparison between what is predicted by Crory and Johnston's equations with what was calculated by the model for the bore radius simulations.*

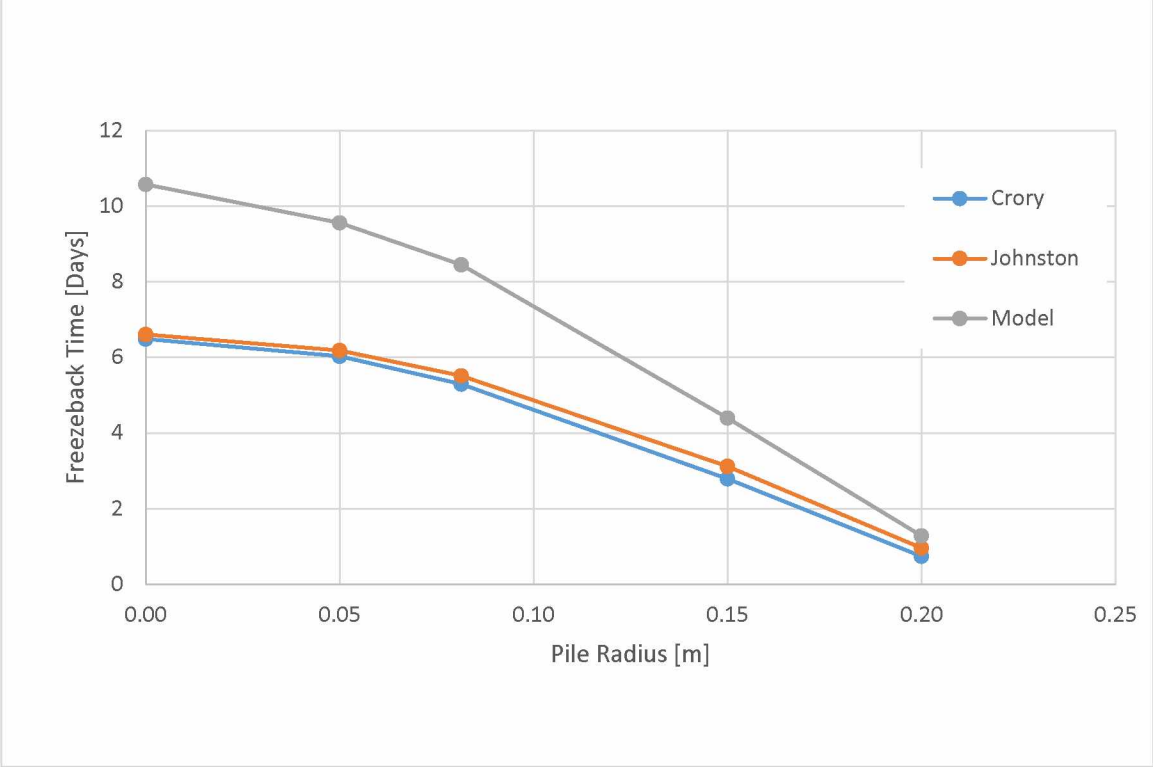

Figure 5.01.02: *Comparison between what is predicted by Crory and Johnston's equations with what was calculated by the model for the pile radius simulations.*

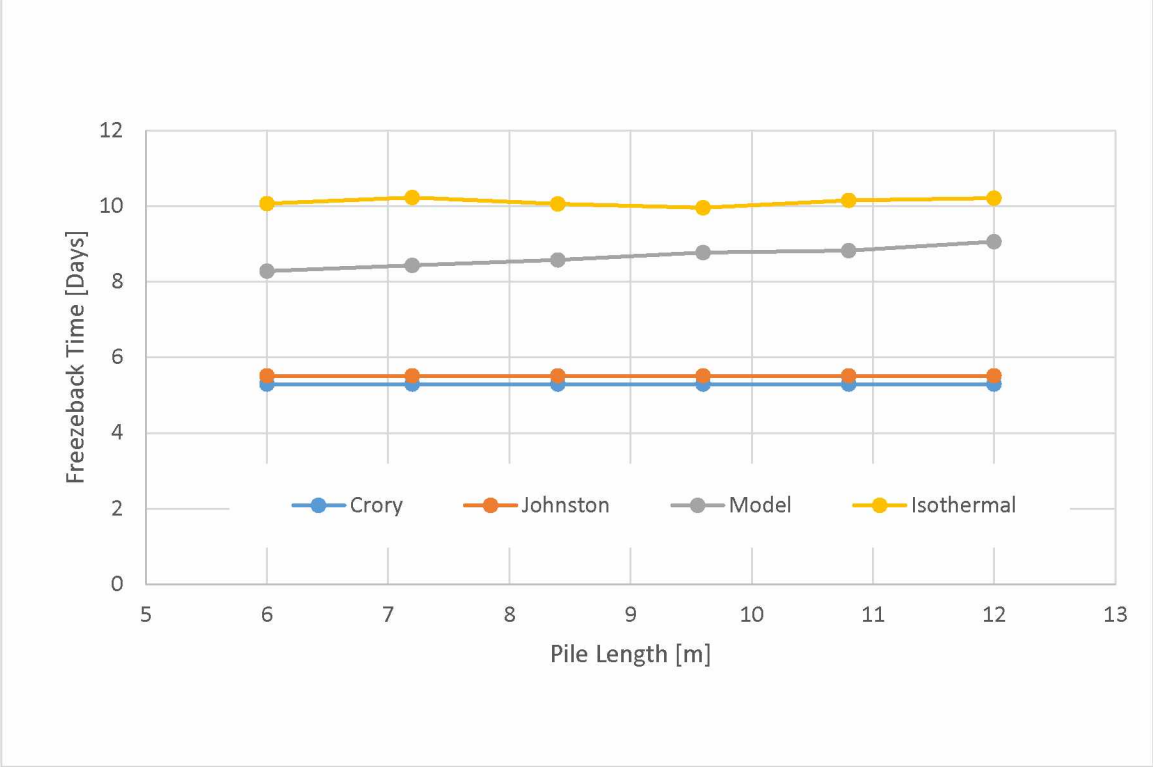

Figure 5.01.03: *Comparison between what is predicted by Crory and Johnston's equations with what was calculated by the model for the pile length simulations. The Model series is for the standard temperature gradient within the permafrost while the Isothermal series is for when the permafrost was set to a constant temperature.*

A difference in freezeback time found by modeling and results predicted by equations of Crory and Johnston increases as the volume of slurry increases.

Table 5.01.04: *Results from the slurry density simulations.*

γ_{sand} [kg/m^3]	w_s	k_f [W/(m·K)]	k_t [W/(m·K)]	$C_{vs,t}$ [kJ/m^3·K]	$C_{vs,f}$ [kJ/m^3·K]	Q kJ/m	t_{Crory} (days)	$t_{Johnston}$ (days)	t_{Model} (days)
1280	0.36	2.08	1.12	2840	1876	2.21E+04	10.70	10.30	14.52
1440	0.29	1.99	1.30	2773	1899	2.00E+04	9.23	9.03	13.05
1600	0.22	1.99	1.56	2613	1876	1.69E+04	7.14	7.19	10.67
1760	0.17	1.99	1.73	2506	1879	1.43E+04	5.60	5.79	8.83
1920	0.15	2.25	1.92	2572	1970	1.38E+04	5.29	5.50	8.28

Table 5.01.05: *Results from the slurry density with constant moisture content simulations.*

γ_{sand} (kg/m^3)	w_s	k_f (W/(m·K))	k_t (W/(m·K))	$C_{vs,t}$ (kJ/m^3·K)	$C_{vs,f}$ (kJ/m^3·K)	Q (kJ/m)	t_{Crory} (days)	$t_{Johnston}$ (days)	t_{Model} (days)
1280	0.24	2.08	1.12	2197	1554	1.47E+04	5.82	6.00	8.86
1440	0.24	1.99	1.30	2472	1748	1.65E+04	6.95	7.02	10.33
1600	0.24	1.99	1.56	2747	1943	1.84E+04	8.14	8.08	11.79
1760	0.24	1.99	1.73	3021	2137	2.02E+04	9.39	9.17	13.32
1920	0.24	2.25	1.92	3296	2331	2.21E+04	10.70	10.30	14.28

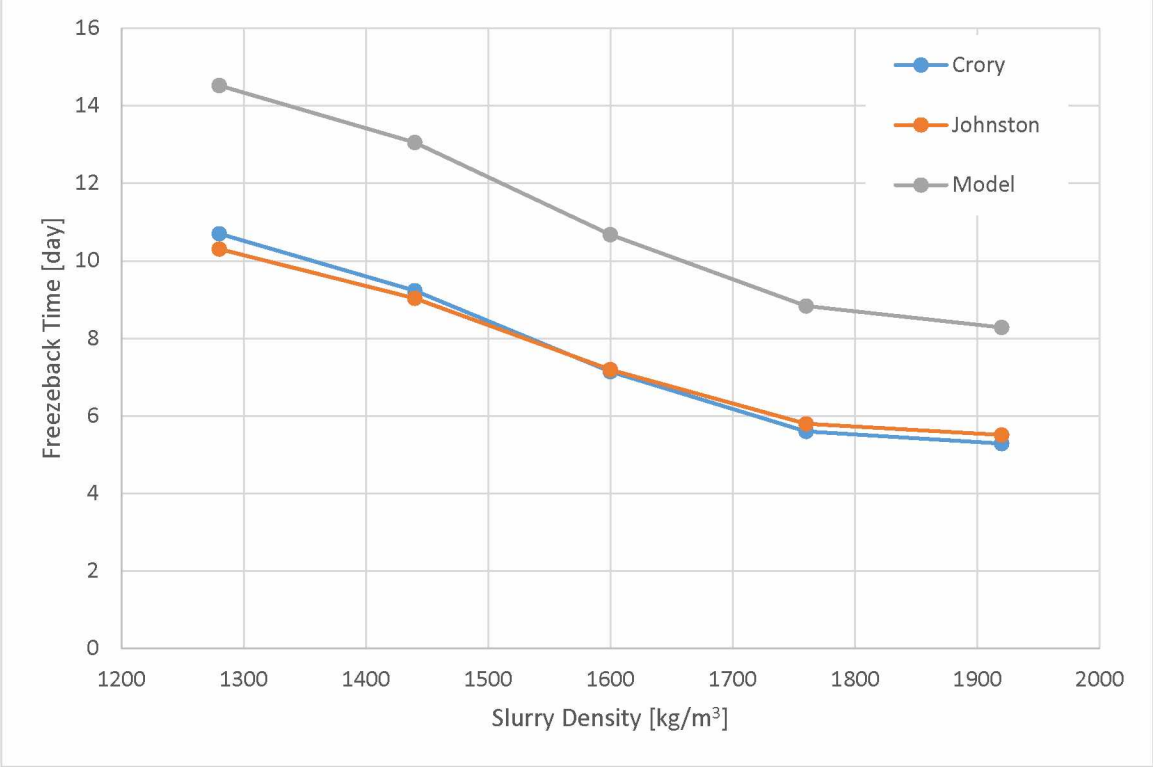

Figure 5.01.04: *Comparison between what is predicted by Crory and Johnston's equations with what was calculated by the model for the slurry density simulations.*

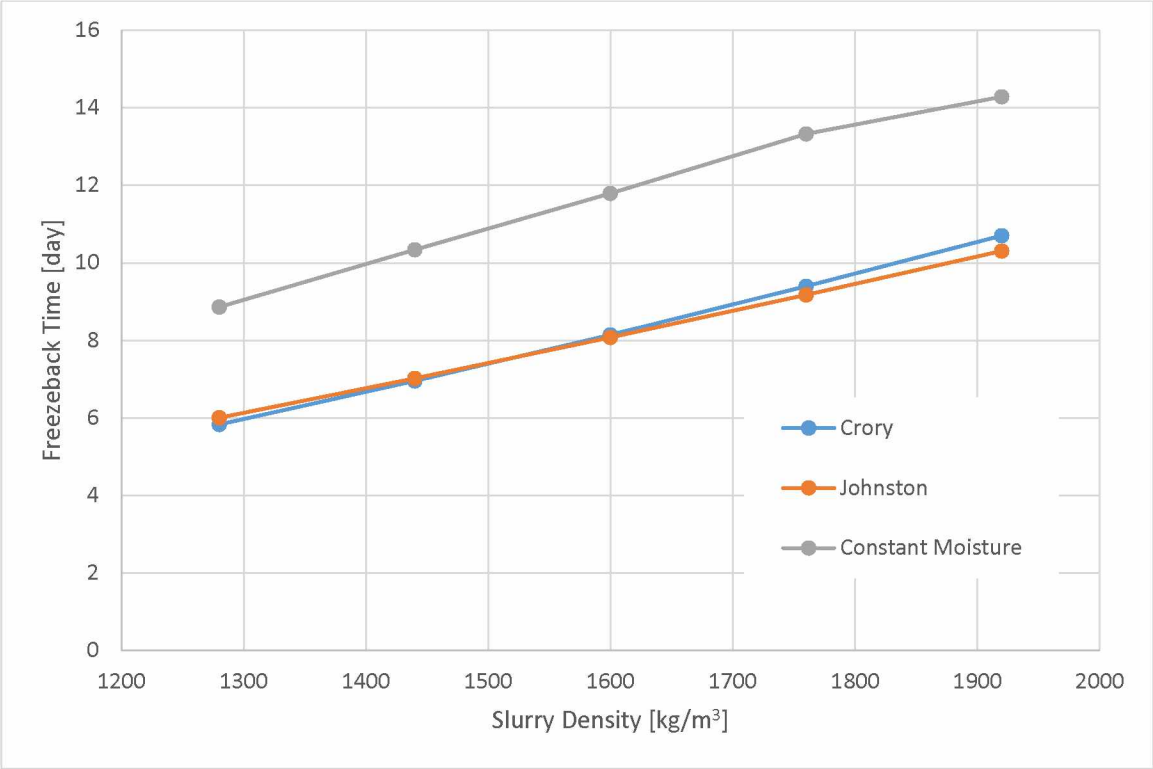

Figure 5.01.05: *Comparison between what is predicted by Crory and Johnston's equations with what was calculated by the model for the slurry density with constant moisture content simulations.*

Tables 5.01.04 and **5.01.05** corresponding with **Figures 5.01.04** and **5.01.05** compare the model results with Crory and Johnston's equations for the slurry density and the slurry density with constant moisture content simulations respectively. While it is again clear that there is a large difference in freezeback time predicted by the model and what is predicted by Crory and Johnston there are some differences from the pile and bore radius simulations. Namely there is no significant reduction in the difference between the model and calculated results like with what was seen with the decreasing slurry volume. While there is some change in the difference it is slight and negligible. Another difference is that unlike the bore and pile radius simulations where Johnston's equation was consistently larger than Crory's in these simulations the two actually interchange with each other in terms of which one produces the larger freezeback time.

Table 5.01.06: *Results from the pile length simulations.*

T_{PT} (°C)	T_p (°C)	t_{Crory} (days)	$t_{Johnston}$ (days)	$t_{Model,ins}$ (days)	$t_{Model,iso}$ (days)
-2.35	-0.90	27.0	23.5	52.3	48.5
-4.00	-2.00	8.2	8.1	12.4	12.3
-5.00	-2.67	5.3	5.5	8.3	8.3
-6.00	-3.33	3.8	4.1	6.1	6.3
-8.00	-4.67	2.3	2.6	4.1	4.1

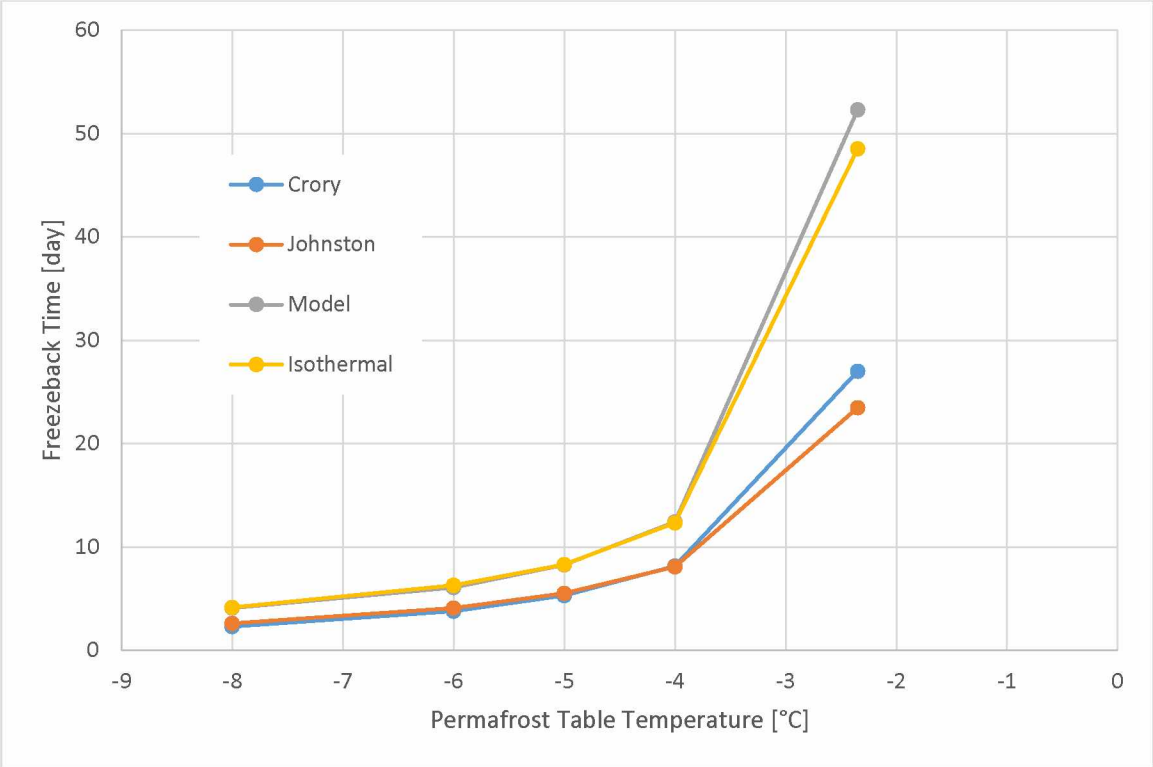

Figure 5.01.06: *Comparison between what is predicted by Crory and Johnston's equations with what was calculated by the model for the permafrost table temperature simulations.*

Table 5.01.06 and **Figure 5.01.06** show the comparison results between the permafrost table temperature simulations and the results predicted by Crory and Johnston. As the permafrost

temperature lowers the closer results of modeling are to those predicted by Crory and Johnston however the difference between them grows significantly at warmer permafrost temperature. This correlates with the results in **Tables 5.01.07** and **5.01.08** with **Figures 5.01.07**, **5.01.08**, **5.01.09**, **5.01.10**, and **5.01.11** which show the comparison results for the temperature gradient simulations for a permafrost table temperature of -2°C, -4°C, -6°C, -8°C, and -10°C respectively. As can be seen with the results for the warmer permafrost, with temperatures of -2 and -4°C, there is a significant difference between the model and the predicted results of Crory and Johnston that is exacerbated as the permafrost temperatures are warmed. This difference decreases for the permafrost table temperature simulations of -6°C and the model overlaps with minimal difference for the permafrost table temperatures of -8 and -10°C. As the permafrost temperatures decreases the freezeback time of the model and the predicted values converge however for warm permafrost, such as what might be found in the discontinuous zone, the equations of Crory and Johnston vastly underestimate the freezeback time.

Table 5.01.07: *Results from the permafrost temperature gradient simulations for permafrost table temperatures of -2, -4, and -6°C.*

T_{PT} (°C) = -2					T_{PT} (°C) = -4					T_{PT} (°C) = -6				
T_{bot} (°C)	T_p (°C)	t_{Crory} (days)	$t_{Johnston}$ (days)	t_{Model} (days)	T_{bot} (°C)	T_p (°C)	t_{Crory} (days)	$t_{Johnston}$ (days)	t_{Model} (days)	T_{bot} (°C)	T_p (°C)	t_{Crory} (days)	$t_{Johnston}$ (days)	t_{Model} (days)
-8.0	-4.00	8.15	8.09	13.63	-2.0	-3.33	3.79	4.09	6.79	-6.0	-6.00	1.57	1.87	3.13
-4.0	-2.67	8.15	8.09	16.07	0.0	-2.67	5.29	5.51	8.82	-2.0	-4.67	2.29	2.61	3.13
-2.0	-2.00	8.15	8.09	17.48	2.0	-2.00	8.15	8.09	12.42	4.0	-2.67	5.29	5.51	7.82
0.0	-1.33	14.98	13.89	30.07	4.0	-1.33	14.98	13.89	21.24	8.0	-1.33	14.98	13.89	18.28
1.3	-0.90	27.00	23.45	60.02	5.3	-0.90	27.00	23.45	36.88	9.3	-0.90	27.00	23.45	30.15

Table 5.01.08: *Results from the permafrost temperature gradient simulations for permafrost table temperatures of -8 and -10°C.*

T_{PT} (°C) = -8					T_{PT} (°C) = -10				
T_{bot} (°C)	T_p (°C)	t_{Crory} (days)	$t_{Johnston}$ (days)	t_{Model} (days)	T_{bot} (°C)	T_p (°C)	t_{Crory} (days)	$t_{Johnston}$ (days)	t_{Model} (days)
0.0	-5.33	1.87	2.19	3.53	4.0	-5.33	1.87	2.19	3.40
4.0	-4.00	2.88	3.21	4.81	8.0	-4.00	2.88	3.21	4.55
8.0	-2.67	5.29	5.51	7.29	12.0	-2.67	5.29	5.51	6.80
12.0	-1.33	14.98	13.89	16.09	16.0	-1.33	14.98	13.89	14.41
13.3	-0.90	27.00	23.45	27.35	17.3	-0.90	27.00	23.45	24.43

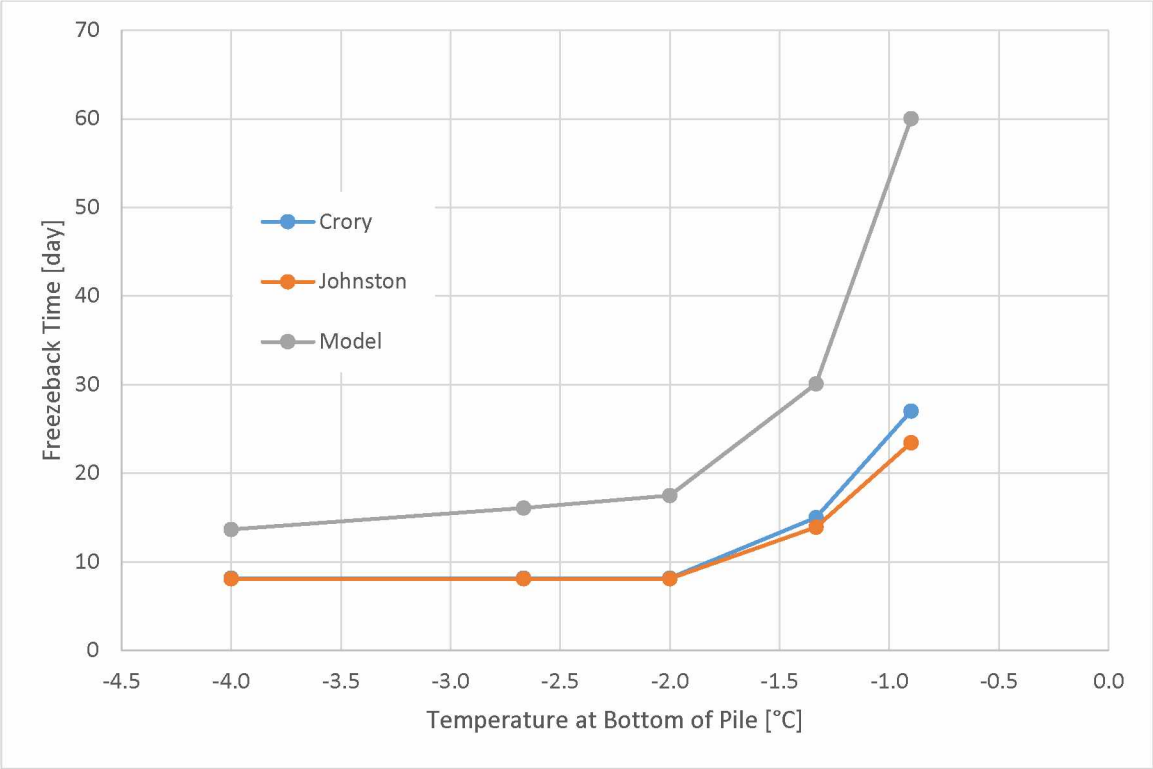

Figure 5.01.07: *Comparison between what is predicted by Crory and Johnston's equations with what was calculated by the model for the permafrost temperature gradient simulation for a permafrost table temperature of -2°C.*

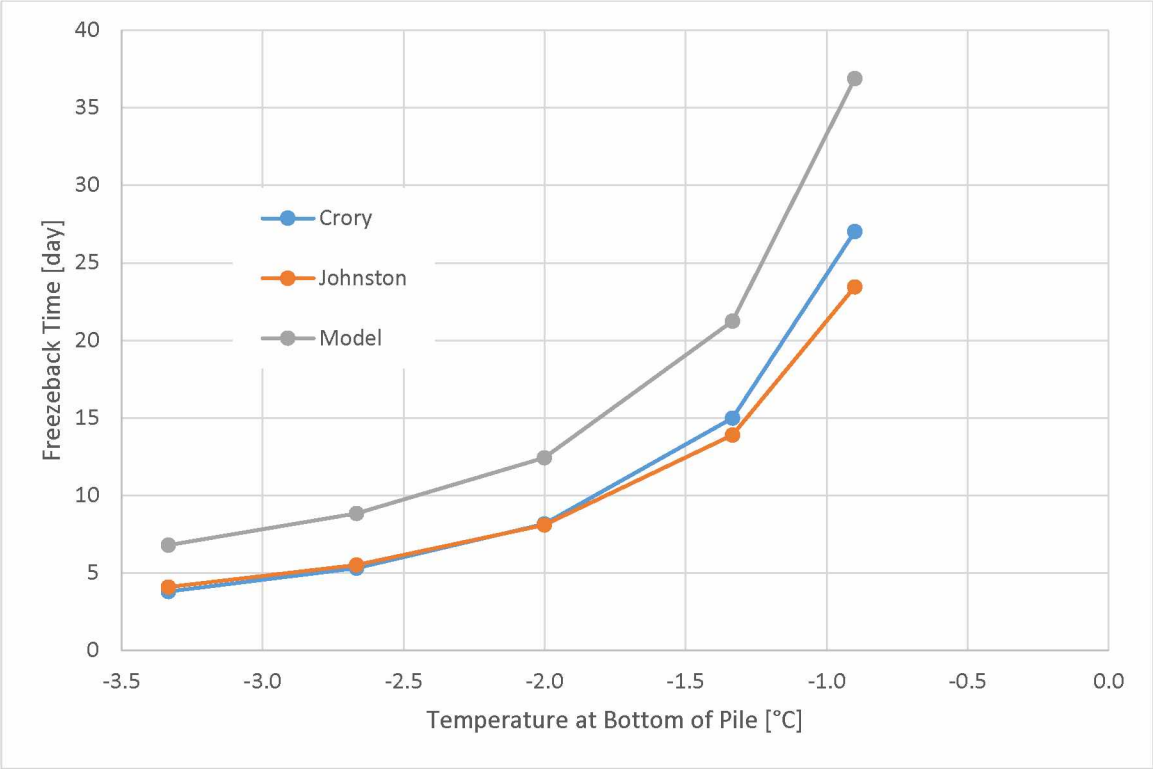

Figure 5.01.08: *Comparison between what is predicted by Crory and Johnston's equations with what was calculated by the model for the permafrost temperature gradient simulation for a permafrost table temperature of -4°C.*

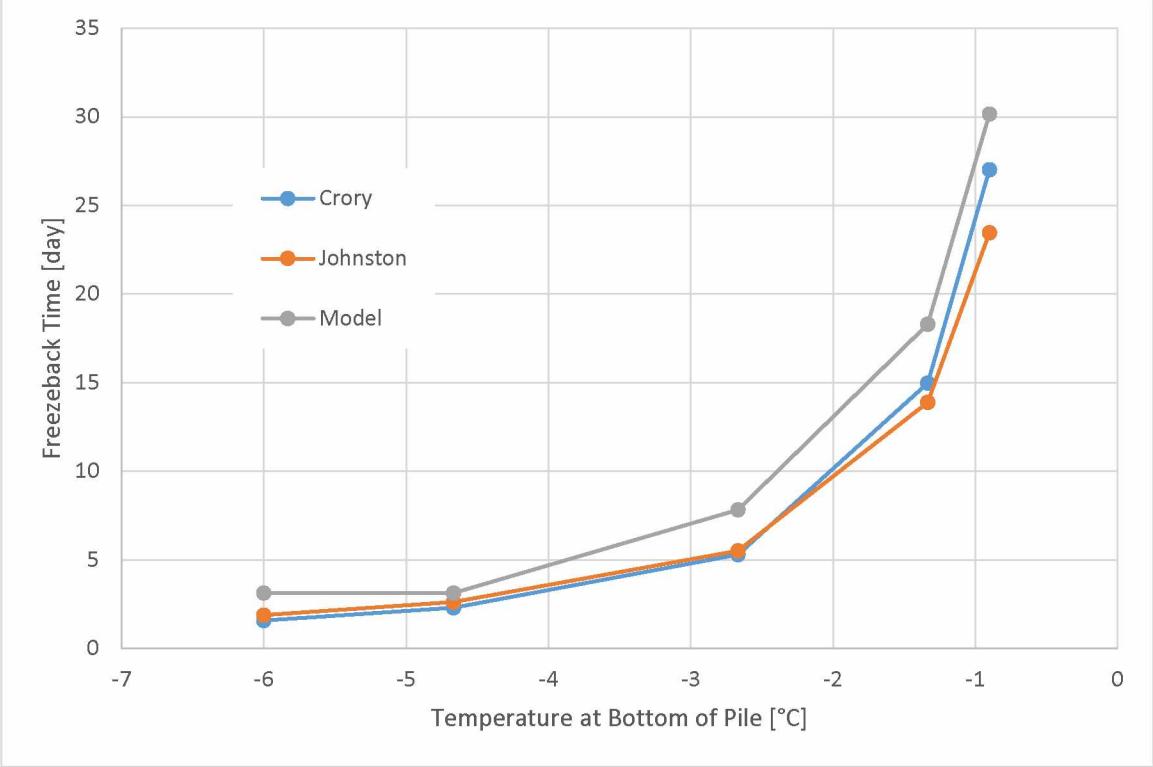

Figure 5.01.09: *Comparison between what is predicted by Crory and Johnston's equations with what was calculated by the model for the permafrost temperature gradient simulation for a permafrost table temperature of -6°C.*

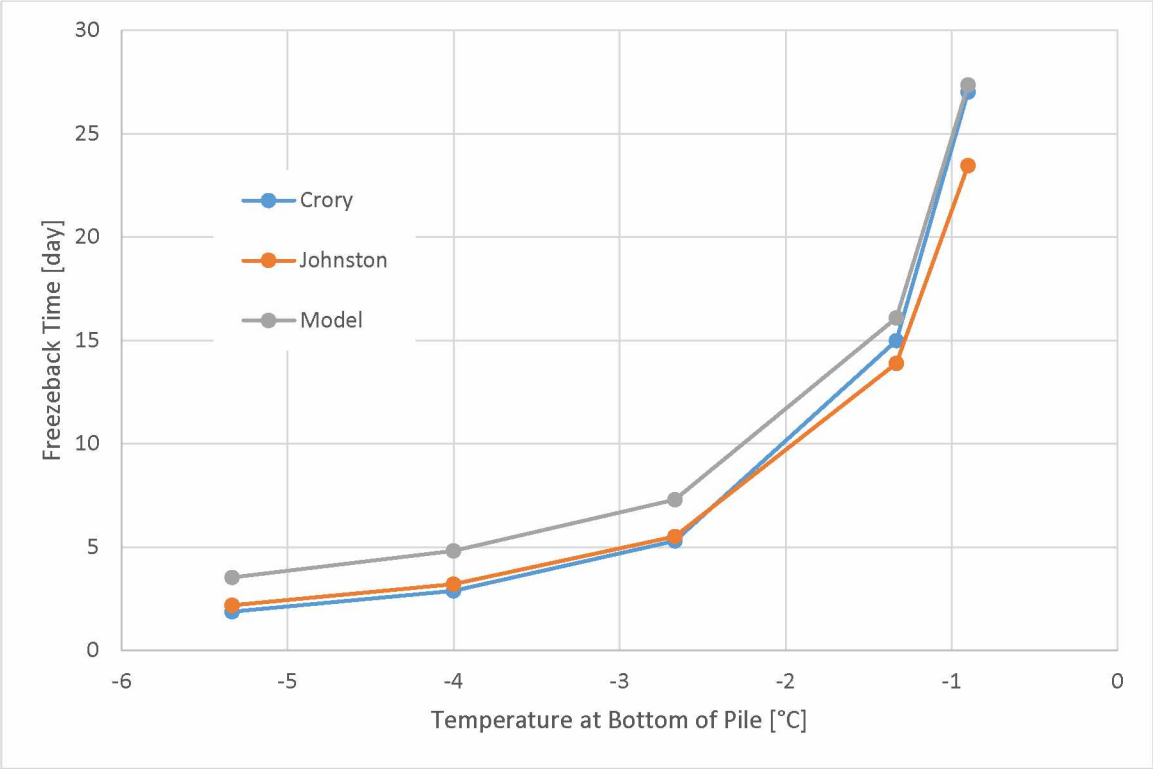

Figure 5.01.10: *Comparison between what is predicted by Crory and Johnston's equations with what was calculated by the model for the permafrost temperature gradient simulation for a permafrost table temperature of -8°C.*

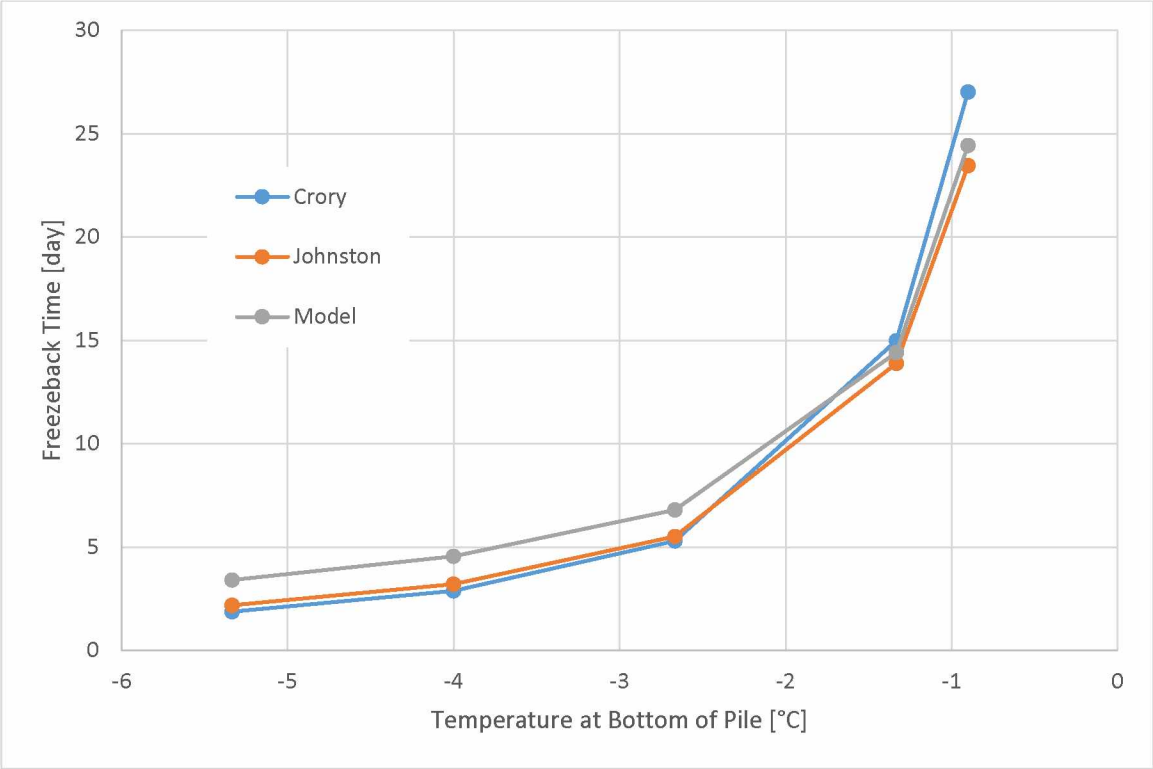

Figure 5.01.11: *Comparison between what is predicted by Crory and Johnston's equations with what was calculated by the model for the permafrost temperature gradient simulation for a permafrost table temperature of -10°C.*

Section 6: Conclusion

6.01: *Implications of Results*

The simulations in general shows similarity in trends predicted by Crory and Johnston in many of the simulations. It is important to notice that modeling shows greater time that can be predicted by equations of Crory and Johnston. The closest the model ever came with their equations was when the slurry volume was extremely small or when the permafrost was abnormally cold. When these situations weren't the case the model produced times several days larger than Crory and Johnston on a consistent basis often following the same general trends.

It is clear that Crory and Johnston's equation are not conservative and under predict the freezeback time for most reasonable cases. The root cause of this difference is difficult to ascertain due to the lack of detailed information on how the original data looked and was interpreted. This lack of background, explanation, and data coupled with the lack of any field results to challenge or check Crory's original field work in over 50 years while being cited and referred to by people in various major publications led people to believe that what was published in 1966 was accurate and the authority on natural pile freezeback.

6.02: *Where to Go from Here*

There are four distinct aspects that future research should consider in light of these results. The first of which is determining a new freezeback equation for slurried piles based on the model results. Because it is clear that what has been accepted for so long is not conservative it would be beneficial to the scientific community and to the design engineers to have a more definitive and accurate method of determining slurry freezeback. For a contractor installing piles and waiting for freezeback to continue construction a freezeback time that is too short by a factor of days can lead to premature pile loading, which can create unsafe working conditions and the potential to ruin the expensive work done up to that point.

Another direction to continue research in is expanding the examination of varying multiple parameters at once. For example varying the bore and pile radius so that the thickness of slurry remains constant while the surface area of the slurry permafrost interface increases. Similar

simulations could be done to see the relationship between the volume of slurry and surface area of contact between the slurry and permafrost. Also, the relationship between the pile and bore radius as a fixed ratio as this ratio is at the core of theoretical cylindrical heat flow. An examination into these connections would give a more thorough representation of what factors influence slurry freezeback.

Consideration should also be given to check the influence of pile spacing. This study assumed that each pile was far away from the closest pile such that the thermal influence of the slurry and its installation was negligible however Crory and his original work remain the only source on determining pile spacing. It would also be beneficial to expand the model to include considering artificial freezeback from various methods. While there has been much discussion given to the freezeback of artificial freezeback it is often assumed that the systems operate so efficiently and quickly that only a few days are needed. This model could be expanded to consider the influence of various types of artificial refrigeration for research and private sector use.

Lastly, all models benefit with some form of ground truthing. It would be very beneficial to check not only the results of this model but the results of Crory, and consequently Johnston. If a freezeback equation were developed to compare with Crory and Johnston then tests could be done to determine which of the three were actually the most accurate for various situations. It is apparent from the results shown here that the widely accepted freezeback equations of Crory and Johnston, as well as the original unpublished fieldwork of Crory, should be subject to question by those that use their results.

References

Andersland, Orlando B. and Ladanyi, Branko. 2004. Frozen Ground Engineering, 2nd Edition. s.l. : John Wiley & Sons, Inc, 2004. 978-0-471-61549-1.

Anderson, D. M. and Tice, A. R. 1972. Predicting Unfrozen Water contents in Frozen Soils from Surface Area Measurements. Washington, D.C. : Frost Action in Soils, 1972.

Carslaw, H. S. and Jaeger, J. C. 1959. Conduction of Heat in Solids. s.l. : Oxford, 1959. 978-0198533689.

Clarke, Edwin S. 2007. Permafrost Foundations: State of the Practice. s.l. : American Society of Civil Engineers, 2007. 978-0-7844-0947-3.

COMSOL. 2011. COMSOL Multiphysics (R) User's Guide Version 4.3. 2011.

Crory, Frederick E. 1966.Pile Foundations in Permafrost. West Lafayette, Indiana : s.n., 1966. Proceedings From the First International Conference on Permafrost. pp. 467-476.

Crory, Frederick E. 1967. Special Report 79 Pile Foundations in Discontinuous Permafrost Areas. s.l. : Cold Regions Research and Engineering Laboratory, 1967.

Crory, Frederick E. 1968. Technical Report 180 Bridge Foundations in Permafrost Areas Goldstream Creek, Fairbanks, Alaska. s.l. : Cold Regions Research and Engineering Laboratory, 1968.

Crory, Frederick E. 1973. Installation of Driven Test Piles in Permafrost at Bethel Air force Station Alaska. s.l. : Cold Regions Research and Engineering Laboratory, 1973.

Crory, Frederick E. 1975. Technical Report 266 Bridge Foundations in Permafrost Areas Moose and Spinach Creeks Fairbanks, Alaska. s.l. : Cold Regions Research and Engineering Laboratory., 1975.

Dagher, E. E., Su, G. and Nguyen, T. S. 2014. Verification of the Numerical Simulation of Permafrost Using COMSOL Multiphysics (R) Software. Boston : s.n., 2014. COMSOL Conference.

Darrow, Margaret M., et al. 2013. Impact of Groundwater Flow on Permafrost Degradation and Transportation Infrastructure Stability. s.l. : INE/AUTC, 2013.

Department of the Air Force. 1966. Calculation Methods for Determination of Depths of Freeze and Thaw Soils – Emergency Construction. Manual AFM 88-40. Chapter 46. Washington D.C.

Gornov, V. F., Stepanov, S. P. and Vasilyev, V. I. 2014. Mathematical Modeling of Heat Transfer Problems in the Permafrost. 2014, Application of Mathematics in Technical and Natural Sciences, pp. 424-431.

Heydinger, Andrew G. 1987.Piles in Permafrost. 1987, Journal of Cold Region Engineering, pp. 59-75.

Jaeger, J. C. and Clarke, M. 1943. A Short Table of I(0, 1;x). 3, s.l. : Proceedings of the Royal Society of Edinburgh Section A: Mathematics, 1943, Vol. 61.

Johnston, G. H. 1966. Pile Construction in Permafrost. West Lafayette, Indiana : s.n., 1966. Proceedings from the First International Conference on Permafrost. pp. 477-481.

Johnston, G. H. 1981. Permafrost Engineering Design and Construction. s.l. : John Wiley & Sons, 1981.

Kersten, Miles S. 1949. Laboratory Research for the Determination of the Thermal Properties of Soils. s.l. : U.S. Arcmy Corps of Engineers, 1949.

Kömle, N. I. and Feng, Wenjie. 2009. Variation of the Frost Boundary below Road and Railway Embankments in Permafrost Regions in Response to Solar Irradiation and Winds. Milan : s.n., 2009. COMSOL Conference.

Ladanyi, B. 1983. Washington, D.C. : s.n., 1983. Final Proceedings of the Fourth International Conference on Permafrost. pp. 43-50.

Ladanyi, B. 1984. Design and Construction of Deep Foundations in Permafrost: North American Practice. Washington D.C. : s.n., 1984. Final Proceedings from the Fourth International Conference on Permafrost. pp. 43-50.

Lee, T. M. 1962. Note on Freeze Back time of Slurry Around Piles in Permafrost. s.l. : Unpublished, 1962.

Linell, Kenneth A. and Kaplar, C. W. 1966. Technical Report 150 Description and Classification of Frozen Soils. s.l. : Cold Regions Research and Engineering Laboratory, 1966.

Linell, Kenneth A. and Lobacz, Edward F. 1980. Special Report 80-34 Design and Construction of Foundations in Areas of Deep Seasonal Frost and Permafrost. s.l. : Cold Regions Research and Engineering Laboratory, 1980.

Luk'yanov, V. S. 1966. Computation of the Depth of Freezing and Thawing in Soils. West Lafayette Indiana : s.n., 1966. Proceedings of the First International Conference on Permafrost. pp. 281-285.

Lunardini, Virgil J. 1981. Heat Transfer in Cold Climates. s.l. : Van Nostrand Reinhold Company, 1981. 978-0442262501.

Luscher, Ulrich, Black, William T. and McPhail, James F. 1984. Results of Load Tests on Temperature-Controlled Piles in Permafrost. Washington D.C. : s.n., 1984. Proceedings From the Fourth International Conference on Permafrost. pp. 756-761.

Marchenko, Sergei, Romanovsky, Vladimir and Tipenko, Gennady. 2008. Numerical Modeling of Spatial Permafrost Dynamics in Alaska. Fairbanks Alaska : s.n., 2008. Nineth International Conference on Permafrost. pp. 1125-1130.

Noetzli, Jeannette, Gruber, Stephan and Friedel, Sven. 2007. Modeling Transient Permafrost Temperatures below Steep Alpine Topography. Grenoble, France : s.n., 2007. COMSOL Conference.

Pavement Interactive. 2012. Pavement Interactive. [Online] 2012. http://www.pavementinteractive.org/.

Qin, Yinghong, Hiller, Jacob E. and Bao, Ting. 2013. Modeling Cold Region Ground Temperatures with a Heat Flux Upper Boundary Model. 2013, Journal of Cold Regions Engineering, pp. 29-43.

Research Group on Pile Foundations in Permafrost, Research Institute of Ministry of Railways, The People's Republic of China. 1978.Testing of Pile Foundations in Permafrost Areas. Edmonton, Alberta, Canada : s.n., 1978. Proceedings From the Third International Conference on Permafrost Volume 2. pp. 179-185.

Rongved, Johanna Lohne and Instanes, Arne. 2012. Foundation Engineering in Svalbard, 1950-2012. Salekhard, Russia : s.n., 2012. Proceedings From the Tenth International Conference on Permafrost, Volume 1. pp. 355-360.

Sanger, Frederick J. 1969. Cold Regions Science and Engineering Monograph III-C4 Foundations of Structures in Cold Regions. s.l. : Cold Regions Research and Engineering Laboratory, 1969.

Sheppard, Marsha I., Kay, B. D. and Loch, J. P.G. 1978. Development and Testing of a Computer Model for Heat and Mass Flow in Freezing Soils. Lafayette Indiana : s.n., 1978. The Third International Conference on Permafrost, Vol. 1. pp. 75-81.

Shur, Yuri and Osterkamp, Thomas E. 2007. Thermokarst. Fairbanks, Alaska : University of Alaska Fairbanks, Institute of Northern Engineering, 2007. Report INE06.11.

U.S. Army Air Force. 1983. TM 5 Volume 4 Arctic and Subarctic Construction Foundations for Structures. s.l. : Department of the Army and the Air Force, 1983.

U.S. Army Air Force. 1988. TM 5 Volume 6 Arctic and Subarctic Construction Calculation Methods for Determination of Depths of Freeze and Thaw in Soils. s.l. : Departments of the Army and the Air Force, 1988.

Wan, Richard and Booshehrian, Ahmad. 2015. Permafrost Degradation within Continuous Permafrost Zones due to Mining Disturbances in Canadian Northern Regions. Calgary, Alberta Canada : University of Calgary, 2015.

Weaver, Jeffrey Stephen. 1979. Pile Foundations in Permafrost. A Thesis. Edmonton, Alberta, Canada : The University of Alberta, Fall 1979.